**US Army Corps
of Engineers** ®
Engineer Research and
Development Center

Strengthening of Concrete Beams with Fasteners and Composite Material Strips–Scaling and Anchorage Issues

Lawrence C. Bank, David T. Borowicz, Dushyant Arora,
Anthony J. Lamanna, Gerardo I. Velázquez,
and James C. Ray

July 2004

Strengthening of Concrete Beams with Fasteners and Composite Material Strips–Scaling and Anchorage Issues

by   Lawrence C. Bank, David T. Borowicz, Dushyant Arora, Anthony J. Lamanna

Department of Civil and Environmental Engineering
University of Wisconsin-Madison
Madison, WI 53706

Gerardo I. Velázquez, James C. Ray

Geotechnical and Structures Laboratory
U.S. Army Engineer Research and Development Center
3909 Halls Ferry Road
Vicksburg, MS 39180-6199

Final report

ABSTRACT: A system to rapidly strengthen concrete beams and slabs, known as the Mechanically-Fastened Fiber-Reinforced Polymer (MF-FRP) system, has been developed. In the fourth year of research on the subject, the focus was on scaling and anchorage issues. The effect of increasing the number of strips, the fastener spacing, termination distances, and the use of expansion anchors at the strip ends were considered. The scaling study also investigated the use of the MF-FRP system on a full-scale highway bridge.

A second series of tests was conducted on large-scale T-beams at the U.S. Army Engineer Research and Development Center, Vicksburg, MS, in the summer of 2002. The results of this testing and of parametric design studies conducted were used to design the strengthening system for a flat-slab bridge built in 1930 in the city of Edgerton, WI, and slated for replacement in 2003. The bridge was strengthened with the MF-FRP system in the summer of 2002 and tested to failure in the summer of 2003. An investigation was also conducted into the properties of the FRP strips with different constituent material properties. An optimal strip design to produce the best ultimate longitudinal strength and stiffness, as well as bearing strength, has been recommended to the manufacturer.

The research conducted revealed a number of important scaling related issues with the MF-FRP system. It was found that multiple strips were not as effective as single strips, that a double row of fasteners at 2 in. on center is less effective than a single row of fasters at 3 in. on center, and that mechanical anchor bolts at the ends of the strip significantly improved performance and delayed the onset of end-delamination failures. The importance of a small termination distance from the support was confirmed in testing. Fatigue testing to 2 million cycles showed no degradation of the MF-FRP strengthening system. The full-scale bridge application proved the versatility of the system. Strips were easily and rapidly attached to a severely deteriorated concrete soffit that would not have permitted the use of an epoxy-bonded FRP (EB-FRP) strengthening system.

Ten (10) months of environmental exposure did not appear to reduce the effectiveness of the system, and no degradation in material properties of the FRP strips was seen. The ultimate failure test on the bridge proved the ability of the MF-FRP system to increase the strength of a reinforced concrete bridge. Analytical models to predict the strengthening were shown to produce reasonable predictions. These models can be used for design purposes.

Contents

SF 298

List of Figures

List of Tables

Conversion Factors, Non-SI To SI Units Of Measurement

Non-SI units of measurement used in this report can be converted to SI units as follows:

Multiply	By	To Obtain
cubic feet	0.028317	cubic meters
Fahrenheit degrees	(F-32)/1.8	Celsius degrees
feet	0.304800	meters
feet per second	0.304800	meters per second
inches	0.025400	meters
inches	25.4	millimeters
miles	1.609	kilometers
pounds (force) per square inch	0.006894757	megapascals
pounds (mass)	0.453592	kilograms

* The primary units presented in the report are those that were used during fabrication of experiment setup or those calibrated and recorded by instruments during experiment execution.

Preface

1   Introduction

This research study continued to investigate the use of mechanically fastened fiber-reinforced polymer (MF-FRP) composite materials using powder-actuated fasteners (PAFs) and expansion anchors (EAs) to rapidly rehabilitate and strengthen concrete members (Bank et al. 2002a, b). The MF-FRP system is an alternative to the epoxy-bonded fiber-reinforced polymer (EB-FRP) system and is ideally suited to rapid installation on poor concrete substrates.

The first year of the study focused on analytical models, materials testing, and small-scale experiments (Lamanna et al. 2001a), while second year investigations included testing of full-size retrofitted rectangular beams at the ERDC in Vicksburg, MS, and comparisons to epoxy-bonded specimens (Bank et al. 2002a, Lamanna et al. 2001b). Third year studies included the strengthening and testing of large-scale concrete T-beams at ERDC in the summer of 2001 with varying steel reinforcement quantities, testing retrofitted full-size rectangular beams under different loading conditions, and the development of an MF-FRP design and installation procedure (Bank et al. 2002b; Velázquez et al. 2002; Borowicz 2002). Overall, the results of the first three years of research indicated that the MF-FRP system was viable for application to real-world structures.

In the fourth year of research on the subject the focus was on scaling and anchorage issues. The effects of increasing the number of strips, the fastener spacing, termination distances, and the use of expansion anchors at the strip ends were considered. The scaling study also investigated the use of the MF-FRP system on a full-scale highway bridge. A second series of tests was conducted on large scale T-beams at ERDC in the summer of 2002. The results of this testing and of parametric studies conducted, were used to design the strengthening system for a bridge application in the State of Wisconsin. A flat-slab bridge built in 1930 in the city of Edgerton, WI, and slated for replacement in 2003 was strengthened with the MF-FRP system in the summer of 2002 and tested to failure in the summer of 2003. An investigation was also conducted into the properties of the FRP strips with different constituent material properties and an optimal strip design to produce the best ultimate longitudinal strength and stiffness, as well as, bearing strength has been recommended to the manufacturer.

2 Technical Objective and Scope

The objective of this research study was to test the MF-FRP system on both full-scale concrete T-beams and a reinforced concrete bridge to determine its viability for military applications. The report is focused on the testing and analysis of results of an experimental investigation of both full-sized T-beams and an actual bridge strengthened with FRP composite strips and mechanical fasteners.

The scope of work for the research report is as follows:

a. *Test Full-Sized T-Beams*. Testing was carried out at the U.S. Army Corps of Engineers Research and Development Center in Vicksburg, MS. Beams were tested in four-point bending using two 110 kip actuators. Data acquired included actuator load, actuator stroke, beam displacement (via Linear Variable Differential Transformer (LVDT)), and strains in both the composite strip and concrete. In prior research (Bank et al. 2002b), a series of nine 29 ft long full-scale T-beams had been tested. In the prior work T-beams with three different steel reinforcement ratios (designated A3, A5 and A8 to represent the number of No. 9 grade 60 reinforcing bars in each type) and three different strengthening levels (no FRP, one FRP strip, and two FRP strips) were tested. All strengthened beams tested in the first series failed by delamination of the FRP strips. The current work revisited the A5 series beams to study the delamination issues in more detail in an attempt to obtain more ductility in the MF-FRP strengthened beams. Six beams were tested in the summer of 2002. These consisted of one control and five strengthened beams. Variables included varying the termination length (3 or 18 in. from the support), the number of strips (one, two, or three), and the use of anchor bolts at the strip ends. In addition, a fatigue test to 2 million cycles was conducted to investigate the effect of long term cyclic loading on the MF-FRP system.

b. *Conduct Parametric Studies*. Using analytical models developed in prior years of the research, parametric studies were conducted to determine maximum moment capacities for MF-FRP strengthened beams. Design moment envelops for standard vehicles were developed for a flat-slab bridge. These studies were used to design the MF-FRP strengthening

system for the strengthening of a flat-slab bridge in Edgerton, Wisconsin. The design requirement was to increase the bridge load rating from HS 17 to HS 25. This required a 29 percent increase in the moment capacity of the slab. Parametric studies were conducted to determine the number of strips and fasteners that would be needed to achieve the required strengthening considering a range of in situ material properties for the existing structure. Based on the results of this study and the results of the T-beam testing an MF-FRP strengthening design was recommended for the bridge.

c. *Optimize Pultruded FRP Strips for the MF-FRP System.* A study was conducted to determine the optimal combination of glass fiber mats, glass fiber rovings, and carbon fiber tows in the FRP strips used for strengthening with the MF-FRP method and to develop a recommendation for a "standard" specification FRP strengthening strips. In the previous year's research (Bank et al. 2002b), low strength FRP strips were obtained when pigments were added to the resin system. The research team worked with a local pultrusion company to produce seven different FRP strips. Strips were tested for their longitudinal strength and stiffness, their open-hole longitudinal strength, and their bearing strength. An optimal configuration was developed and "guaranteed" design properties for this strip according to ACI (ACI 440.2R 2002) procedures were developed.

d. *Strengthen and Test a Real-World Structure.* The flat-slab reinforced concrete bridge was strengthened with 21 composite strips attached to the underside of the deck with powder-actuated fasteners spaced at 3 in. on center and expansion anchors at their ends. The strengthened bridge was exposed to the environment for 10 months and then tested to failure. Data from this test, to include load, deflection, and strain readings, were analyzed to determine the strengthening effect of the MF-FRP system.

e. *Document Environmental Effects on System.* Ten (10) months of exposure to Wisconsin weather had some impacts on the MF-FRP strengthening system. These effects were identified and documented to assist in future investigations.

3 Testing of Full-Scale T-Beams

Introduction

In 2001 nine full scale T-beams were tested at the Vicksburg site of the Engineering Research and Development Center (Bank et al. 2002b). The T-beams were 29 ft long and had a 60 × 8 in. top flange and a 22 × 12 in. web section. They were reinforced with No. 9 grade 60 main longitudinal bars in the bottom of the web and No. 4 stirrups at 12 in. on center (o.c.). The flange was reinforced with a double layer of No. 4 bars at 12 in. o.c. in both directions. Beams were fabricated at ERDC with 5000 psi concrete. Three different levels of tensile reinforcement were used, identified by the number of No. 9 main bars: A3, A5, and A8. For each reinforcement level 3, different strengthening levels were used–no strengthening, one FRP strip, and two FRP strips. A termination length of 18 in. was used in all beams. All beams had the FRP strips fastened with Hilti X-ALH power actuated fasteners in two rows spaced at 2 in. and spaced at 2 in. along the length. In the A3 and A5 controls it was not possible to achieve ultimate failure of the beams resulting from the large displacement required. Only the A8 beam reached its ultimate load. All the strengthened beams failed resulting from strip delamination prior to achieving compressive failure in the concrete. Beams showed increases of between 10 and 20 percent in strength at yield and at ultimate load. Figure 1 shows the moment versus displacement data for all nine Phase I tests.
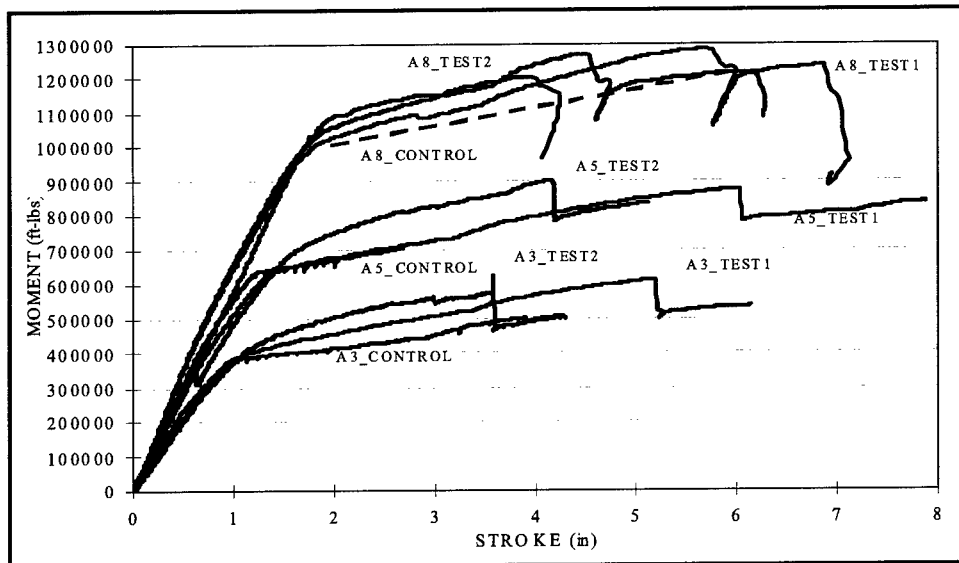
Figure 1. Moment-stroke data for Phase I (2001) tests

To further understand the influence of the different material and geometric parameters on the behavior of the MF-FRP strengthened beams a second phase of full-scale T-beam tests was conducted in the summer of 2002. The A5 series was chosen as the T-beam configuration for the second series of tests since the data from this set were inconclusive in the first phase and this level of reinforcement was felt to be the most representative of real bridges. The parameters investigated in the this series of six beams were:

a. Termination length. A 3 in. termination length was compared to the 18 in. termination length. The shorter termination length was expected to increase the capacity and delay the onset of end-delamination failures.

b. Fastener spacing. Three inch spacing along the length of the strip was used to compare to the 2 in. spacing used previously. Two rows at 2 in. apart were again used in the second phase. The effect of greater spacing along the length was expected to decrease the likelihood of interior-delamination failure.

c. Mechanical Anchors. The 2.5–3 in. long 1/2–in. diameter mechanical expansion anchors were used at the ends of the strips to determine their influence on end-delamination.

d. Number of strips. A beam was tested with three FRP strips to see if an increased level of strengthening could be achieved relative to the Phase I tests which had one or two strips only.

e. One beam was tested under fatigue loading to 2 million cycles to investigate the long-term durability under repeated service load of the MF-FRP system.

f. Since a control beam was not successfully tested to failure in the Phase I tests, an unstrengthened control beam was tested to obtain data for comparison purposes.

Experimental Setup

The experimental setup, shown in Figure 2, placed the simply supported beam into four-point bending through the use of two load points equally spaced from the ends of the beams. This setup was identical to the one used in the nine phase one T-beam tests in 2001 (Bank et al. 2002b). The constant moment span was 60 in., the shear spans equaled 138 in. each, and the total span length was 336 in.
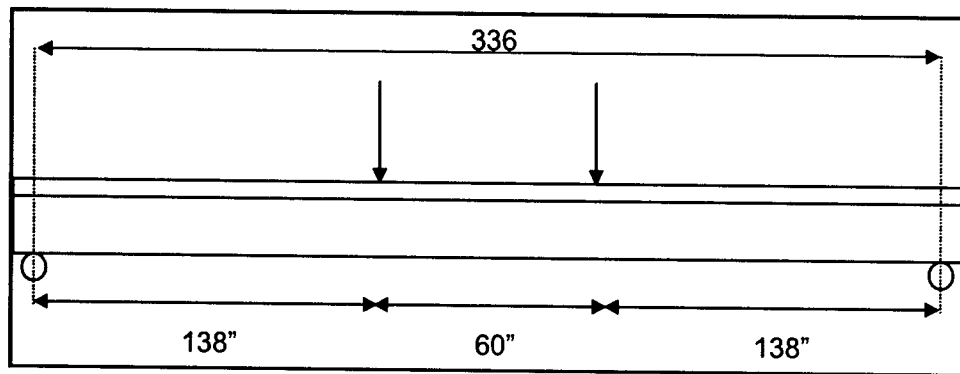
Figure 2. Experimental setup

A MTS Testar system was used to control the two 110 kip actuators (each load point was a separate actuator) at a rate of 0.1 in./min. The data acquisition system consisted of an Optimum Megadac reading and recording the data from the following inputs:

a. *Concrete Strain Gages*: seven 120-ohm gages along the top flange spaced at 8 in. along the length of the beam.

b. *Internal Steel Strain Gages*: three 120-ohm gages placed at the centroid of the tensile steel.

c. *Composite Strip Strain Gages*: varying number of 350 ohm strain gages placed at various locations along the length of the strip.

d. *Freestanding LVDTs*: three LVDTs measuring the deflection of the span at midspan and under each load point, and two LVDTs measuring the deflection of the flange at the midspan.

e. *Load*: both actuators registered separate readings.

f. *Stroke*: measured stroke of each actuator separately.

6

Stroke data was chosen instead of LVDT data in all graphical and theoretical comparisons because the stroke data was more complete and therefore more useful. Not all data was recorded for all beams tested. Beams were cast at ERDC using 5,000-psi strength concrete. For details of beam fabrication see Bank et al. 2002b.

Figure 3 shows an overhead view of the experimental setup. Note the size of the load frame and the positioning of the LVDTs along the bottom of the specimen.
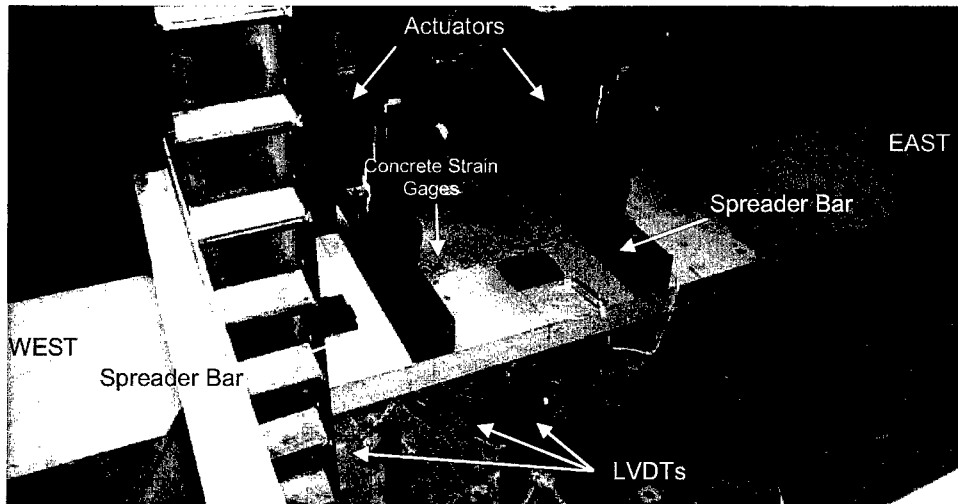
Figure 3. Full-scale T-beam ready for testing

Results of Full-Scale T-Beam Testing

All beams contained 5 No. 9 rebars (A5 beams) and were strengthened with one or more FRP strips (except for the control beam). Strips were stacked on top of one another for beams that were strengthened with more than one FRP strip. Table 1 provides a summary of critical variables in the full-scale beam tests. Termination distance is defined as the distance from the support at the ends of the span to the first row of powder actuated fasteners attaching the FRP strip. End distance is the distance from the support at the ends of the span to the first anchor bolt. Beams that had anchor bolts had two anchor bolts on each end of the strip for a total of four anchor bolts.

Table 1
Strip Attachment Data

Beam	No. of Strips	PAF Type	PAF Spacing (in.)	No. of PAF	No. of PAF in Shear Span	Termination Distance (in.)	End Distance (Anchor Bolts) (in.)
Control							
DS 18	2	AL-52	2	302	120	18	NA
DS 3	2	AL-52	3	222	90	3	NA
SS 18	1	AL-47	3	222	90	18	7
TS 18	3	AL-57	3	222	90	18	7

Notes: SS – single strip; DS – double strip; TS – triple strip
Two SS 18 beams were tested - one static load and one fatigue load.

Tests were typically carried out through 10 in. of midspan displacement. When large cracks opened near one actuator, the actuator began to shed load to the other actuator. Table 2 summarizes the results of the tests. Shown in the table are the values at yield and the values at a deflection of 2.5 in. The value of 2.5 in. equals a deflection ratio of L/135; a value well beyond typical design limits of L/360. In addition to gains in the moment capacity, each beam displayed an increase in the postyield stiffness as described by the slope of the moment vs. stroke diagram.

Table 2
Test Results at Yield and 2.5-in. Deflection

Beam	Actuator	Yield Moment (k-ft)	Average Yield Moment (k-ft)	% Inc. Yield Moment	Moment @ 2.5" (k-ft)	Average Moment @ 2.5 in. (k-ft)	% Inc. @ 2.5"
Control	A	622	600	-	628	604	-
	C	577			579		
DS 18	A	651	665	10.9	661	676	12.0
	C	679			691		
DS 3	A	628	695	15.9	702	758	25.6
	C	762			814		
SS 18	A	648	662	10.4	719	732	21.2
	C	676			745		
TS 18	A	665	679	13.3	714	722	19.6
	C	694			730		

As explained in the following descriptions of each test, the strengthened beams without anchor bolts ultimately failed by the detachment of the FRP strip from either the end of the strip or from the interior of the strip as was seen the Phase I tests. The beams with anchor bolts either failed at extremely large displacements in bearing of the strip around the anchor bolt, or from the powder actuated fasteners failing in the interior of the strip.

The moments and displacements of the strengthened beams are shown in Table 3. The percent increase over the unstrengthened beam was calculated using the difference in strength between the strengthened beam at failure and the strength of the control beam at the displacement of failure of the strengthened beam, as opposed to comparing the capacity to the ultimate strength of the control beam.

Table 3
Test Results at Failure

Beam	Actuator	Ultimate Moment (k-ft)	Average Ultimate Moment (k-ft)	Average Control Ultimate Moment @ Ult. Displ. (k-ft)	% Inc. Ultimate Moment	Deflection Ratio
DS 18	A	729	744	639	16.5	L/96
	C	760				
DS 3	A	906	912	687	32.8	L/71
	C	919				
SS 18	A	867	877	702	24.9	L/65
	C	887				
TS 18	A	790	767	622	23.3	L/100
	C	743				

Description of T-Beam Tests

The goal of the T-Beam tests was to determine the configuration of strip attachment that would result in the best combination of moment capacity, ductility, and failure mode. A discussion of each test and a description of the failure mode for each beam follow. Yield strengths were determined from the moment vs. stroke plots. Since the loads were applied by each actuator moving at a constant displacement rate, the loads were not identical in the two actuators. Therefore, the moment was computed by averaging the moment from each of the two actuators.

Control Beam

The control beam achieved concrete compression failure. The test showed that the beam was very ductile, capable of significant displacements even after the initial compression failure of the concrete. The first flexural cracks in the moment span became visible soon after the start of loading. Then flexural cracks began to open about 3 ft outside of the moment span, then progressed vertically to the bottom rebar where they leaned toward the load points at roughly a 45 degree angle. Well past the tensile rebar had yielded, shear cracks opened in the shear spans in the middle of the web. These shear cracks did not reach the bottom or top of the web. This crack pattern was the same for all beams tested. Concrete compression failure occurred along the interior of the east load point.

The control beam yielded at a moment of 600 ft-k, reached a moment of 604 ft-k at a deflection of 2.5 in., and failed in concrete compression at about 720 ft-k. The beam continued to carry additional load after failing in concrete compression. At a stroke of about 8 in., Actuator A began to shed load to Actuator C. The moment vs. stroke curves for the two actuators for the control beam are shown in Figure 4.
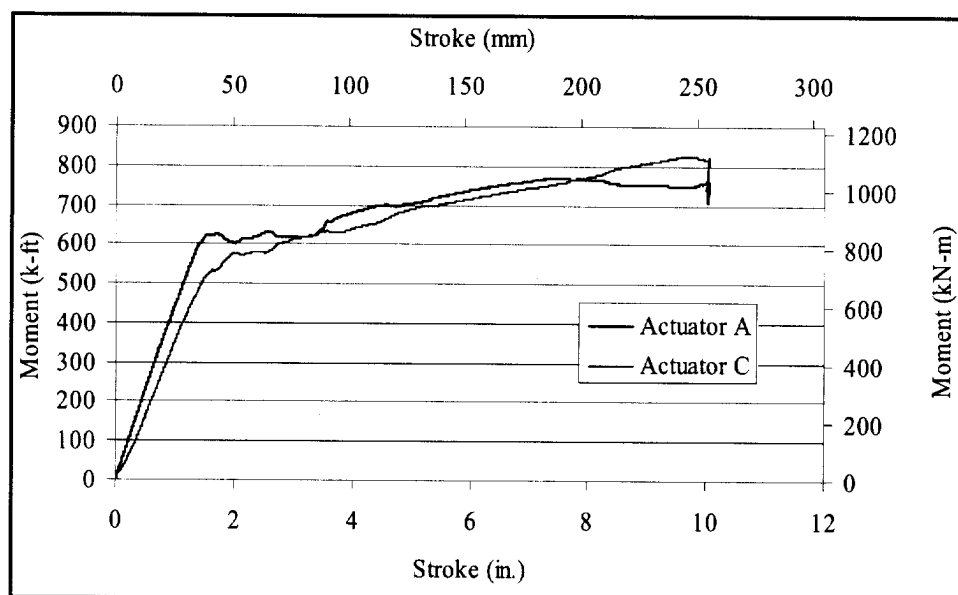
Figure 4. Moment vs. stroke curves for the control beam

Beam DS 18

Beam DS 18 was strengthened with two FRP strips, one on top of the other. The strips were taped together, and then aligned on the soffit of the web with carpenter's clamps. Holes were predrilled in groups of four, then fasteners driven into the four holes from the centerline out toward one support. The process was repeated from the centerline out towards the other support. The termination distance, the distance from the support to the first set of fasteners, was 18 in. The spacing between the fasteners along the length of the strip was 2 in. Spacing between the two rows was also 2 in.

The beam failed by strip detachment, beginning at the east end of the beam. Figure 5 shows the strip detached from the beam, resting on the support block. The fasteners were still partially attached to the beam about 2 ft from the end of the strip, but this partial attachment had very little strength, as the strip was easily removed from the beam with a claw hammer. The partial attachment continued through the moment span, approximately 4 ft into the shear span on the other side of the beam. After an initial load drop following strip detachment, the beams began to reload. The beam ultimately failed resulting from concrete compression failure. The concrete compression failure is shown in Figure 6. This is typical of concrete compression failure for all beams.

Figure 5. Strip detached from the end of Beam DS 18, shown resting on the support block

Figure 6. Concrete compression failure for Beam DS 18

Beam DS 18 yielded at a moment of 665 ft-k, reached a moment of 676 ft-k at a deflection of 2.5 in., delaminated at 744 ft-k, and failed in concrete compression at about 730 ft-k. The beam continued to carry additional load after failing in concrete compression. The moment vs. stroke curves for Beam DS 18 and the control beam are shown in Figure 7. The curves shown for each beam are the average between the two actuators. Beam DS 18 showed an increase in capacity of 10.9 percent at yield, 12.0 percent at a deflection of 2.5 in., and 16.5 percent at strip detachment.
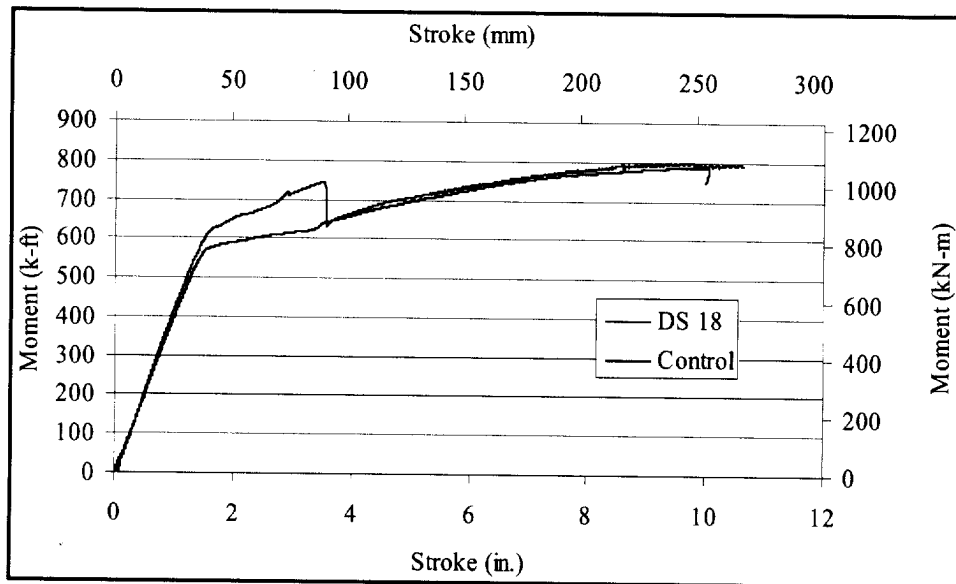
Figure 7. Moment-Stroke curves for Beam DS 18 and control beam

Beam DS 3

Beam DS 3 was strengthened with two FRP strips, one on top of the other. The strips were attached in the same manner as the strips for Beam DS 18. The termination distance was 3 in. The spacing between the fasteners along the length of the strip was 3 in.

The beam failed by strip detachment initiating at the west end of the beam. The delaminated strip is shown in Figure 8. After the strip detached from the beam, the beam continued to reload. The beam then failed resulting from concrete compression failure, and still continued to carry additional load.

Beam DS 3 yielded at a moment of 695 ft-k, reached a moment of 758 ft-k at a deflection of 2.5 in., and a moment of 912 ft-k at delamination failure. The beam continued to carry additional load after failing in concrete compression. The moment vs. stroke curves for Beam DS 3 and the control beam are shown in Figure 9. The curves shown for each beam are the average between the two actuators. Beam DS 3 showed an increase in capacity of 15.9 percent at yield, 25.6 percent at a deflection of 2.5 in., and 32.8 percent at strip detachment.
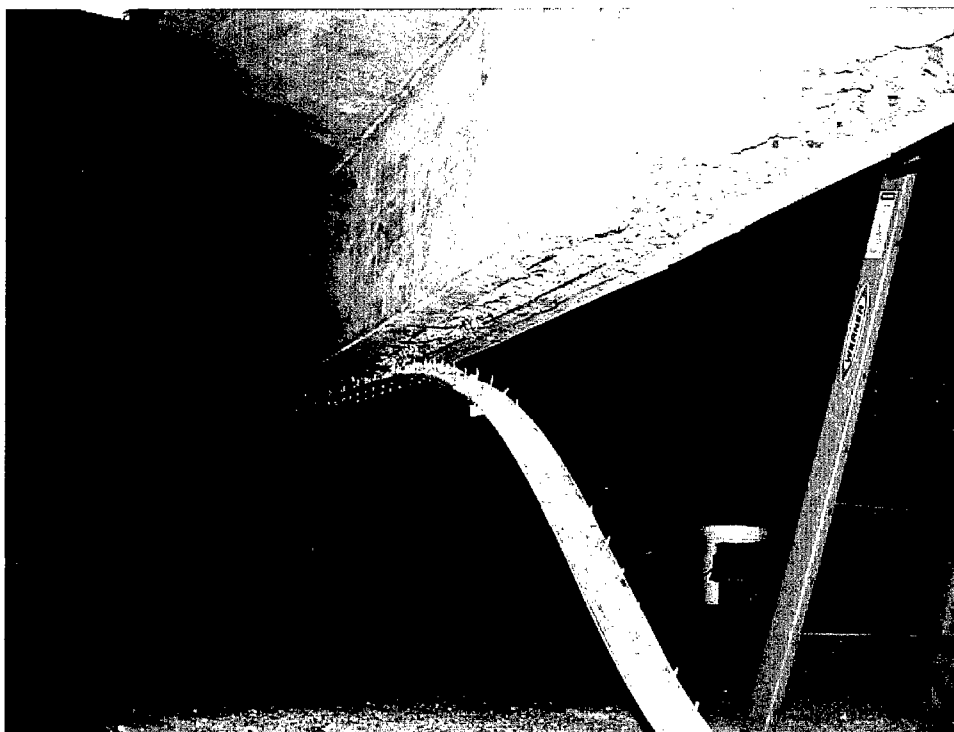
Figure 8. Detached strip from Beam DS 3
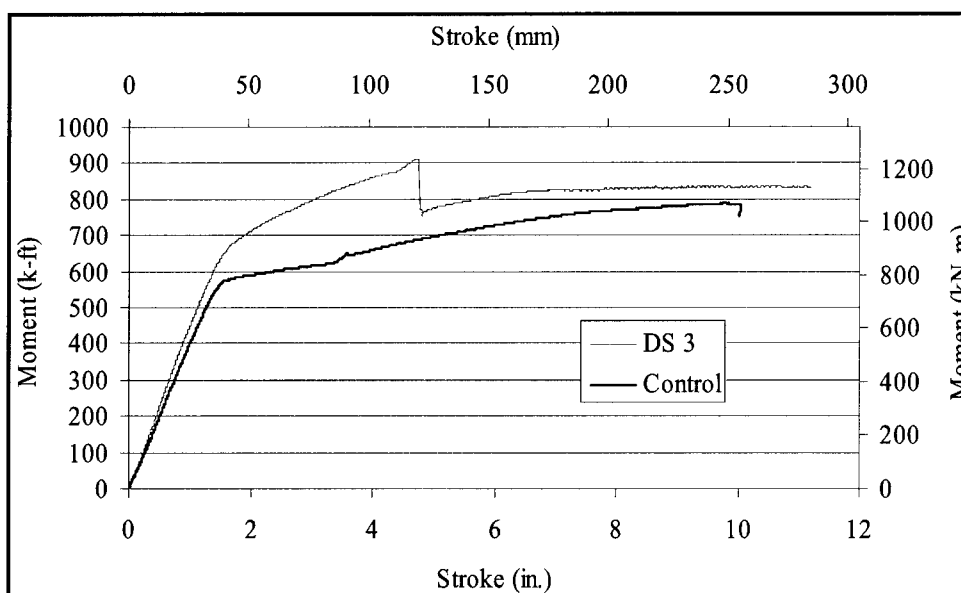
Figure 9. Moment-Stroke curves for Beam DS 3 and control beam

Beam SS 18

Beam SS 18 was strengthened with one FRP strip. The strip was attached in the same manner as the strips for Beam DS 18. The termination distance, the distance from the support to the closest powder actuated fastener was 18 in. The spacing between the powder-actuated fasteners along the length of the strip was 3 in. Two anchor bolts were placed on each end of the strip, and the end distance from the first anchor bolt and the support was 7 in. The anchor bolts used are shown in Figure 10. The anchor bolts were 1/2 in. diameter and 3 in. long. An additional 1-1/2 in. diameter washer was used in conjunction with the provided 1 in. diameter washer. A 1/8-in. red-rubber-packing sheet for washers and gaskets was placed between the 1-1/2 in. washer and the FRP strip to prevent the anchor bolt assembly from damaging the strip. Figure 11 shows the anchor bolts in the end of the strip. The anchor bolts were installed into predrilled holes that were 2 in. deep.
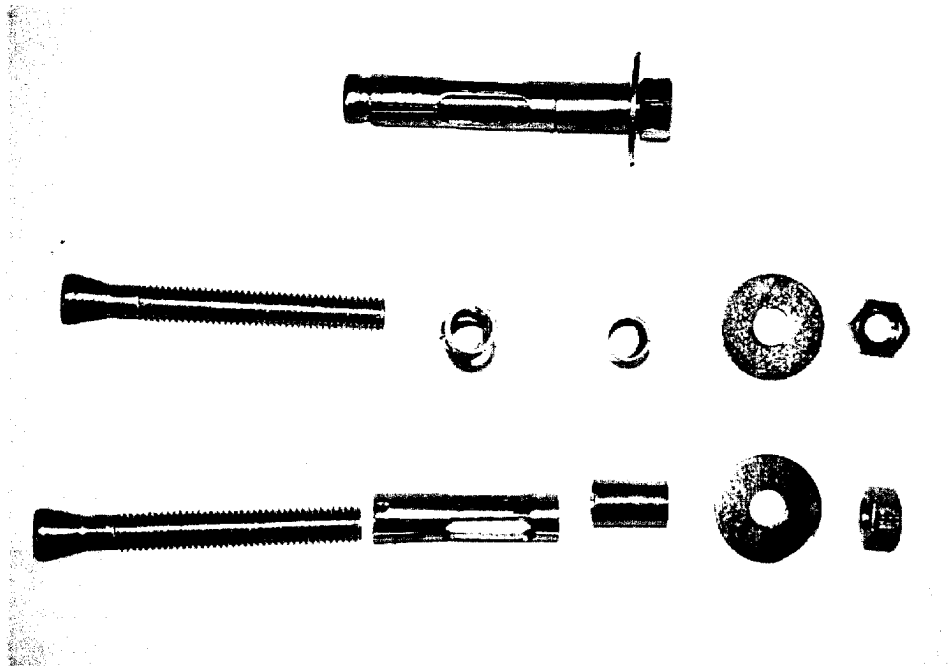
Figure 10. Anchor bolt assembly used for Beam SS 18
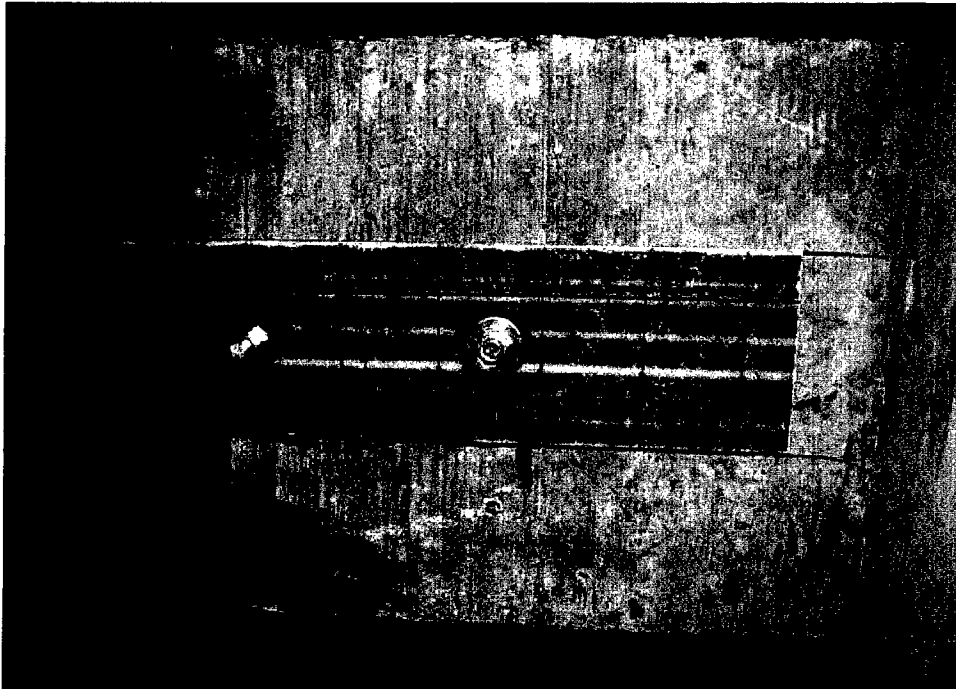
Figure 11. Anchor bolts in the end of the strip in Beam SS 18

The first drop in capacity for Beam SS 18 occurred when the powder actuated fasteners pulled out of the concrete. The strip was still firmly attached to the beam by the two anchor bolts at each end, shown in Figure 12. These anchor bolts remained in place through concrete crushing in the moment span of the beam. When the test was discontinued at the maximum stroke, the strip exhibited an extreme bearing failure, shown in Figure 13.
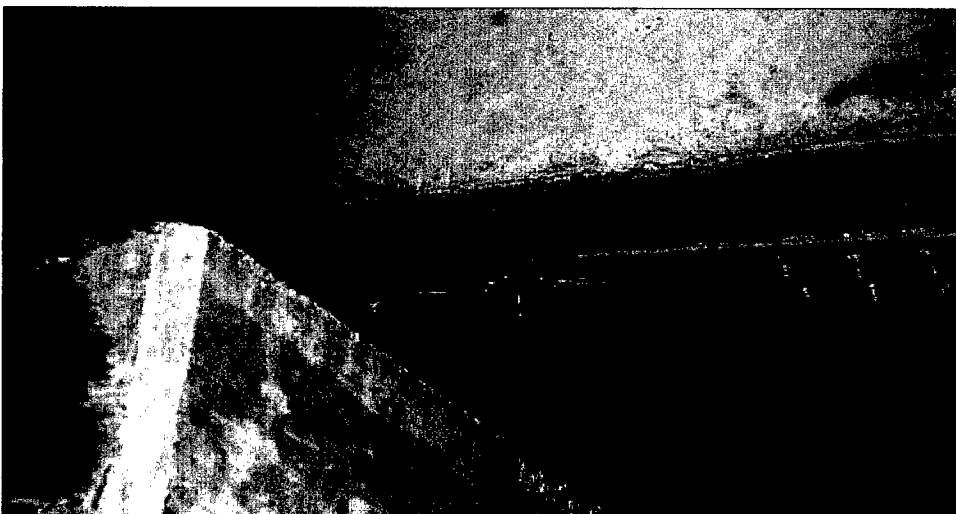
Figure 12. Powder actuated fasteners have failed but the anchor bolts continued to hold

Figure 13. Extreme bearing failure in the strip around the anchor bolts on Beam SS 18

When the test was concluded, the strip was removed from the beam with a pry bar. The anchor bolts remained partially embedded in the concrete, having pulled out of the holes roughly 1/2-in. The concrete around the anchor bolts exhibited no visible signs of distress except for minor crushing on the edges closest to the midspan. One big crater existed extending the entire length of the strip where powder actuated fasteners had been used. This crater was as wide as the strip. The anchor bolts and the end of the crater can be seen in Figure 14.

Figure 14. Anchor bolts and crater left in the concrete after testing of Beam SS 18

Beam SS 18 yielded at a moment of 662 ft-k, reached a moment of 732 ft-k at a deflection of 2.5 in., and a moment of 877 ft-k at delamination failure. The beam continued to carry additional load after failing in concrete compression. The moment vs. stroke curves for Beam SS 18 and the control beam are shown in Figure 15. The curves shown for each beam are the average between the two actuators. Beam SS 18 showed an increase in capacity of 10.4 percent at yield, 21.2 percent at a deflection of 2.5 in., and 24.9 percent at failure.
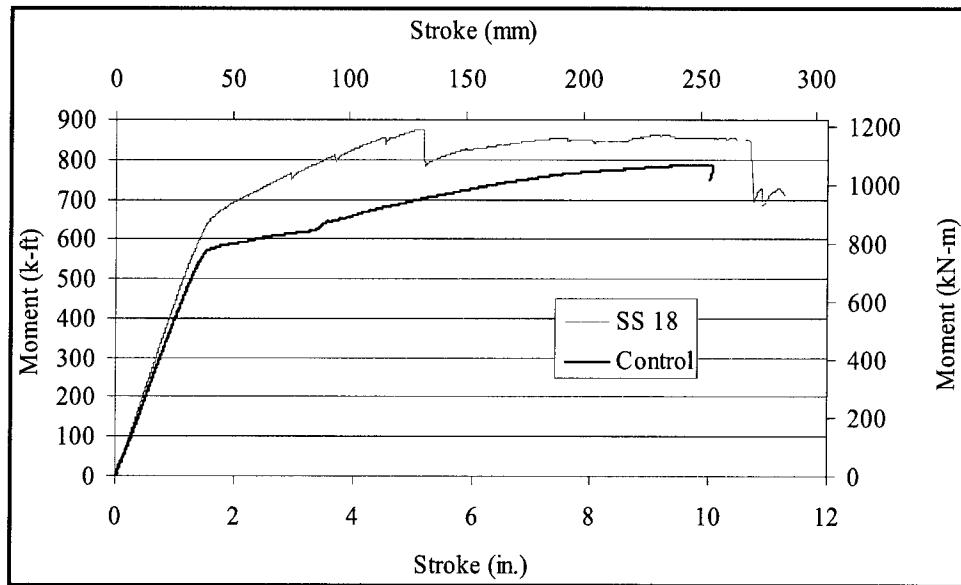
Figure 15. Moment-stroke curves for Beam SS 18 and the control beam

Beam TS 18

Beam TS 18 was strengthened with three FRP, stacked on top of each other. The strips were attached in the same manner as the strips for Beam DS 18. The termination distance, the distance from the support to the closest powder actuated fastener was 18 in. The spacing between the powder-actuated fasteners along the length of the strip was 3 in. Two anchor bolts were placed at each end of the strip, and the end distance from the first anchor bolt and the support was 7 in. The anchor bolts used are shown in Figure 16. The anchor bolts were 1/2-in. diameter and 3 in. long. An additional 1-1/2 in. diameter washer was used in conjunction with the provided 1 in. diameter washer. A 1/8-in. red-rubber-packing sheet for washers and gaskets was placed between the 1-1/2 in. washer and the FRP strip to prevent the anchor bolt assembly from damaging the strip. The anchor bolts were installed into predrilled holes that were 2 in. deep.
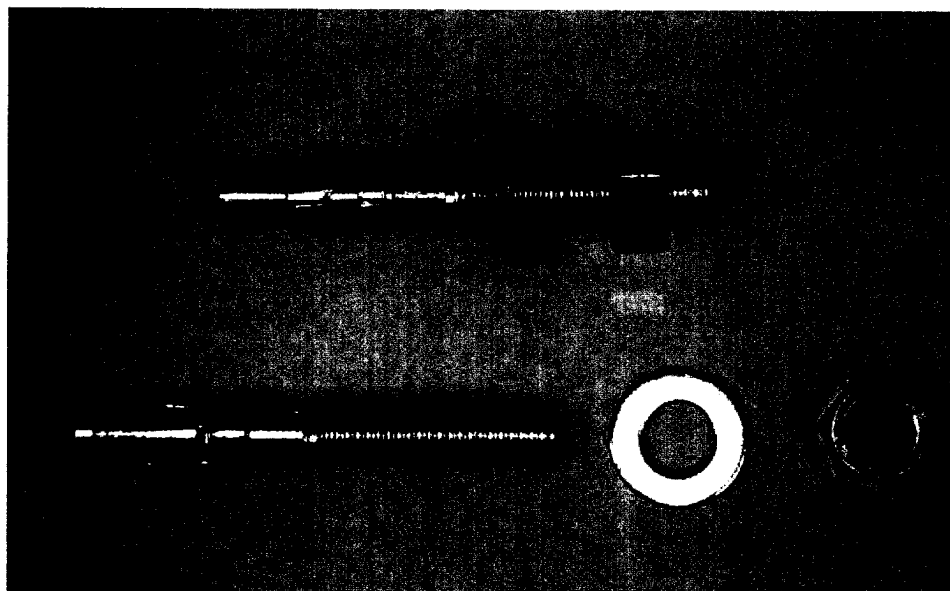
Figure 16. Anchor bolts used for Beam TS 18

Failure occurred for Beam TS 18 when the FRP strips suddenly detached from the beam, starting at one end of the beam. The anchor bolts as well as the powder-actuated fasteners were pulled out of the concrete, as shown in Figure 17. Concrete can be seen on the anchor bolts on the side of the bolts that were bearing against the concrete while under load. The anchor bolts on the end of the strip that was still attached to the beam had pulled partially out of the concrete.
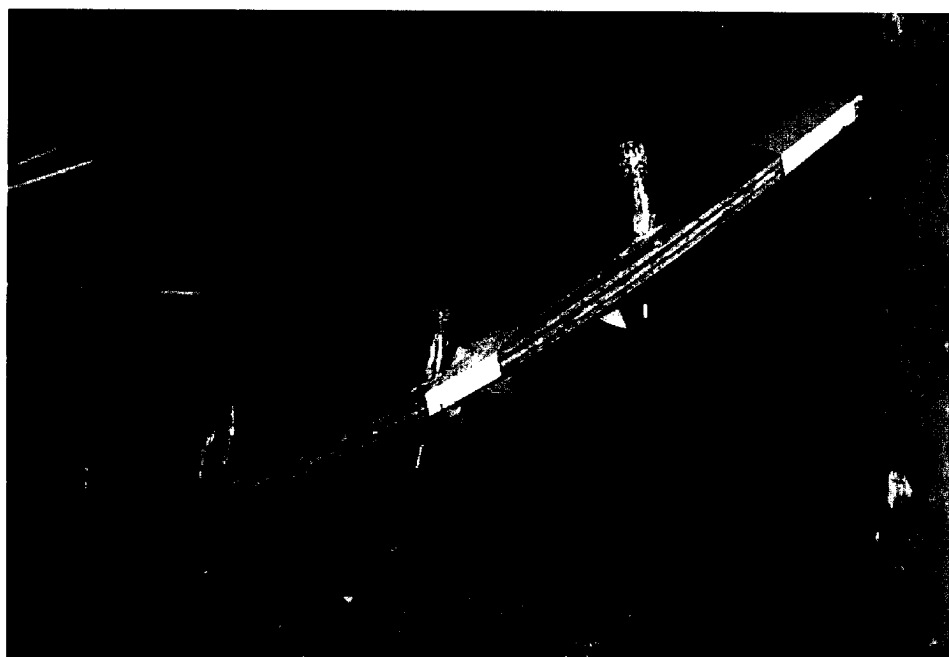
Figure 17. The detached strip with end anchor bolts from Beam TS 18

Beam TS 18 yielded at a moment of 679 ft-k, reached a moment of 722 ft-k at a deflection of 2.5 in., and a moment of 767 ft-k at delamination failure. The beam continued to carry additional load after failing in concrete compression. The moment vs. stroke curves for Beam TS 18 and the control beam are shown in Figure 18. The curves shown for each beam are the average between the two actuators. Beam TS 18 showed an increase in capacity of 13.3 percent at yield, 19.6 percent at a deflection of 2.5 in., and 23.3 percent at failure.
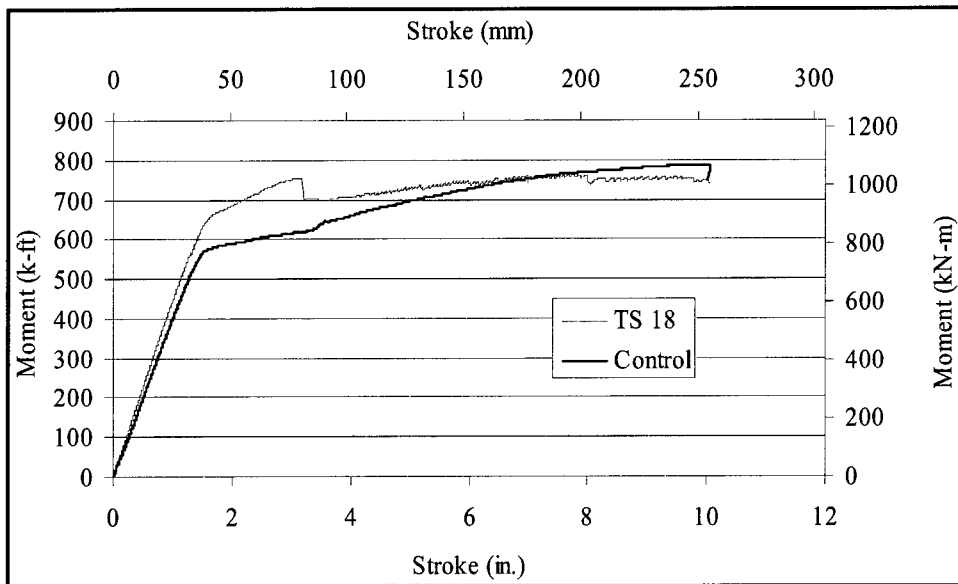
Figure 18. Moment-stroke curves for Beam TS 19 and control beam

Comparison

The moment-stroke plots for all five beams are shown in Figure 19. It can be seen from the plot that Beams TS 18 and DS 18 failed with the least amount of ductility. The deflections for these beams at failure were both around L/100, much more deflection than is anticipated in bridge design. Beam DS 18 failed suddenly by strip detachment because the distance between the support and the first type of anchorage was 18 in. The larger this distance the greater the forces placed on the first anchors. A large termination distance will result in detachment of the strip from the end. Beam TS failed suddenly by strip detachment from the end powder actuated fasteners, followed by the anchor bolts being pulled out of the concrete. The early failure of Beam TS is attributed to the thickness of the strip. The resultant of the force placed on the fasteners by the thicker strip was farther away from the face of the concrete than the force placed on the thinner strips. This larger distance created a greater moment on the fasteners leading to early failure.
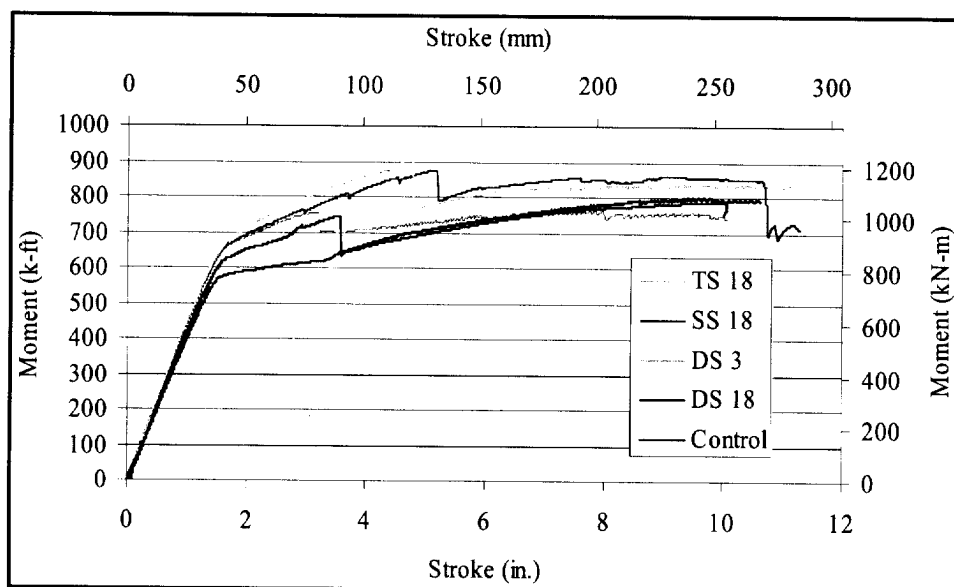
Figure 19. Moment-stroke plots for all five beams

Beam DS 3 had a greater postyield stiffness than Beam DS 18. Beam DS 3 also showed twice as much increase in postyield strength than Beam DS 18. Beam DS 3 was the same as DS 18 except for a termination length of 3 in., as opposed to 18 in. in Beam DS 18. The shorter termination length resulted in a higher strength and greater ductility of the strengthened beam.

Beam SS 18 had a termination length to the powder actuated fasteners of 18 in., and an end distance to the first anchor bolt of 7 in. Beam SS 18 behaved much in the same manner of DS 3, but only half as much strengthening material was used. The two anchor bolts at the end of the strip in Beam SS 18 increased the connection strength of the strip at the ends, the critical locations.

Fatigue Test

One T-beam was tested cyclically to 2 million cycles. The beam was strengthened with a strip attached in a similar manner to Beam SS 18. The beam was cycled at 2 Hz between a load of 10k and 30k on a single actuator at midspan. The cycles were conducted for 8 hr a day. The test was shut down at night so that it would not run unattended.

The load–stroke data for the cycles during which data was collected is plotted in Figure 20. It can be seen from the plot that there was about 0.02 in. of drift. This is a very small amount of drift, with very little change in the overall stiffness of the plot. Around 1-1/2 million cycles, the plots exhibit a slight "wave" characteristic. The source of this "wave" is unknown.
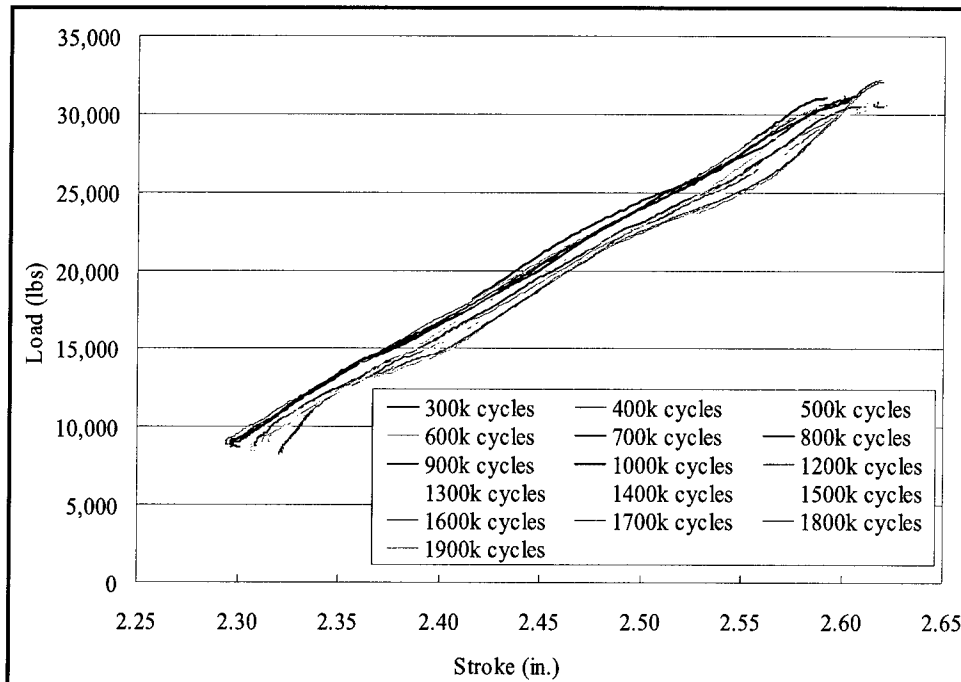
Figure 20. Load-Stroke during cycles for cycles in which data was collected

After the full 2 million cycles were completed the beam was lifted to be positioned under two actuators; so that the ultimate load testing would be conducted in the same configuration as the other T beams. During the move, one of the swivel anchors pulled out, which caused the east end of the beam to fall to the floor. The cause of the swivel anchor failure was found to be resulting from the anchor not being fully threaded into the embedded fixture. One anchor bolt lined up with an open tie-down hole in the floor, but the other anchor bolt on the east end was crushed when the beam impacted the floor. The crushed anchor bolt was the bolt closest to the interior of the strip. The beam was placed on the supports and tested; however, no additional data could be obtained from the failure test resulting from to the damage sustained.

Conclusions and Recommendations from T-Beam Testing

Based on the results of the two phases of full scale T-beam tests conducted in 2001 and 2002 in which a total of 15 full scale beams were tested to failure (11 with MF-FRP strengthening and 4 control beams) the following overall conclusions can be drawn and recommendations made:

a. The shorter the termination length the better the performance of the MF-FRP system. Beams with a 3 in. termination length performed better than those with an 18 in. termination length. The shorter termination length provides for more fasteners, but more importantly terminates the strengthening at a point of smaller moment in the beam. This is a well know fact from epoxy-bonded (EB) FRP systems. The recommendation

used for EB-FRP systems, that the strengthening strip be extended past the point of the cracking moment in the beam, is also recommended for the MF-FRP system.

b. A 3 in. spacing of fasteners along the length of the strip is better than a 2 in. spacing. The 3 in. spacing reduces the likelihood of shear cone failures in the concrete substrate with leads to interior delamination. Although 2 in. spacing was used between rows and the precise effect of row spacing was not studied, the recommendation should also be applied to the row spacing. Hence, a 3 in. minimum gage and pitch spacing (side-by-side and along the length) is recommended. Since the currently produced FRP strip is only 4 in. wide, a single row of fasteners is recommended wherever possible. However, it is also important to note that the number of fasteners required by the design must be consider together with this recommendation. If the required number of fasteners needed for the design cannot be accommodated in the single row with 3 in. spacing, then two rows in a wider strip should be considered.

c. A single FRP strip performs relatively better than multiple FRP strips. Since the strips are not bonded together in the MF-FRP method, the load transfer into the outermost strips decreases resulting from slip and fastener rotation. In addition, the likelihood of end-delamination in double or triple strips is larger resulting from the larger peeling stresses (and bending stresses) in the thicker strip at its end. It is therefore recommended that single strips be used wherever possible.

d. Mechanical expansion anchors (EAs) delay the occurrence of end-delamination failures. The use of two expansion anchors is recommended for all strips. The length of the anchor should be approximately 2–2.5 in. provided the tension steel does not interfere with the embedment. A 1/2 in. diameter anchor has been shown to be suitable for use with the current FRP strip.

e. In T-beams with wide compression flanges, it is unlikely that compression failure in the concrete will occur before strip delamination. Strip delamination from the interior (when anchors are used) will be the most likely failure mode. However, this will occur at sufficiently large deflection ratios for design purposes.

f. Fatigue loading to 2 million cycles under service load levels was shown not to degrade the performance of the MF-FRP system when a single strip with end anchors was tested. Neither the power actuated fasteners, nor the FRP strips showed fatigue related damage. However, a postfatigue failure test could not be not conducted to determine if the fatigue loads affected the ultimate loads.

g. A direct quantitative numerical comparison between the results of the Phase I and Phase II tests was not possible resulting from slight variations in the test-setup, the testing procedure, the concrete properties and the different parameters used. However, the behavior exhibited by

the beams in the two phases was very similar and indicated similar trends. As can be seen in Figures 1 and 19, the load capacity and deformation behavior of the beams tested in the two phases was similar although not directly comparable.

h. For the T-beams tested in this study an increase of 10-15 percent in yield moment and an increase in 25-30 percent in ultimate moment can be achieved using the MF-FRP system.

i. The time taken to strengthen a single beam was approximately 3 hr (including the expansion anchors). Two people are needed to attach the strip. Beams could be tested immediately after the attachment of the strip.

j. The approximate material cost of the system is $11 per ft for a single strip including the cost of the fasteners and anchors ($9 /ft for the strip and $2/ft for the fasteners). All fasteners and tools are commercially available from a number of suppliers. FRP strips used in this research are currently produced by Strongwell (Chatfield, MN) under the trade name of Safstrip™.

4 Optimization of FRP Strips

Overview

A second generation of FRP strips was produced with a variety of proportions of material constituents in order to optimize the strip properties and to understand the reason for earlier low strength strips. Material characterization tests were conducted to determine the properties of the FRP strips obtained from the manufacturer. An optimal strip design was recommended for the MF-FRP system. The guaranteed minimum properties for design with the recommended strip were calculated using American Concrete Institute (ACI) recommended procedures.

Objectives

FRP strips were produced with different fiber architectures, layouts, and material properties to optimize the FRP strip for attachment with mechanical fasteners. The objectives of this study were:

a. To investigate the properties of the new strips with different fiber architectures and material properties.

b. To report on the tensile properties of the FRP strips produced.

c. To report the net section strength of the FRP strips with a predrilled hole.

d. To report and compare the mechanical properties of the FRP strips with those provided by the manufacturer.

e. To report results of bearing tests on the FRP strips.

f. To analyze the results of the mechanical tests and to recommend an optimal FRP strip design for the MF-FRP method.

g. To calculate the guaranteed mechanical properties of the strip according to ACI procedures.

Second Generation FRP Strips

FRP strip used in prior years research were referred to as "Hybrid 1.5" to signify their construction consisting of a combination of glass rovings and carbon tows and 1.5 oz/ft^2 continuous strand mats (Bank et al. 2002a). The prior year FRP strip ("Hybrid 1.5") had two layers of 4.25 in. wide 1.5 oz/ft^2 continuous strand mat, twenty-one 113 yield E-glass rovings, and 138 Grafil 12 k standard modulus carbon tows. In addition to the standard version of the strip, a version with a gray pigment was also produced. The addition of the pigment caused a dramatic drop in the tensile strength of the strip. The properties of the "Hybrid 1.5" and the "Hybrid 1.5–gray" are show in Table 4 and 5.

Table 4
Properties of FRP Strip "Hybrid 1.5" in 2001 Tests (Bank et al. 2002b).

Type Strength	No. of Tests	Average Strength (ksi))	Standard Deviation (ksi)	Coeff of Variation (COV) (%)	Modulus of Elasticity (ksi)	Standard Deviation (ksi)	Coeff of Variation (COV) (%)
Ultimate ASTM D3039	10	107.80	12.70	11.80	8,200	700	8.70
Open-Hole ASTM D5766	10	95.00	6.20	6.50	8,200	600	7.80

Table 5
Properties of FRP Strip "Hybrid 1.5–Gray" in 2001 Tests (Bank et al. 2002b)

Type Strength	No. of Tests	Average Strength (ksi)	Standard Deviation (ksi)	Coeff of Variation (COV) (%)	Modulus of Elasticity (ksi)	Standard Deviation (ksi)	Coeff of Variation (COV) (%)
Ultimate ASTM D3039	9	71.66	7.80	10.88	8,200	750	9.15
Open-Hole ASTM D5766	9	52.00	4.50	8.65	8,200	625	7.62

Seven different fiber architectures and resin system were produced for the second generation. The quantity and placement of continuous stand mats was varied and the number of glass rovings and carbon tows was varied in order to arrive at the FRP strip having optimal longitudinal and bearing properties. The 4 × 1/8-in. size of the FRP strip was maintained for the second-generation strips. Table 6 shows the fiber architecture for the second generation of FRP strips.

While the use of mats in the FRP strips was expected to increase the bearing strength of the FRP strip, it was expected to reduce the tensile strength. Higher yield 48 k Grafil carbon tows were substituted for the lower yield 12 k tows used in the previous "Hybrid 1.5" strips to reduce cost.
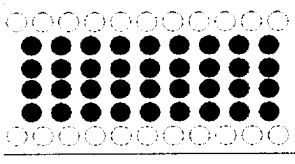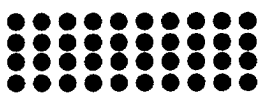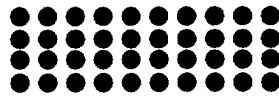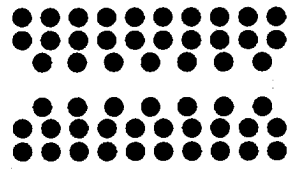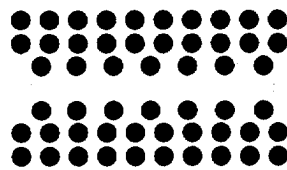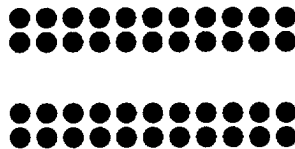
Table 6
Fiber Architectures for Second Generation FRP Strips

Trial	Fiber/Mat constituents	Diagram
Trial 1	1-4.25 in. wide 1.5 oz Mat 11-113 Yield Rovings 34-48 k Tows 11-113 Yield Rovings 1-4.25 in. wide 1.5 oz Mat	
Trial 2	1-4.25 in. wide 1.5 oz Mat 8-113 Yield Rovings 40-48 k Tows 8-113 Yield Rovings 1-4.25 in. wide 1.5 oz Mat	
Trial 3[†]	1-4.25 in. wide 1.5 oz Mat 8-113 Yield Rovings 40-48 k Tows 8-113 Yield Rovings 1-4.25 in. wide 1.5 oz Mat	
Trial 4	1-4.25 in. wide 1.0 oz Mat 8-113 Yield Rovings 20-48 k Tows 1-4.25 in. wide 1.0 oz Mat 20-48 k Tows 8-113 Yield Rovings 1-4.25 in. wide 1.0 oz Mat	
Trial 5	1-4.25 in. wide 1.0 oz Mat 28-48 k Tows 1-4.25 in. wide 1.0 oz Mat 28-48 k Tows 1-4.25 in. wide 1.0 oz Mat	
Trial 6	1-4.25 in. wide 1.0 oz Mat 23-48 k Tows 1-4.25 in. wide 1.0 oz Mat 1-4.25 in. wide 1.0 oz Mat 23-48 k Tows 1-4.25 in. wide 1.0 oz Mat	
Trial 7	Same as Trial # 2 + addition of Gray Pigment	

[†] Different Veil used (same architecture as Trial No.2)
Note: All FRP strips included a top and bottom veil

Table 7 gives the longitudinal tensile strength and elastic modulus provided by the manufacturer, which were conducted in accordance with ASTM D 638. A minimum of seven tests were conducted for each trial. ASTM D 638 uses a 2 in. nominal gage length cut in the shape of a "dog-bone" with a nominal width of 0.5 in. at the middle.

Table 7
Tensile Properties of Second Generation FRP Strips (ASTM D 638)

Trial Number	Tensile Strength			Modulus of Elasticity		
	Mean, (ksi)	SD, (ksi)	COV, (%)	Mean, (ksi)	SD, (ksi)	COV, (%)
1	103.6	10.7	10.3	8,277	880	10.6
2	112.0	9.1	8.1	9,069	1,222	13.5
3	111.9	14.1	12.6	8,516	895	10.5
4	108.4	7.7	7.1	8,908	874	9.8
5	120.2	12.3	10.2	10,715	1,048	9.8
6	104.8	14.2	13.5	8,914	515	5.8
7	77.3	7.6	9.8	8,781	1,200	13.7

The material properties for the constituent materials are provided in Table 8.

Table 8
Properties of the Constituents Used in FRP Strips

Component	Modulus (ksi)	Area or Thickness	Ultimate Strength (ksi)
113 Yield E Glass Roving	10,500	$2.68 \times 10^{-3} \text{ in}^2$	500
48 k Grafil Standard Modulus Tow	34,000	$2.756 \times 10^{-3} \text{ in}^2$	600
Vinylester Resin	490	NA	11.8
[†] Obtained from manufacturers data.			

Trial 1 was the same construction as Hybrid 1.5 except that the 48 k tows were substituted on a proportional basis for the 12 k tows used previously. Since the strength obtained using the 48 k tows was somewhat lower than the Hybrid 1.5, the number of 48 k tows was increased (and the number of rovings decreased). This increased the strength and stiffness in Trial 2. Trial 3 and 7 were conducted to attempt to improve the appearance of the FRP strip with either a veil or a pigment. The veil did not cause much visual improvement and the pigment once again significantly reduced the strength properties (although it did improve the appearance (Bank et al. 2002b)). Trial 7 in the second-generation tests was also produced to determine the reason for the low strength in the prior year strips when the gray pigment was used. As can be seen from Table 7, the pigment once again significantly reduced the strength of the strips. An explanation for this is still not known and further studies are needed to determine the cause of the low strength when the pigment is used. Based on this result the use of a pigment in the resin system is not recommended until this problem is understood and rectified. Trials 4, 5, and 6 were conducted to investigate ways of improving the bearing strength by increasing the number of mats in the strip.

The trial strips were also tested at the University of Wisconsin-Madison for open-hole strength and bearing strength. In addition, the tensile strength and stiffness were obtained using the American Society for Testing Materials (ASTM) D3039 test with a 1 in. wide flat-sided coupon to see if this would yield different values from the manufacturer tests conducted according to ASTM D638 with a 1/2 in. wide dog-bone coupon. Detailed results can be found in Gulbrandsen (2002). A summary of the key results is presented here.

Tensile Tests

Longitudinal tests according to ASTM D3039 were conducted on the strips to determine their longitudinal elastic modulus and longitudinal tensile strength. This specification is used as one standard for FRP materials. Two different sets of tensile tests were conducted on uniform FRP composite specimens to determine the ultimate strength and modulus of elasticity. The first set consisted of the six different trials. The dimensions of all thirty specimens were 14 in. × 1 in. × 0.125 in. with a 10 in. effective gage length (2 in. on both ends of the strips were enclosed by the machine grips).

The second set was composed of specimens with a hole drilled directly in the center of each specimen to evaluate the properties based on the net section of the FRP strips in accordance with ASTM D5766. A 0.188 in. diameter hole was drilled to represent the net section present in the FRP strips when a 0.177 in. diameter X-ALH fastener is attached. The hole was located 7 in. from either end of the specimen.

The result of the D3039 tests is shown in Table 9 while the results of the D5766 tests are shown in Table 10. Table 11 shows a comparison between the tensile properties reported by the manufacturer and measured using ASTM D638 and those measured at the University of Wisconsin (UW) using ASTM D3039. Tensile strength results for Trial 7 reported by the manufacturer were so poor that coupons from this trial were not included in the University of Wisconsin-Madison testing.

Typical failure modes of the tensile specimens are shown in Figure 21 and Figure 22. Typical load-displacement plots for the specimens are shown in Figure 23 and 24.

Table 9
Tensile Properties of Second Generation FRP Strips (ASTM D3039)

Trial Number	Tensile Strength			Modulus of Elasticity		
	Mean (ksi)	SD (ksi)	COV (%)	Mean (ksi)	SD (ksi)	COV (%)
1	109.8	4.8	4.4	8,037	516	6.4
2	122.4	11.2	9.2	8,893	765	8.6
3	123.9	13.2	10.7	9,320	679	7.3
4	114.2	5.3	4.6	8,549	209	2.4
5	138.1	8.3	6.0	10,439	685	6.6
6	131.1	2.7	2.0	9,307	516	5.5

Table 10
Open-hole Strength Properties of Second Generation FRP Strips (ASTM D5766)

Trial Number	Open-Hole Tensile Strength			Open-Hole Strength/Ultimate Strength
	Mean, (ksi)	SD, (ksi)	COV, (%)	%
1	82.7	6.8	8.2	75.3
2	92.8	7.1	7.6	75.8
3	95.5	8.4	8.8	77.1
4	96.0	3.7	3.9	84.1
5	104.4	9.4	9.1	75.6
6	97.2	3.2	3.3	74.1

Table 11
Comparison between D638 and D3039 Tensile Properties

Trial Number	Tensile Strength (ksi)			Modulus of Elasticity (ksi)		
	D638	D3039	%Diff	D638	D3039	%Diff
1	103.6	109.8	-6.0	8,277	8,037	+2.9
2	112.0	122.4	-9.3	9,069	8,893	+1.9
3	111.9	123.9	-10.7	8,516	9,320	-9.4
4	108.4	114.2	-5.4	8,908	8,549	+4.0
5	120.2	138.1	-14.9	10,715	10,439	+2.6
6	104.8	131.1	-25.6	8,914	9,307	-4.4

Figure 21. Typical failure mode for tension test specimens
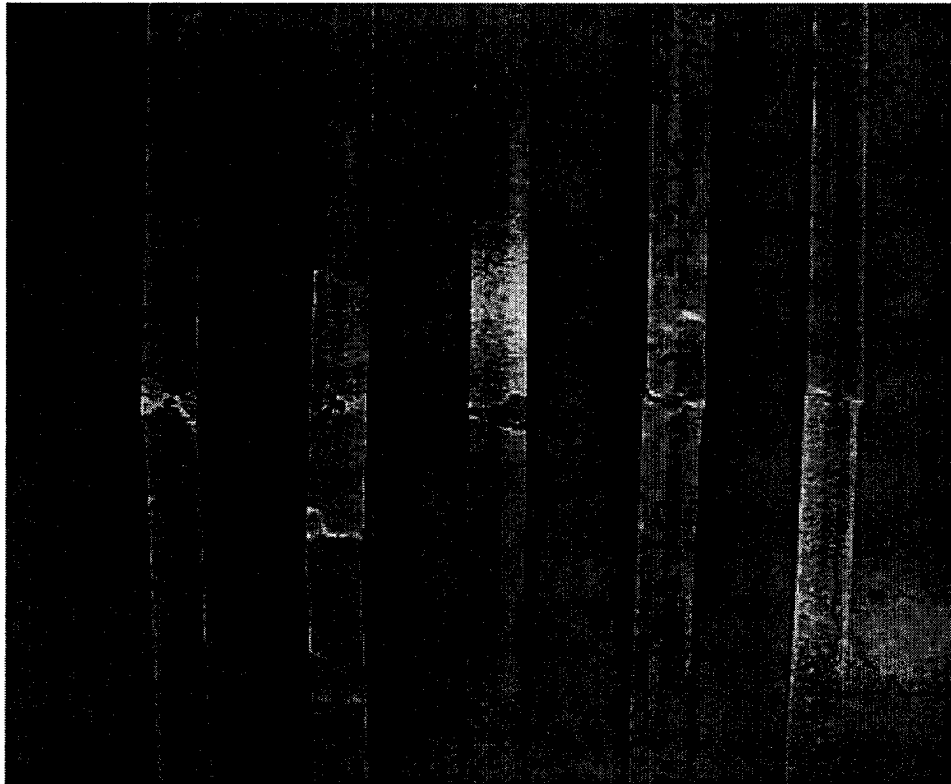
Figure 22. Typical failure mode for open hole tension test specimens
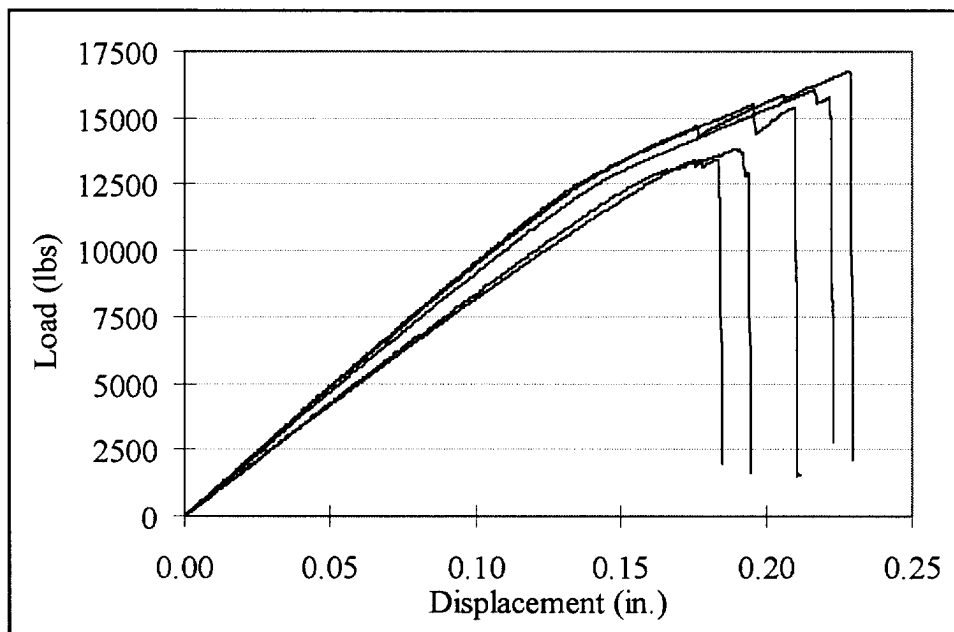
Figure 23. Load vs. Displacement plot for typical tension test (Trial No. 2)
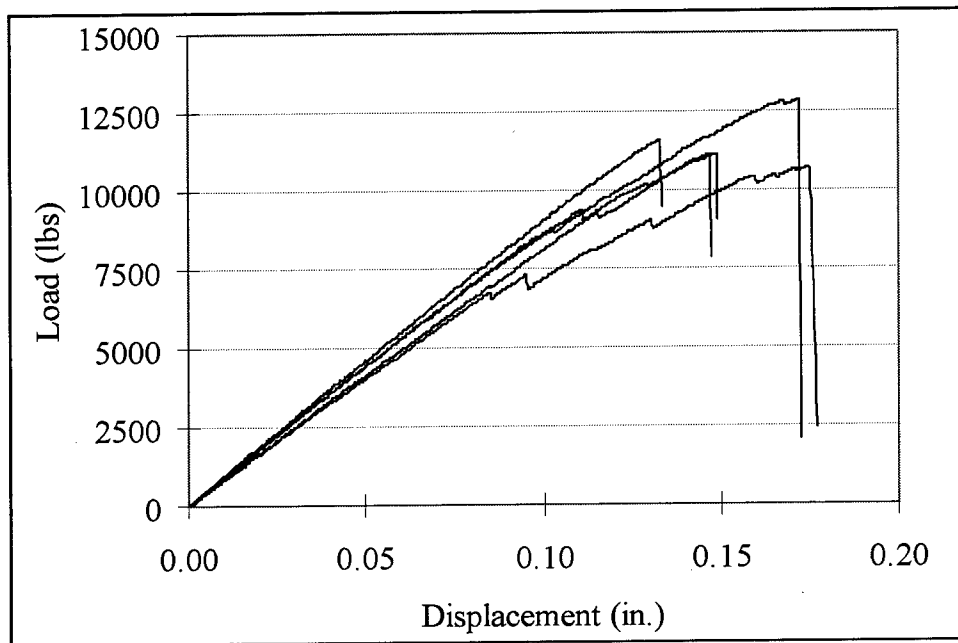
Figure 24. Load vs. Displacement plot of typical open-hole tension test (Trial No. 2)

Comparing the results of the tensile testing between D3039 and D638 a general trend can be noticed. Using D3039 the strength values appear to be somewhat higher and the modulus values appear to be somewhat lower than those obtained from D638. The coefficients of variation in the D3039 tests were generally lower than those from the D638 tests.

Bearing Strength Tests

Bearing tests were conducted on uniform FRP composite specimens to determine the bearing strength of the FRP trial strips. Figure 25 shows the bearing test setup in an MTS 100-kip testing machine. Ten specimens from each of the six designed trials were tested, each measuring 7 in. × 1 in. × 0.125 in. A 0.188 in. diameter hole was drilled 2 in. from the top of the specimen directly into the center of the width.
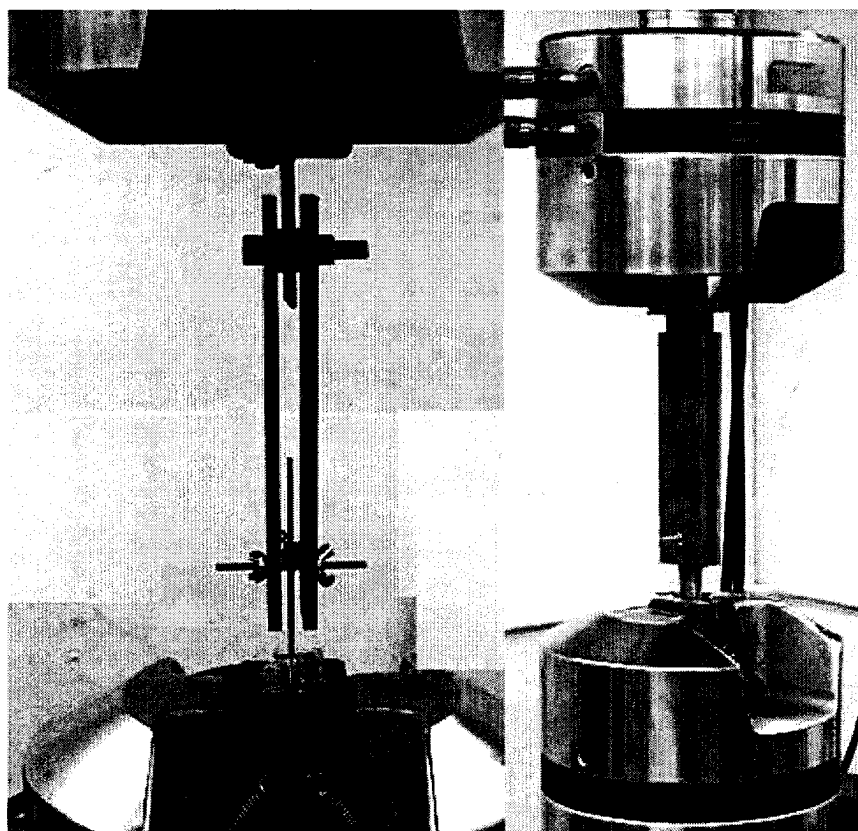
Figure 25. Setup for bearing strength tests

An MTS TestStar IIs was used to control the deformation of each sample at 0.10 in./min and to collect the data. The maximum load, the average load over 0.05 in. to 0.20 in. deformation, and the 4 percent deformation load were calculated for every specimen.

The definition of bearing strength varies in different standard test methods. ASTM D953 defines the bearing strength at the bearing stress at which the bearing hole is deformed 4 percent of its diameter. Four percent of the hole diameter corresponds to 0.0075 in. However, ASTM D5961 defines the bearing strength as the value of bearing stress occurring at a significant event on the bearing stress/strain curve. Accordingly, both bearing strength values were calculated and reported. In addition, the average bearing strength value for each specimen was calculated over the interval from 0.05 in. to 0.20 in. on the load vs. displacement chart. This number represents the load at which each specimen appeared to maintain a constant bearing stress as the hole elongated in a "slotting" or "shear-out" failure mode.

The results of the bearing tests are shown in Table 12. In addition to the maximum and the 4 percent bearing capacities a "sustained bearing capacity" when the specimen reached a stable progressive slotting failure (between 0.05 and 0.20 in. of displacement) was determined. The sustained bearing capacity for the different trials is given in Table 13. Figure 26 shows the typical bearing failure in the specimens and Figure 27 shows the typical load displacement plot

for the bearing tests. It was clear that all specimens tested for the bearing tests produced a desirable bearing failure in accordance to the definition of a bearing failure by ASTM D5961. The failure modes were as desired and no lateral, shearout, tearout, or cleavage (block shear) failures were observed (Gulbrandsen 2002). Most of the specimens reached their maximum load capacity at approximately 0.035 in. displacement.

Table 12
Bearing Test Results of Second Generation FRP Strips

Trial Number	Maximum Bearing Capacity (ASTM D5961)			4% Deformation Bearing Capacity (ASTM D953)		
	Mean, (lb)	SD, (lb)	COV, (%)	Mean, (lb)	SD, (lb)	COV, (%)
1	944	81	8.5	184	42	22.7
2	897	94	10.5	248	44	17.6
3	835	39	4.7	169	78	46.1
4	777	58	7.5	239	62	25.9
5	730	39	5.3	263	45	17.19
6	853	45	5.3	221	52	23.5

Table 13
Sustained Bearing Results of Second Generation FRP Strips

Trial Number	Sustained Bearing Capacity		
	Mean, (lb)	SD, (lb)	COV, (%)
1	811	93	11.5
2	798	34	4.3
3	704	50	7.1
4	614	21	3.5
5	599	31	5.2
6	683	54	8.0

Figure 26. Typical bearing failure mode observed
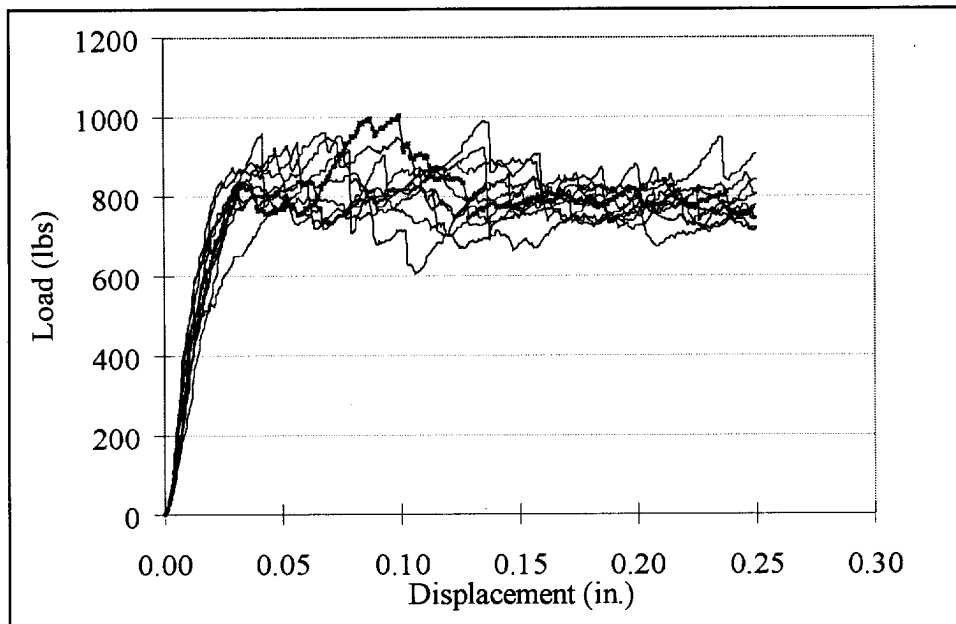
Figure 27. Load vs. Displacement of typical bearing failure of Trial No. 2 strip

Analysis of Test Results

An analysis of the tensile, open hole, and bearing test results indicates the following:

a. The inclusion of additional mats in Trials 4, 5, and 6 did not increase the bearing strength of the strips. On the contrary, resulting from fact that glass rovings were removed and carbon tows were added to these strips the bearing strength actually decreased. The use of a small number of glass rovings appears to have much more of a beneficial effect on the bearing strength than does the use of additional mats.

b. The tensile strength and stiffness of Trials 4, 5, and 6 did show an increase resulting from the increased number of carbon tows; however, this comes at a price of deceased bearing strength. Since the FRP strip for the MF-FRP system must be able to sustain a bearing stress through large displacement, an increase in tensile properties without an increase in sustained bearing does not add value.

c. The open-hole tensile strength is the maximum effective tensile strength of the FRP strip in the MF-FRP method, since the strip will fail in net-tension at this load before it can reach its ultimate strength. The open-hole strength also appears to benefit from the inclusion of a small number of glass rovings. In general the open-hole strength of all Trials was about 75 percent of the ultimate strength of the material.

Based on the analysis of the results of the tests Trial 2 was considered to have the optimal combination of tensile, open-hole and sustained bearing strength properties and was chosen as the "standard" for the FRP strip architecture for the MF-FRP method. This strip was used in the Phase II T-beams tests conducted in 2002 at ERDC and for the strengthening of the Edgerton Bridge in Wisconsin.

Determination of Guaranteed Properties of the FRP Strip

Ultimate Tensile Strength

The results obtained on the mechanical properties of the FRP strip Trial 2 were analyzed to evaluate the Ultimate Tensile Strength as defined by the statistical value based on 20 replicate specimens in accordance with ASTM D3039 (ACI 440. 2R 2002). Since similar strength results were seen in the ASTM D3039 and ASTM D638, values from ASTM D638 provided by the manufacturer were taken because a larger sample was available for this data. In total, 49 samples of Trial 2 strips were tested by the manufacturer. The mean tensile strength minus three times the standard deviation (σ) is required to be reported as the "guaranteed" ultimate strength and "guaranteed" ultimate strain of FRP materials used for strengthening.

$$f_{fu} = \overline{f_{fu}} - 3\sigma \qquad \qquad \text{(ACI 440 2R. 2002)}$$

$$\varepsilon_{fu} = \overline{\varepsilon_{fu}} - 3\sigma \qquad \qquad \text{(ACI 440 2R. 2002)}$$

This value will provide a 99.87 percent probability that the values are exceeded in any given sample. The modulus is calculated as the modulus between in 0.003 and 0.006 strain values in accordance with ASTM D3039. Guaranteed ultimate values are shown in Table 14.

| Table 14 | | | |
| Guaranteed Tensile Properties for Trial No. 2 FRP Strip | | | |
Test	Ultimate Tensile Strength, (ksi)	Modulus of Elasticity, (ksi)	Ultimate Tensile strain, (in./in.)
Tension (D638)	84.7	9,069	0.0093
Open-hole (D5766)	71.6	--	--

As noted earlier the open-hole strength is used in design as the FRP strip strength. The "guaranteed" ultimate failure strain of the strip is then calculated using the open-hole strength as the "guaranteed" tensile strength of the strip and the modulus of the strip. The final specified guaranteed ultimate properties of the MF-FRP strip are

$$f_o = 71.6 \; ksi$$

$$E_{frp} = 9,069 \; ksi$$

$$\varepsilon_o = 0.0079$$

Bearing Strength

The sustained bearing capacity is used to calculate the "sustained bearing strength" of the FRP strip for use in the MF-FRP design process. The bearing strength of the FRP strip may therefore be calculated as

$$f_b = \frac{P_{max}}{d \times t_{frp}}$$

where

P_{max}:   Sustained bearing capacity (798 lb)
d: Diameter of Hole (0.188 in.)
t_{frp}:   Thickness of FRP strip (0.125 in.)

The calculated Bearing strength for the FRP strip is therefore:

$$f_b = 33.95 \; ksi \sim 34 \; ksi$$

Fastener Force for Bearing Failure

The characteristic bearing strength value for the FRP strip may be used to calculate the sustained force transferred per fastener that will cause bearing of the FRP strip from

$$P_{fu,b} = f_b \times d_f \times t_{frp}$$

where

$P_{fu,b}$:   Load per Fastener to cause bearing
d_f: Diameter of fastener
t_{frp}:   Thickness of FRP strip (0.125 in.)

Table 15 shows the load per fastener for different types of mechanical fasteners.

Table 15 Sustained Load Per Fastener Corresponding to Bearing of the FRP Strip			
Fastener Type	Bearing Strength, ksi	Diameter (d_f), in.	Average Sustained Load, lb
X-ALH 47		0.177	752
X-CR-44	34	0.158	672
Anchor Bolt KBII		0.5	2,125

From the above table, the ratio of force per anchor bolt to fastener can be calculated as a ratio of diameters. Based on the above calculation an anchor bolt provides approximately 2.5–3.0 times the fastener force at bearing failure.

Tensile Force in the Strip at Bearing Failure

The maximum load per fastener calculated above may be related to the stress in 4 in. wide FRP strip using equilibrium. Figure 28 shows the load at the fastener corresponding to a bearing failure of the FRP strip.
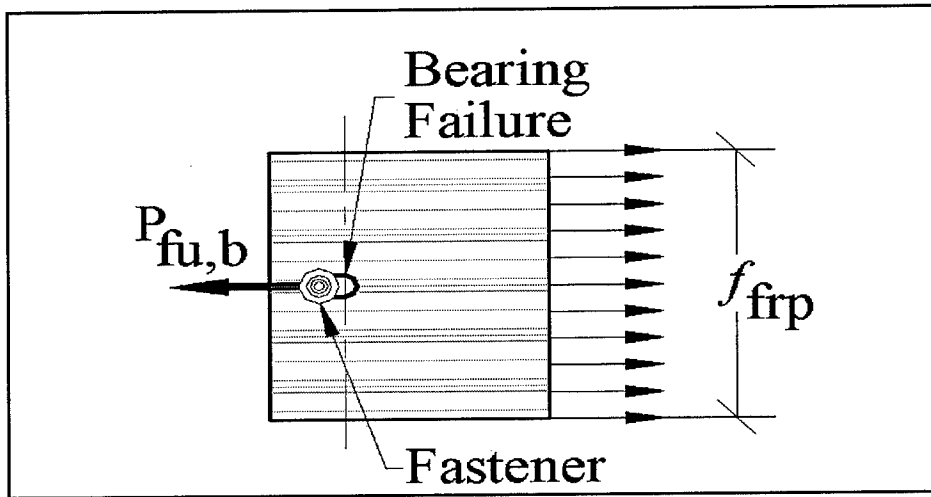
Figure 28. Force transfer at bearing failure of FRP strip

For force equilibrium in the x-direction

$$\sum F_x = 0;$$

$$f_{frp} = \frac{P_{fu,b}}{A_{frp}}$$

where

A_{frp} = Area of FRP strip and $P_{fu,b}$ as before.

The idealized load versus deformation plot for the FRP strip at bearing failure is shown in Figure 29. This shows bearing (yielding) behavior of the mechanically fastened FRP strip.
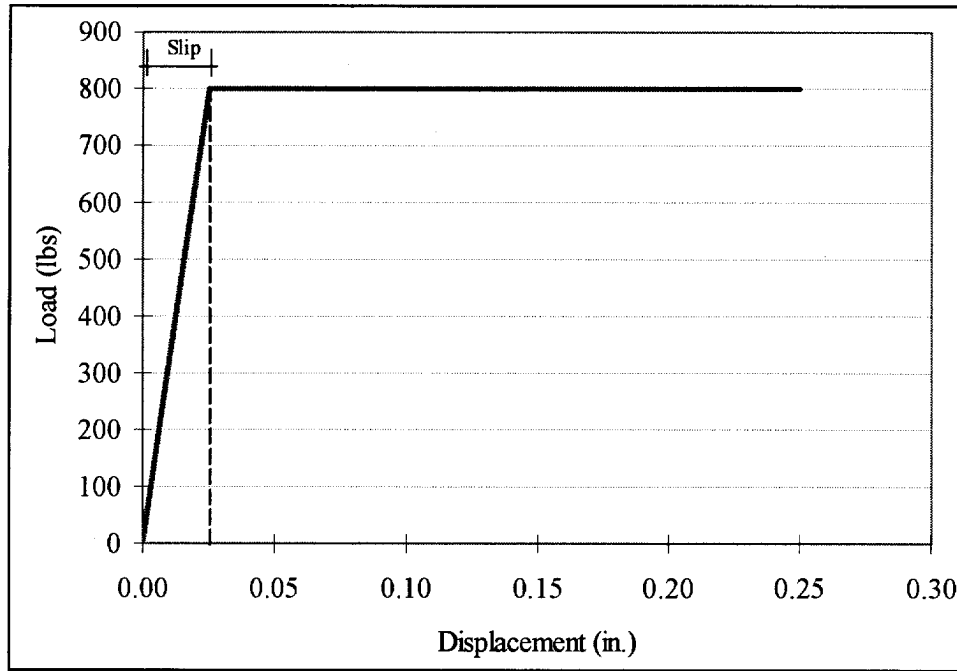
Figure 29. Idealized load versus displacement behavior of the FRP strip

The slip seen in the above graph is relatively small and does not affect the maximum load per fastener. For strength calculations it can be ignored. This results in a pseudo elasto-plastic behavior of the FRP strip at the sustained capacity of the fastener.

The strain in the FRP strip at the sustained bearing stress for an X-ALH fastener can therefore be calculated from

$$\varepsilon_{frp,b} = \frac{f_{frp}}{E_{frp}}$$

$$\varepsilon_{frp,b} = 0.00017$$

This strain corresponds to the strain in the FRP strip with a single fastener. The maximum strain in an FRP strip with multiple fasteners (n) along its length, assuming all fasteners attain the sustained bearing capacity, is

$$\varepsilon_{frp,b}^{max} = \frac{nP_{fu,b}}{A_{frp}E_{frp}}$$

For example, for the case in which 40 X-ALH fasteners are used, the maximum strain corresponding to the sustained bearing failure of the FRP strip at all fastener locations is

$$\varepsilon_{frp,b}^{max} = 0.0066$$

Note that this strain is close to the strain corresponding to net tension failure of the FRP strip, previously determined to be $\varepsilon_0 = 0.0079$. Therefore, if too many fasteners are used, then FRP net tension failure may occur prior to bearing failure at all locations of the fasteners.

Conclusions of FRP Strip Study

Based on the results of a parametric study conducted to determine an optimal configuration for the FRP strip for use in the MF-FRP system the following are concluded:

a. The optimal design for the FRP strip for the MF-FRP system that provides a high value of sustained bearing strength and a high value of tensile strength and stiffness is the one produced as Trial 2. This strip consists of two surface veils, two 4.25 in. wide 1.5 oz/ft^2 E-glass continuous strand mats, sixteen 113 Yield E-glass rovings, and forty 48 k carbon tows, in a vinylester resin matrix with no pigment.

b. A sustained bearing strength has been determined for the FRP strip for use in the MF-FRP system. At the load corresponding to this strength the FRP strip will undergo a continuous and progressive slotting failure similar in nature to a perfectly plastic load carrying response.

c. The open-hole tensile strength of the FRP strip is approximately 75 percent of its ultimate tensile strength.

d. Guaranteed properties of the FRP strip have been determined for use in design in accordance with ACI practice. The guaranteed tensile strength is based on the open-hole tensile strength of the strip. The guaranteed design properties for the FRP strip for use in the MF-FRP system are

Ultimate tensile strength: f_o = 71.6 ksi

Sustained bearing strength: f_b = 34.0 ksi

Modulus of Elasticity: E_{frp} = 9,069 ksi

Ultimate failure strain: ε_o = 0.0079

5 Full-Scale Implementation of the MF-FRP System

Introduction

As part of the proposed research to investigate the constructability and performance of the MF-FRP system on existing deteriorated bridge structures, a capacity deficient reinforced concrete flat slab bridge built in 1930 was strengthened and tested to failure. The full-scale application of the proposed system on an existing bridge in the State of Wisconsin was conducted to demonstrate the performance of the MF-FRP system. A procedure was developed in collaboration with the Wisconsin Department of Transportation (WisDOT) to identify a bridge that represented a large percentage of "Structurally Deficient" (SD) bridges in the Wisconsin Highway Bridge Inventory. A schedule for the rapid strengthening of the existing bridge was developed to demonstrate the installation procedure with the aid of the county maintenance personnel. In addition, an analysis and design of the existing bridge for retrofit was conducted to improve its load carrying capacity. This portion of the research study was conducted in collaboration with the WisDOT through the Wisconsin Highway Research Program (WHRP).

Objectives of the Application of MF-FRP System on an Existing Bridge

The objectives of this part of the research were intended to demonstrate the effectiveness of the MF-FRP system to strengthen an existing bridge and are highlighted below:

a. To identify a below HS20-44 rated deteriorated reinforced concrete slab bridge in the Wisconsin Highway Bridge Inventory.

b. To determine the existing Load Rating (LR) and Sufficiency Rating (SR) of the candidate bridge according to American Association of State Highway and Transportation Officials (AASHTO) and Federal Highway Administration (FHWA) standard procedures.

c. To design a strengthening system for the bridge using the MF-FRP strips to increase the Inventory Load Rating of the bridge to HS25 and to account for moving loads in the design procedure.

d. To develop a schedule, materials, personnel, and methods plan for strengthening the bridge.

e. To strengthen the bridge and to conduct service load testing.

f. To conduct a preliminary investigation of the durability of the in situ strengthening system.

g. To conduct ultimate load testing to determine the actual strengthening level achieved with the MF-FRP system.

Bridge Identification

To identify a candidate bridge, the research team proposed the following general method to WisDOT to select an under capacity bridge with potential for rehabilitation:

a. A bridge earmarked for replacement between 2002 and 2004.

b. A reinforced concrete flat slab bridge with a 20-30 ft long span with simple supports.

c. A vintage bridge constructed between 1930 and 1940 with available existing plans (if possible).

d. A bridge rated for loads lower than HS20-44.

Three bridges were identified from the Wisconsin bridge inventory. The descriptions and characteristics of the three bridges are provided in the next sections.

Bridge 1

Candidate Bridge 1 was a 20 ft long slab bridge designated B-13-518 located northwest of the city of Dane. The bridge was located on STH 113 over Spring Creek. Figure 30 and Figure 31 show the characteristics of the bridge.
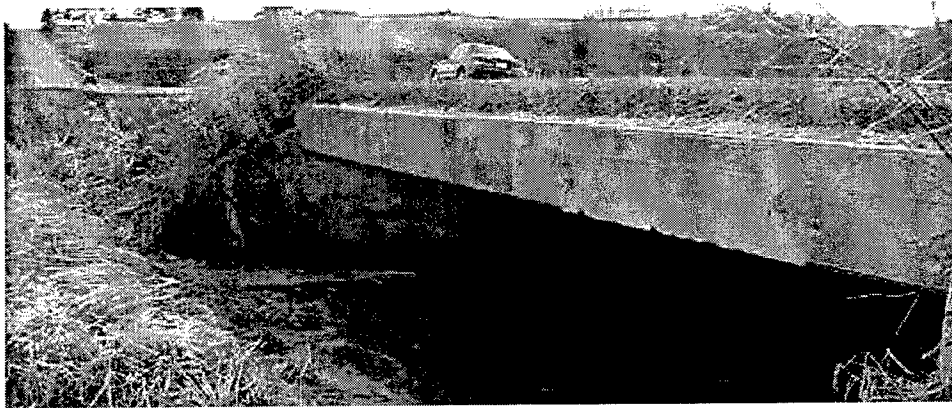
Figure 30. Bridge B-13-518, one of the selected bridges
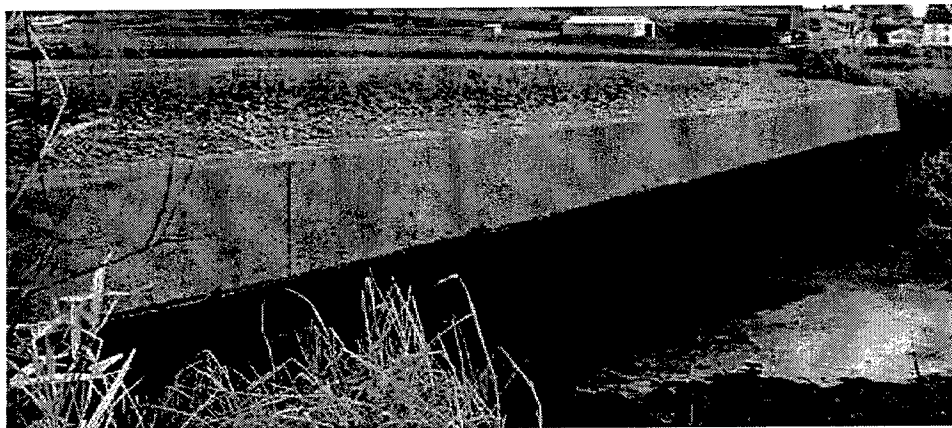
Figure 31. Flat slab of bridge B-13-518

The width of the bridge was measured to be 38.1 ft. As can be seen in the figures, no traffic barriers or guardrails were installed on the bridge. The "Sufficiency Rating" of the bridge was 41, which qualified it for replacement and it was scheduled for reconstruction as part of a roadway project in 2003. The head clearance of the bridge was measured between 2-3 ft and the depth of the slab was 20 in. No extreme deterioration or section loss was observed in the slab; however, the bridge was posted for its under-capacity. While the bridge was a suitable candidate for the project, other bridges were considered for easier access to the bridge soffit.

Bridge 2

Candidate Bridge 2 was a 23 ft long slab bridge designated P-53-71 located on Marsh Road over a branch of Bass Creek in the Town of Magnolia, Rock County. The bridge was due for replacement in the 2002-2003 cycle. The letter "P" designates that bridge plans for the structure were not available. The bridge was built in 1930 and was 26.9 ft wide. In 1950 the bridge was widened utilizing four steel girders. Resulting from the complexity of the structural system the bridge was not investigated further.

Bridge 3

Candidate Bridge 3 was a 23 ft long flat slab bridge designated P-53-702 located on Stoughton Road over Saunders Creek in the City of Edgerton, Rock County. The bridge was originally constructed in 1930 for an H15 truck loading and was 25.9 ft wide. Figure 32 and Figure 33 show the details of the bridge.
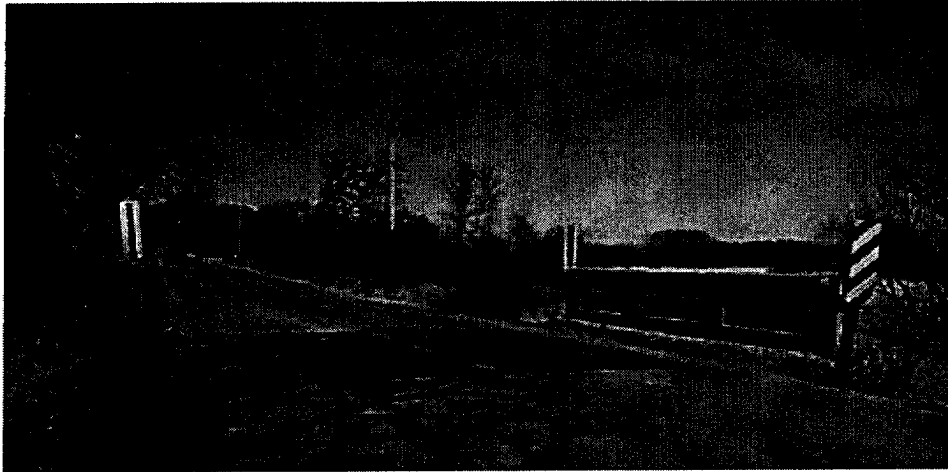
Figure 32. Bridge P-53-702 view of roadway
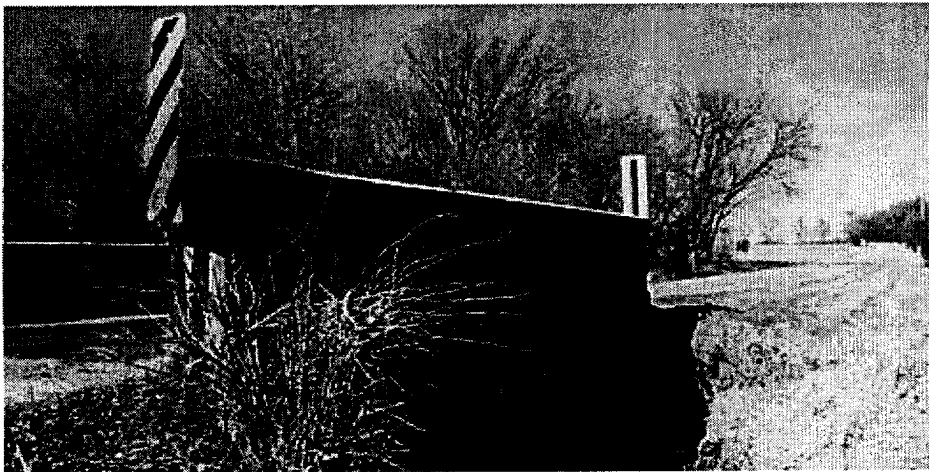
Figure 33. Bridge P-53-702 over Saunders Creek in City of Edgerton

Upon preliminary assessment, the underside of the bridge looked in reasonable (but deteriorated) condition with a clearance of 4 to 5 ft. A large number of stalactites were seen on the underside of the slab and one of the edges showed some section loss. Figure 34 shows the underside of the bridge.

Figure 34. Large amount of stalactites and efflorescence seen on the bottom surface of the slab of P-53-702

Efflorescence was seen on the edge of the bridge slab, which was around 24-28 in. thick. The creek that ran under the bridge was shallow, but had a decent flow to it. The concrete guardrail that appeared to be constructed monolithically with the slab showed some spalling on the edges. The bridge was scheduled for replacement in the summer of 2003 and was considered ideal for the research study even though plans did not exist. The bridge was considered representative of structurally deficient bridges in the age group and of the type needed for the research study. Based on the criteria developed candidate Bridge 3, P-53-702, was selected for the strengthening study.

Preliminary Investigations of Bridge P-53-702

Following the selection of the bridge, a detailed investigation was required to determine the properties of the constituent materials. The bridge was owned by the City of Edgerton and was maintained by the county's maintenance department. Since the owner of the bridge was other than the Wisconsin Department of Transportation, an owner approval was required prior to any investigations on the bridge could be conducted. The City officials raised concerns regarding the project, including responsibilities of additional costs and liability to the city. The main items of concern of the City of Edgerton were the following:

a. *Liability*: The insurance and liability for the personnel and equipment to be used in conducting the research on the bridge, including the research team from the UW.

b. *Financial Responsibilities*: Additional costs incurred during the research project for traffic control and detour.

c. *Logistics*: The loading techniques and traffic control during the testing of the bridge.

d. *Environmental Considerations*: Coordination with the Department of Natural Resources (DNR) on the impact on the surrounding flora and fauna needed to be considered. A purple parsnip plant, a particularly rare species, and the trout in the creek were items of concern.

e. *Schedule*: The time frame for the installation and load testing of the bridge needed to avoid the activities scheduled in the park next to the bridge. In addition, the strengthening work had to be conducted in the DNR "construction window" from June to August to prevent damage to the creek and the adjacent watershed.

On August 5, 2002, a motion to conduct research on the bridge was brought before the Common Council of the City of Edgerton. The UW research team presented details of the project to the City Common Council. An agreement was reached between the City of Edgerton and WisDOT relieving the City of any liability and financial responsibilities related to the research. The City Council was impressed by the intended purpose of the research as it has difficulty finding funds for replacement of deteriorating bridges. After the concerns of the city were addressed by the UW and the WisDOT, the Common Council gave unanimous approval for the research study to be conducted on the bridge.

Investigations were conducted on the 70-year old bridge selected for the project. The Bridge Inspection Report and the Load Rating Sheets of the bridge were obtained from the WisDOT maintenance department. Key information on the bridge was reviewed. Appendix A provides the Bridge Inspection Report and Load Rating Sheet for P-53-702. The main properties of the bridge as per the inspection report are listed in Table 16.

Table 16 Key Properties of Bridge P-53-702						
Span (ft)	Width (ft)	Inventory Rating	Operating Rating	Sufficiency Rating	Rate Score	Comments
23	25.9	HS 17.6	HS 29.3	32.7	64	Deep deterioration of the concrete slab. Recommended for replacement or other (action)

The Average Daily Traffic (ADT) for the bridge in 1980 was recorded at 600. The last inspection conducted on the bridge in January of 2001 recommended a re-rating of the bridge for its capacity. Other comments noted on the inspection report were "deep deterioration of the deck edges and cracks" and "spalls about the abutments at the corners." Over the years a 3-5 in. bituminous overlay was placed on the bridge; however, no record of when this was done was found. Figure 35 and Figure 36 show more details of the selected bridge.
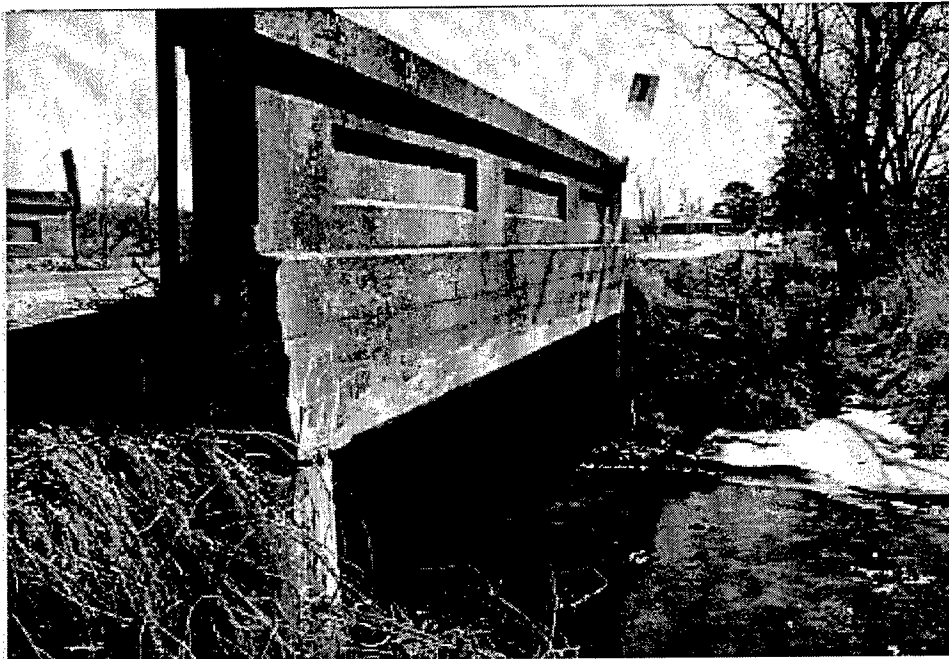
Figure 35. Bridge P-53-702 with a span of 23 ft over Saunders Creek
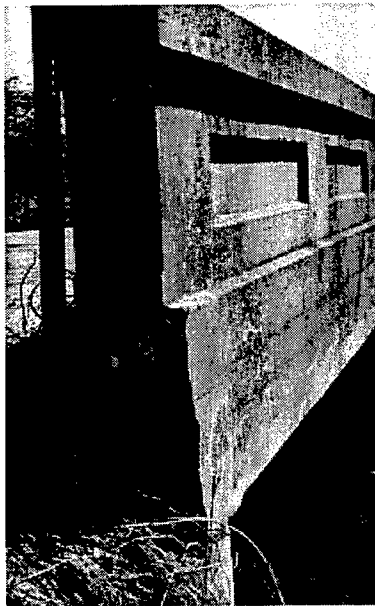
a. Profile of the monolithic guardrail   b. Deterioration and section loss

Figure 36. Bridge rails details

Table 17 provides the measured properties of the bridge elements.

Table 17
Measured Properties of Bridge P-53-702

Total Length	Span	Clear Span	Width	Abutment Width	h (Mid-span) est.	h (Edge)	d (Mid-span) est.	d (Edge)
(ft)	(ft)	(ft)	(ft)	(in.)	(in.)	(in.)	(in.)	(in.)
24	22.75	21.33	26	16	20	28	18	26

The details of the bridge deck reinforcement and material properties were unknown resulting from the unavailability of the bridge plans. A historical search for plans of similar bridges built during the same time period was undertaken. Relevant literature was reviewed along with information obtained from the Department of Transportation on the load rating of the bridge. These were used to estimate the existing properties of the bridge. To determine the steel reinforcement in the selected bridge, a bridge plan for a 23 ft bridge built in 1940 was studied. In addition, properties for a 20 ft bridge built in 1956 as detailed in the revision of "Standard Plans for Highway Bridge Structures" by U.S. Department of Commerce, Bureau of Public Roads (USDC 1956) was also studied. A design for a new flat slab bridge in accordance with the latest AASHTO LRFD specifications (AASHTO 1998) was also conducted. Table 18 lists the comparison of reinforcement details obtained from the historical research and analysis of the existing bridge.

Table 18
Comparison of Reinforcement Properties for Bridges to Determine the Reinforcement of the Selected Bridge

Type	Span	Width	Depth	Bar Size	Spacing	Area per ft	Yield Strength	Shear Reinforcement
	(ft)	(ft)	(in.)	(No.)	(in.)	(in.^{2})	(ksi)	
1930*(In Situ)	23	25.9	18.5	1 in. sq. bar	6	2.0	33**	Bent long. bars 4 ft from each support
1940 Standard Plan	23	28.0	18	7	4	1.8	33**	Bent long. bars 4 ft from each support
1956 Standard Plan	20	24	10.5	8	8.5	1.6	33**	Bent long. bars 4-5 ft from each support
1998 LRFD Bridge Design	23	26	24	7	4.5	1.6	60	NA***

* Selected bridge P-53-702 from Inspection Report
** Expected considering the time period.
*** Not required if designed in accordance with AASHTO LRFD 4.6.2.3 (1998)

Based on the above, the existing steel reinforcement for the selected bridge was assumed to be 1 in. square bars at 6 in. o.c., which provided an area of 2 in.^{2} per ft of the bridge deck. These assumptions were correlated with visual field inspection. The location of a number of visible corroded square rebars was noted and this confirmed the assumed reinforcement details. The location of a bent longitudinal bar near the support for shear resistance was seen on the edge of the bridge section that was deteriorated.

The strength properties of the concrete and the reinforcing steel were determined based on the recommendations provided by AASHTO in the *Manual For Condition Evaluation of Existing Bridges* (AASHTO 2000.) Ultimate strength of concrete is based on the year of original construction of the bridge and shown in Table 19.

Table 19
Ultimate Strength of Concrete (AASHTO 2000)

Year Built	f'_c (psi)
Prior to 1959	2,500
After 1959	3,000

While it was intended to extract cores from the bridge deck to experimentally determine the concrete strength, this was not possible and it was decided to evaluate the existing capacity using concrete properties of the bridge as defined in the standard procedure by AASHTO (AASHTO 2000). Table 20 lists the allowable unit stresses in tension for reinforcing steel as specified by AASHTO (2000).

Table 20
Yield Strength of Steel in Tension (AASHTO 2000)

Type	Yield Strength (psi)
Structural or unknown grade prior to 1954	33,000
Grade 40 billet, intermediate, or unknown grade (after 1954)	40,000
Grade 50 rail or hard	50,000
Grade 60	60,000

In addition to longitudinal tension reinforcement, field inspections showed evidence of relatively small reinforcing steel bars in the transverse direction of the bridge. It was also believed that some reinforcement near the top surface of the concrete deck was present. Figure 37 and Figure 38 show assumed sections of the bridge.
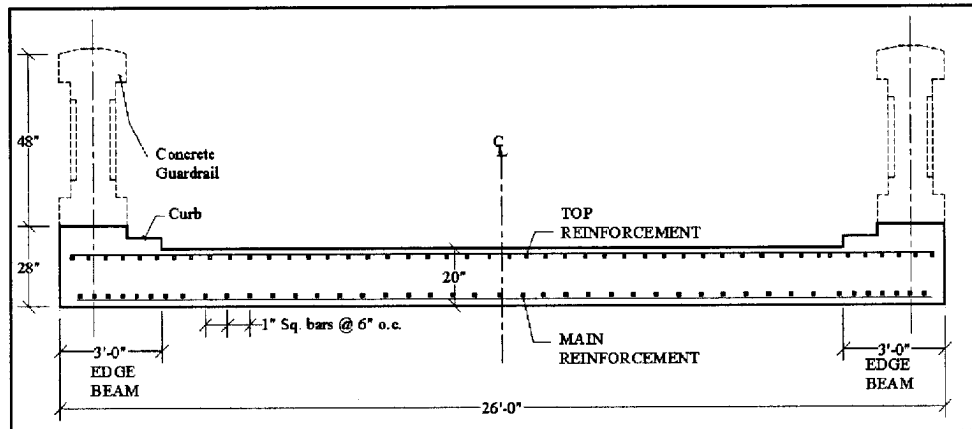
Figure 37. Transverse bridge section with main reinforcement running parallel to traffic
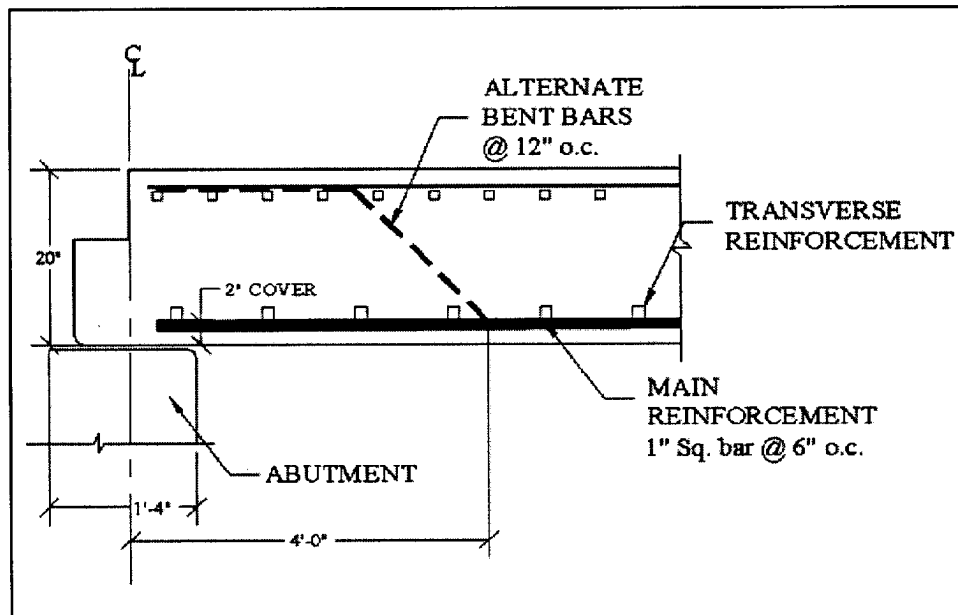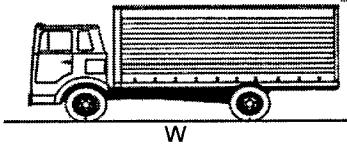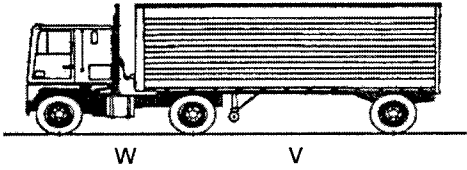
Figure 38. Bridge section at abutment with alternating bent bars for shear

Investigation of Design Loads on Bridges

A highway bridge must be designed for the vehicular live loads as they move across the span. The loads produced by standard trucks specified by AASHTO are used to analyze bridge structures for vehicular live loads. Since the 1930s, AASHTO has specified the standard truck weights and configurations for bridge design. Since then, truck loadings have evolved to better represent the increased weight of trucks. Table 21 shows the configurations of standard trucks specified by AASHTO (1996).

Table 21
Standard Truck Configurations and Weights as Specified by AASHTO (AASHTO 1996)

Type	Front Axle (k)	Rear Axle1 (k)	Rear Axle 2 (k)	Weight (Tons)	Description
H15-44	6	24	-	15	
H20-44	8	32	-	20	
HS15-44	6	24	24	27	
HS20-44	8	32	32	36	
HS25-*44	10	40	40	45	

Note: W = 14 ft, V = varies between 14 ft and 30 ft.
* Denotes anticipated in future codes.

While the H class loadings were used in the early 1930s, heavier and larger HS class trucks have since replaced the lighter and smaller trucks. According to the latest AASHTO specifications, the HS20-44 standard truck must be used to design all highway bridges. Furthermore, latest trends show a further increase of 25 percent in the weight of standard trucks indicating a standard HS25 truck may be used for design in the upcoming years.

Load envelopes corresponding to the axle loads of standard trucks as they move along the length of the span are used to analyze the maximum load effects on a bridge structure. The bridge for the project was built in 1930 and was originally designed for an H15 standard truck loading. The moment envelopes for the different types of truck loadings on the bridge are shown in Figure 39. A significant increase in the demand for the bridge from the original H15 load to the current demands is noted. The increased live load moment demand for the existing bridge for different standard trucks specified by AASHTO is provided in Table 22.
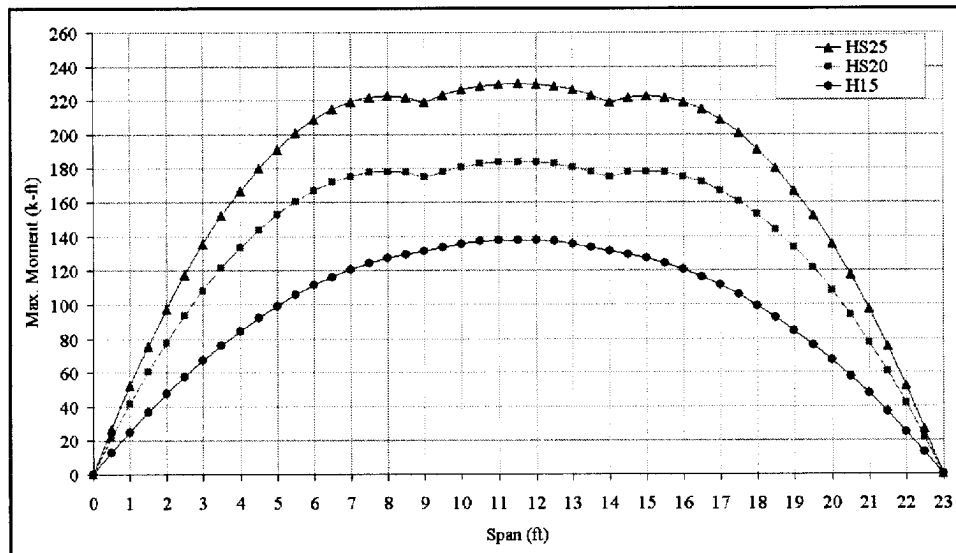
Figure 39. Moment envelope for the 23ft span bridge P-53-702

Table 22
Increase in Moment for the Bridge for Current Truck Loads

Type	Maximum Moment (Live Load), (k-ft)	Increase, %
H15-44	138	-
HS20-44 *	184	33.33
HS25-44 *	230	66.67
* Denotes anticipated in future codes.		

Review of Bridge Inspection and Rating Procedures

The Federal Highway Administration U.S. Department of Transportation, National Bridge Inspection Standard (NBIS) establishes the requirements for the inspection and maintenance of bridges located on or over all public roads. The NBIS further establishes the requirements for inspection procedures, frequency of inspections, load ratings, qualifications of personnel, inspection reports, and preparation and maintenance of bridge inventory records (AASHTO 2000). The NBIS standard uses the *Recording and Coding Guide for the Structure Inventory and Appraisal of Nation's Bridges* (FHWA 2000) to record and code the structural and nonstructural elements of a bridge. The *Manual for Condition Evaluation of Existing Bridges* (AASHTO 2000) and the *Bridge Inspector's Training Manual/90*, supplement the Guide. These manuals are used by federal, state, and local agencies as the basis for Bridge Replacement and Rehabilitation Programs and recordings in the National Bridge Inventory (NBI) Database (FHWA 2001). This National Bridge Inventory Database is used to evaluate and make recommendations for the nation's infrastructure.

The WisDOT has established its own set of guidelines for the inspection of bridges in the State of Wisconsin. These guidelines use the *Pontis Bridge Inspection Program* for bridge inspections. The *Pontis Manual* specifies numerical values for the condition state information and actions for the various elements of the bridge. These values are used in the bridge inspection report and are used to evaluate the overall condition of the bridge. While these values are different from those used in the federal guidelines, a direct conversion can be made to the NBI ratings by the bridge inspector. The Inspection report in Appendix A for Bridge P-53-702 shows the additional NBI ratings.

These recordings are used to determine three major criteria or "ratings" of the bridge. These ratings are numerical values that are recorded to indicate the existing condition, strength, and serviceability of the structure and are further used to determine maintenance and replacement schedules for the bridge. The three types of ratings are:

1. Condition Rating
2. Load Rating
3. Sufficiency Rating

These ratings are further subdivided into various categories that describe in detail the properties of a particular bridge. Details of each rating are described in the following sections.

Condition Rating (CR)

The condition rating of a bridge is defined as "the results of the determination of the functional capability and the physical condition of bridge components including the extent of deterioration and other effects," (AASHTO 2000).

The observations made during the inspection of the bridge are interpreted numerically in the inspection report by assigning an environment for the physical condition of the bridge component. These environments are assigned such that they allow different values (or limit states) of deterioration for each element. The limit states have a high value to signify severe deterioration and a low value to signify minimal deterioration. For example, the concrete deck of a bridge may have a condition state of 5 representing "area of distress" (potholes etc.) > 25 percent of the deck area, or a condition state of 1 to represent an area of distress < 2 percent. The condition ratings of bridge components are provided in the inspection report.

Load Rating (LR)

According to the AASHTO specification, the *Manual for Condition Evaluation of Bridges* (AASHTO 2000), load rating is defined as, "the determination of the live load carrying capacity of an existing bridge using existing bridge plans supplemented by information gathered from a field

inspection." Bridge load ratings are a basis for determining the safety and serviceability of a bridge under usage. They are reviewed periodically and updated to reflect any changes in the condition of the bridge. The ratings are required under federal regulations to be maintained in conjunction with inspection reports. The load ratings are used to monitor and manage the load posting, rehabilitation, and replacement schedules of bridges.

The load rating is a calculated numerical value that defines the safe load carrying capacity of a bridge. Load ratings are calculated at different levels to determine the safe load carrying capacity of the bridge for different levels of usage. On occasions a bridge may be used to carry special vehicles and therefore the load rating for such an atypical loading may be considered as well. Primarily, levels of rating provide an effective means of determining limitations on the bridge under service and ultimate conditions. The two levels of load rating suggested by AASHTO are *Inventory Level* and *Operating Level*. The two rating levels are described below.

Inventory Rating (IR)

The Inventory Rating corresponds to the customary design level of stresses but reflects the existing bridge and material conditions with regard to deterioration and loss of section. Load ratings based on the Inventory level allow comparisons with the capacity for new structures and; therefore, results in a live load, which can safely be used on an existing structure for an indefinite period of time (AASHTO 2000).

Operating Rating (OR)

The maximum permissible live load, to which a bridge structure may be subjected to, corresponds to the Operating Rating of the bridge. This maximum load is generally associated with special occasions and may shorten the life of the bridge if used consistently (AASHTO 2000).

These rating levels may be calculated using the Allowable Stress method (AS), Load Factor method (LF), or the Load and Resistance Factor Rating method (LRFR) to evaluate the capacity of the bridge members. The AS method or working stress method is a traditional method used to calculate the structural capacity of a member under actual loadings, which are combined to produce maximum stresses in a member (AASHTO 2000). These limiting stresses are based on the safety and reliability of the material under service conditions. The LF method is based on factored loads, which are multiples of the actual loads experienced by the candidate structure. These factors reflect the effects of different types of loads and are used to ensure that strength of the member is maintained under uncertain loading conditions (AASHTO 2000).

Load ratings are calculated for each of the elements of the structure and the member with the lowest rating controls the bridge rating. The following general

equation is used in evaluating the load rating of a candidate structure based on the wable Stress (ASD) method or the LF method.

$$RF = \frac{C - A_1 D}{A_2 L(1+I)}$$

Equation 6-1a (AASHTO 2000)

$$RT = (RF) \times W$$

Equation 6-1b (AASHTO 2000)

Where

RF: Rating Factor for the live-load carrying capacity. The rating factor multiplied by the rating vehicle in tons gives the rating of the structure

C: Capacity of the member based on Allowable Stress Design or Load Factor Design

D: Dead Load effect on the member

L: Live Load effect on the member

I: Impact Factor to be used with Live Load to amplify static loading to dynamic loading

A_1: Factor for Dead Load

A_2: Factor for Live Load

RT: Bridge Rating and

W: Weight of Rating Truck

In the above expression, the "load effect" is the effect of the applied loads on the element and is typically axial force, vertical shear force, bending moment, axial stress, shear stress, and bending stress (AASHTO 2000). Based on current load requirements specified by AASHTO for a HS20 truck an $RT < 20$ or $RF < 0.56$, reflects under capacity of the bridge.

Sufficiency Rating (SR)

The sufficiency rating of a bridge is indicative of its sufficiency to remain in service and is calculated to determine the strength and serviceability of the bridge. The sufficiency rating of a bridge is based on the condition ratings of the bridge components and the load ratings as explained above. The SR is a calculated numerical value that defines the usage of the bridge based on four factors each of which corresponds to the strength and serviceability of the bridge (FHWA 2000). These four factors are:

1. The Structural Adequacy and Safety (S_1)
2. Serviceability and Functional Obsolescence (S_2)

3. Essentiality for Public Use (S_3) and
4. Special Reductions (S_4)

The result of numerical calculations of the four factors as a percentage are then combined using the following equation:

$$SR = S_1 + S_2 + S_3 - S_4$$
<div align="right">Equation A-1 (FHWA 2000)</div>

where

$$0\% < SR \leq 100\%$$

The equation above yields a percentage value in which a 100 percent would represent an entirely sufficient bridge and zero percent would represent an entirely insufficient or deficient bridge (FHWA 2000). The sufficiency rating is used to implement the maintenance, scheduling, and planning of rehabilitation of existing bridges. According to FHWA regulations the following measures are appropriate based on the SR.

$$SR \leq 80\%$$ Bridge qualifies for rehabilitation techniques;

$$SR \leq 50\%$$ Bridge qualifies for Federal funds for replacement.

Analysis and Rating Calculations for Bridge P-53-702

Following the selection and investigation of the bridge for demonstration of the MF-FRP system to strengthen existing bridges for increased flexural strength, the next part of the project was to investigate the existing flexural capacity of the bridge and to calculate its load rating.

Condition Rating for P-53-702

The Inspection Report for Bridge P-53-702 provided the CR of various bridge components reflecting their level of deteriorated physical condition. Table 23 shows the CR for the bridge elements. It should be noted here that a rating of "4" for *Poor Condition* is similar to a rating of "3" for *Serious Condition* except for the absence of fatigue cracks in steel rebar or shear cracks in concrete and can be improved upon if improvements in strength are shown.

Table 23
Condition Rating for Key Components for Bridge P-53-702

Component	Condition Rating (NBI)	Description
Concrete Slab	3	*Serious Condition*: loss of section, deterioration, spalling or scour, have seriously affected primary structural components. Local failures are possible. Fatigue cracks in steel or shear cracks in concrete may be present.
Superstructure	3	
Substructure	5	*Fair Condition*: all primary structural elements are sound, but may have minor section loss, cracking, spalling or scour.

The effects of fatigue in the reinforcing steel can be reduced if the stresses in the steel are reduced. The addition of FRP strips on the bridge soffit will decrease the stresses in the steel. Since the condition rating influences the SR (inherent in factors S_1, S_2, and S_3) of the bridge the potential improvement in the SR was calculated for the proposed retrofit in what follows.

Load Rating for P-53-702

According to available records the load ratings for the bridge were last conducted in 1979. The rating calculations are shown in Appendix A. Resulting from the uncertainty over the rating procedures adopted for load ratings in 1979, it was not possible to determine the exact methodology used at the time. Furthermore, current practice is to use the Load Factor method of rating for all bridges except for prestressed girders and must be used to re-rate all bridges (WBM 1994).

The load rating of the existing bridge was conducted using the load rating equation given by AASHTO (AASHTO 2000). The procedure to calculate the IR and OR levels essentially represents the calculation of the capacity of the bridge in the service and ultimate conditions. The rating procedure requires the placement of the rating truck at critical locations on the bridge span that will create the maximum load effects. The location of the critical sections are found from envelopes as the live loads are moved across the bridge span as discussed previously. The calculated load effects (for example dead and live load moments) are then distributed to the bridge elements, which are subsequently analyzed for their existing capacity.

Table 24 shows the calculated Rating Factors for the bridge for its existing capacity and for an increased rating factor for HS20 and HS25. The calculations for the bridge Load Ratings and the improved Inventory ratings of HS20 and HS25 are provided in the following sections.

Table 24
Rating Factors for Bridge P-53-702

Level	Existing	Future	
	HS17	HS20	HS25
Inventory	0.49	0.56	0.69

Sufficiency Rating for P-53-702

The Sufficiency Rating for the Bridge P-53-702 provided by the WisDOT was 32.7 percent, which qualifies it for replacement with Federal funds. Calculations based on the FHWA criteria result in a SR of 36.83 percent (see Arora 2003 for details). The difference between the calculated and the reported value is small and is attributed to the lack of accurate information on some non-structural conditions of the bridge. The effect of increasing the Inventory (Load) Rating from HS17 to HS25 on the Sufficiency Rating was calculated for a variety of scenarios. Table 25 shows a summary of SR rating levels for the bridge for these scenarios. It can be seen that if the Inventory Rating of the bridge is improved from HS17 to HS25, the Sufficiency Rating of the bridge may also be improved. However, increasing the load rating alone will not improve the sufficiency rating that significantly. If, however, in addition to improving the load rating, repairs are carried out together with the strengthening to improve the deck condition rating, the bridge life may be improved beyond the 50 percent mark that qualifies it for replacement.

Table 25
Summary and Comparison of Ratings

#	Scenario	Sufficiency Rating	
		Calculated	Reported*
0	Existing Bridge	36.83 %	32.70 %
1	Increase Inventory Rating (HS17 to HS25)	40.45 %	36.30 %
2	Increase Inventory Rating (HS17 to HS25) + Increase NBI Condition Rating of Item # 59 (Superstructure) from 3 to 4**	52.65 %	51.60 %
3	Increase Inventory Rating (HS17 to HS25) + Increase NBI Condition Rating of Item # 59 (Superstructure) from 3 to 4** + Increase NBI Condition Rating of Item # 58 (Deck) from 3 to 4***	54.67 %	53.70 %
4	Increase Inventory Rating (HS17 to HS25) + Increase NBI Condition Rating of Item # 58 (Deck) from 3 to 4***	42.49 %	38.40 %
* As provided by WisDOT			
** Superstructure: Serious to Poor			
*** Deck: Serious to Poor			

Capacity of existing Bridge P-53-702. The existing capacity "C" of the bridge was calculated using the analytical model specified by AASHTO 2000. For a concrete flat slab subjected to live load effects on a unit width, the flexural capacity of the bridge is calculated using strain compatibility, internal force equilibrium, and the constitutive relationships of the materials. The Whitney stress-strain model for concrete is used, while an elastic-perfectly plastic model for steel reinforcement in tension is used. The strength properties for the constituent materials as specified by AASHTO (AASHTO 2000) were used to calculate the exiting flexural capacity of the bridge. The capacity of a unit (12 in.) slab section for the bridge was calculated using the properties in Table 26.

Table 26
Section Properties Used to Calculate the Existing Capacity of Bridge P-53-702

Width	Depth	Area of Steel	Depth to Tension reinforcement	Concrete Strength	Yield Strength
b	h	A_s	d_s	f'_c	f_y
(in.)	(in.)	(in.²)	(in.)	(psi)	(psi)
12	20	2*	18.5	2,500	33,000

*For 1 in. square bar @ 6 in. o.c.

Figure 40 shows the stress-strain distribution and the internal force equilibrium for a unit section of the existing slab. Note that the contribution of the compression steel is ignored.
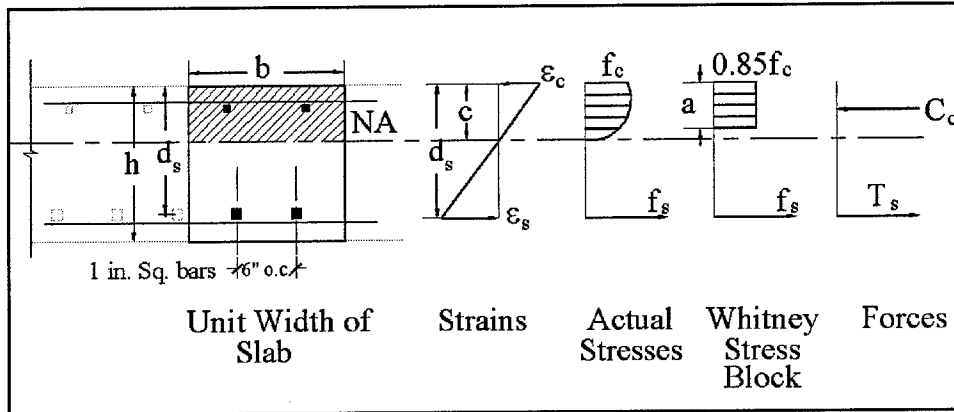
Figure 40. Internal force distribution for calculating capacity of existing slab

The nominal moment capacity of the unit section of the existing slab was determined from

$$M_n = A_s f_y \left(d_s - \frac{a}{2} \right)$$

where

$$a = \frac{A_s f_y}{0.85 f'_c cb}$$

The ultimate capacity of the slab is calculated with a strength reduction factor $\phi = 0.9$ for flexure as

$$C = M_u = \phi M_n$$

Table 27 gives the calculated nominal and ultimate capacities of the bridge section.

Table 27			
Nominal and Ultimate Capacities for Bridge P-53-702			
Nominal Capacity M_n		Ultimate Capacity M_u	
(k-in./ft)	(k-ft/ft)	(k-in./ft)	(k-ft/ft)
1135.5	94.6	1022	85.2

Dead Load Effect of Existing Bridge P-53-702. The Dead Load moment for a unit (12 in.) width of the bridge was calculated using the unit weight of concrete and a 3 in. overlay to be 18.9 k-ft/ft.

Live Load Distribution for Bridge P-53-702. The AASHTO load rating equation can be modified to calculate the ratings based on the flexural demand of the bridge. The rating factor for the flexural rating of a bridge can be written in terms of the effective width (E) as

$$RF = \frac{C - A_1 M_{DL}}{A_2 \dfrac{M_{LLHS20}}{E}(1+I)}$$

where the rating of the bridge is given as

$$RT = (RF) \times W$$

and

M_{DL}:	Dead Load Moments
M_{LLHS20}:	Live Load Moments for HS20 (184 k-ft)
E:	Effective width used to distribute the live load moment (ft)
C, I, A_1, A_2:	as before.

The AASHTO specifications (AASHTO 1996; AASHTO LRFD 1998) and the Wisconsin Bridge Manual (WBM 1994) suggest the use of "effective strip" models to determine the live load distribution. AASHTO LRFD (1998) defines the effective strip (E) as "the artificial linear element, isolated from the deck for the purpose of analysis, in which extreme force effects calculated for a line of wheel loads, transverse or longitudinal, will approximate those actually taking place in the deck." The effective strip (E) is essentially the equivalent rectangular width of uniform stress that represents the non-linear stress distribution of the live load on the entire lane. Table 28 lists the different effective strip widths calculated using different specifications.

Table 28
Equivalent Strip Width Calculation for Bridge P-53-702

AASHTO 1998 * One Lane	$E_1 = 10in + 5\dfrac{in}{ft}\sqrt{(S \times W)} < 7ft$	$\dfrac{E_1}{2} = 5.0\,ft$
AASHTO 1998 * Two Lanes	$E_2 = 84in + 1.44\dfrac{in}{ft}\sqrt{(S \times W)} \leq \dfrac{12.0W}{N_L}$	$\dfrac{E_2}{2} = 4.9\,ft < 6ft$
AASHTO Standard Spec. 1996	$E_3 = (4ft + 0.06 \times S)$	$E_3 = 5.38\,ft < 7ft$
Wisconsin Bridge Manual *	$E_4 = (4ft + 0.06 \times S) < 7ft$	$E_4 = 5.38\,ft < 7ft$

Denotes per Axle and are therefore divided by 2 to obtain per wheel line.

The effective width was also back calculated based on the given WisDOT inspection report rating of HS 17.6 as follows:

$$E_5 = \frac{RFA_2 M_{LLHS20}(1+I)}{C - A_1 M_{DL}}$$

For M_{LLHS20} = 184 k-ft, M_{DL} = 18.9 k-ft/ft, RF = 0.49, C = 85.2 k-ft/ft, I = 0.3, A_1= 1.3, A_2 = 2.17 gives

$$E_5 = 4.2\,ft$$

To maintain consistency with the existing rating (i.e., HS 17.6) the effective width distribution factor (E) calculated using the original ratings was used in further calculations to design the strengthening system. It should be noted here that this value is not the same as any of those shown in Table 28. However, it is within the same range as those in Table 28 and was felt to be the most appropriate value for use in the strengthening design. Table 29 provides the uniform live load effects calculated for various trucks using this equivalent width.

Table 29
Live Load Moments Per Foot Width of Slab for P-53-702

Type	Maximum Live Load Moment (k-ft)	Distribution Factor (D) (ft)	Maximum Unit Live Load Moment (k-ft/ft)	Diff %
	(k-ft)	(ft)	(k-ft/ft)	%
H15-44	138	4.2	32.9	-
HS20-44	184	4.2	43.8	33.1
HS25-44 *	230	4.2	54.8	66.6

Denotes anticipated in future codes.

The maximum live load moments per unit width are then be factored and combined with the dead load moments per unit width to calculate the moment capacity required for HS20 and HS25 trucks. As discussed previously, the LF method has been adopted to evaluate the Inventory rating of the bridge. The safety factors as used in the rating calculations are used here. Table 30 provides the summary of the design moments required per unit width of the slab for various standard trucks and compares them with the design moments used originally to design the bridge based on standard H15 truck.

Table 30
Design Moments Per Unit Width of Slab for Bridge P-53-702

Type	LL Moment (M_{LL}) (k-ft/ft)	DL Moment (M_{DL}) (k-ft/ft)	Load Factor Design (LFD) Moments * (k-ft/ft)	Diff. From H15 %	Allowable Stress Design (ASD) Moments *** (k-ft/ft)	Diff. From H15 %
H15-44	32.9	18.9	117.4	-	61.7	-
HS20-44	43.8	18.9	148.1	26.1	75.9	23.0
HS25-44	54.8	18.9	179.2	52.6	90.2	46.2

* Denotes anticipated in future codes

** Using a Dead Load Factor of 1.3 and Live Load Factor of 2.17 plus Impact = 0.3

*** Using a Dead Load Factor of 1.0 and Live Load Factor of 1.0 plus Impact = 0.3

Note that the calculated design moment using the Load Factor method for the H15 truck loading may not be the moment used originally to design the bridge in 1930. The ASD design methodology was probably used. This may reduce the actual design moment for the bridge. In such a case, the design factors A_1 and A_2 may more likely to be 1.0 each. Therefore, 61.7 k-ft/ft is most probably the original design moment value for the bridge. Table 31 provides a comparison between the required design moment (per unit width) from Table 30 and the nominal capacity of the unit width of the bridge for the LFD method.

Table 31 Comparison of Design Moments with Existing Capacity of P-53-702

Type	Ultimate Design Moments (M_u) (k-ft/ft)	Nominal Design Moments (M_n) (k-ft/ft)	Existing Nominal Capacity (k-ft/ft)	Diff. From H15 %
H15	117.4 (61.7) **	105.7 (61.7) **		--
HS20-44	148.1	133.3	94.6	40.1
HS25-44	179.2	161.3		70.5

* Denotes anticipated in future codes

** Denotes for ASD method

A significant increase in the nominal moment is shown to be needed to increase the capacity of the existing bridge. Figure 41 graphically shows an approximate behavior of the existing unit width of the bridge slab using a Moment-Curvature model, which includes strain hardening of tension steel and a non-linear stress-strain distribution for concrete (Lamanna 2002). The existing

nominal capacity is compared with limits of required nominal design capacity for various standard trucks given in the above table.
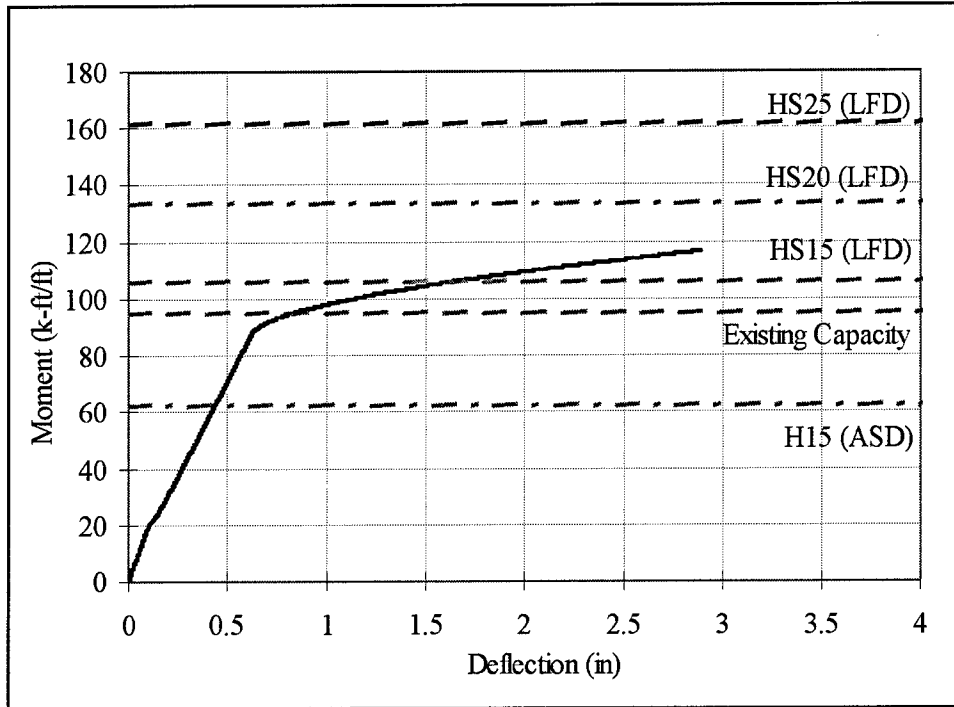
Figure 41. Comparison of existing flexural capacity of the bridge with required moments for different trucks

Strengthening Required for Increased Rating

To increase the Load Rating of the selected flat slab bridge from HS17 to HS25, the analytical model used to determine the existing capacity of the slab was modified to design the strengthening system. The methodology used to calculate the existing Inventory Rating for the bridge using Equation AASHTO equations (AASHTO 2000) was modified to calculate the increased flexural capacity of the bridge slab from the Inventory Rating of HS17 to HS25. The required RF for the increased ratings is calculated as follows

$$RF_{REQ} = \frac{RT_{REQ}}{W_{HS20}}$$

and the required capacity "C" of the section for the required Rating Factor was then calculated from

$$C = RF_{REQ}(A_2 M_{LL}(1+I)) + A_1 M_{DL}$$

where

$C = M_u$ = Required Ultimate Capacity of the section and $M_{DL}, M_{LL}, I, A_1, A_2$ as before for LFD method.

The required nominal capacity was then calculated as

$$M_{n,REQ} = \frac{C}{\phi}$$

Results of the calculations are given in Table 32. It can be seen that a 29 percent increase in the existing capacity of the unit width of the bridge is required to increase the Inventory rating of the bridge from HS17 to HS25.

Table 32
Summary of Required Moment Capacity for Increase in the Rating Level for Bridge P-53-702

Rating Level	Existing Rating (Rating Factor)	Improved Rating (Rating Factor)	Existing Nominal Capacity (k-ft/ft)	Required Nominal Capacity (k-ft/ft)	Increase in Capacity (%)
Inventory	HS 17.6 (0.49)	HS 20 (0.56)		104.3	10.2
		HS 25 (0.69)	94.6	122.1	29.0
Operating	HS 29.3 (0.81)	HS 33 (0.93)		104.3	10.2
		HS 41 (1.15)		122.1	29.0

Design of MF-FRP Strengthening System

Preliminary analytical investigations were required to estimate the number of FRP strips and fasteners for the existing bridge slab corresponding to the increase in the Inventory Rating from HS17 to HS25. The objectives of this task were:

a. To conduct a preliminary design for the strengthening of the existing bridge slab for the required flexural capacity using existing models for the MF-FRP system.

b. To conduct parametric studies to account for varying properties that may exist in the existing bridge and to assess their influence on the design.

c. To find the optimal configuration to produce the increase in capacity with a desirable failure mode.

d. To finalize the MF-FRP system design of the bridge based on the parametric studies

In previous research, an analytical Moment-Curvature (M-C) model was developed to predict the flexural behavior and ultimate capacity of the MF-FRP strengthened section (Lamanna 2002). This model was used to design the strengthening system for the existing bridge slab. The M-C model is an incremental model that predicts the elastic and postyield behavior of the section and includes tension strain hardening. A Strength Model was also developed using material relationships similar to the M-C model to predict the ultimate strength of the section without the affects of strain hardening. The strength model assumes full composite action between the FRP strip and the concrete section with a nonlinear concrete stress-strain model as used in the M-C model. A conventional Whitney Model was used for the unstrengthened section analysis.

As explained previously, the required design nominal moment of 122 k-ft per unit width of the bridge slab, corresponding to an Inventory Rating of HS25 requires a 29 percent increase in the existing flexural capacity of the bridge slab. These nominal design moments were used to design the strengthening system for the bridge using the MF-FRP system.

The preliminary design was conducted with two reinforcement ratios to determine the amount of FRP strips required for the strengthening. The FRP reinforcement ratio is defined as

$$\rho_{frp} = \frac{A_{frp}}{b \times d_{frp}}$$

where

ρ_{frp}:   FRP Reinforcement Ratio
A_{frp}: Area of FRP Reinforcement
b: Width of Cross section (12 in.)
d_{frp}:   Depth of FRP Reinforcement (20.0625 in.)

A unit width of the slab section with one FRP strip (i.e., one FRP strip @ 12 in. o.c.) with a FRP reinforcement ratio of 0.21 percent and an FRP reinforcement ratio of 0.12 percent corresponding to a 20 in. spacing of the FRP strips were considered. Since FRP strips are prefabricated with a cross section 4 in. x 1/8 in., the reduced area of FRP reinforcement for a unit width of section is conveniently accommodated by the increased spacing.

Figure 42 shows the two design reinforcement ratios used for the preliminary design and the parametric study.
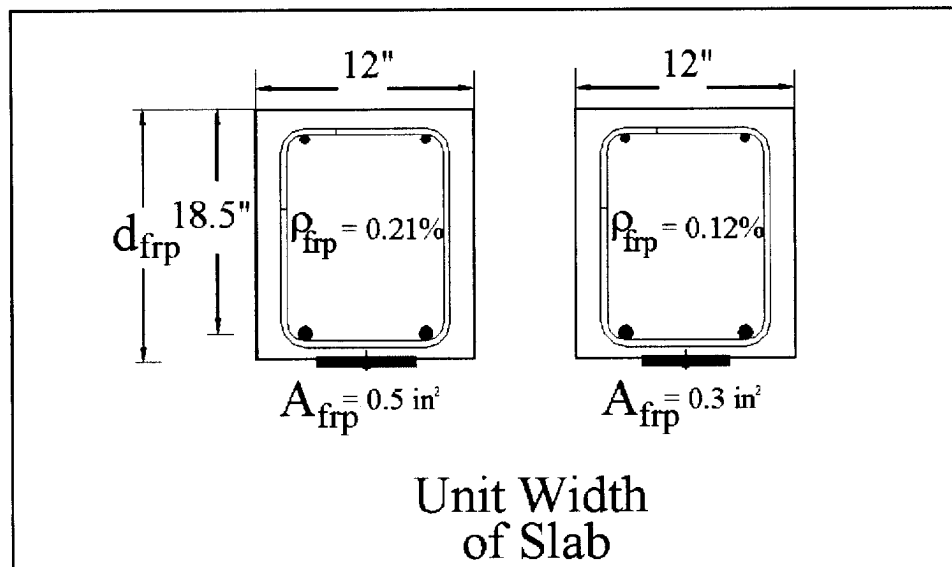
Figure 42. Designs for preliminary analysis and parametric studies

Parametric Design Studies

In addition to the FRP reinforcement ratio, concrete strength, tensile reinforcement strength, and the number of fasteners required were varied in the parametric design studies for the MF-FRP system.

Concrete Strength

The actual concrete compressive strength of the section may be different from the 2,500 psi assumed for the calculation of the existing capacity of the bridge slab. A number of previous studies suggest that concrete strength for bridges built around the same time may be as high as 8,000 psi. (Shahrooz et al. 1994). Therefore, concrete compressive strengths of 2,500 psi, 4,000 psi, and 6,000 psi, were considered in the parametric study.

Yield Strength of Tensile Reinforcement

Yield strength of steel in tension-controlled slab sections may range from 33 ksi for bridges built prior to 1954, to 60 ksi for conventional Grade 60 steel (AASHTO 2000). Table 33 provides a comparison of areas of steel for different yield strengths.

Table 33		
Comparison of Areas of Steel Reinforcement for Different Yield Strengths		
Original Reinforcement	**Yield Strength, (ksi)**	**12 in. Wide Section, (in.^{2})**
1- 33ksi sq. bar @ 6 in. o.c. (2in.^{2} per ft)	33	2
	40	1.65
	60	1.1

The modulus of elasticity of the steel reinforcement was assumed to have remained constant at 29×10^6 psi for the different steels.

Fastener Spacing

The strength and failure mode associated with the strengthened MF-FRP section is highly dependent on the number of fasteners used to attach the FRP strips. Previous tests conducted on the strength of the connections have limited the amount of shear force per fastener to 1,000 lb (Bank et al. 2002a). The force per fastener in the FRP strip is calculated in the Moment – Curvature model and is checked against the 1,000 lb limit (Bank et al. 2002a). While an extensive model for the fastener spacing is needed for the effects of moving loads, resulting from the schedule of the bridge strengthening a simple analysis for the maximum moment at the most critical location (here the midspan) was considered for the strengthening.

Results of Parametric Studies for Preliminary Design

Table 34 and Table 35 show the results of the parametric study for the two reinforcement ratios. For the parametric studies the modulus of the strip was taken as 8,900 ksi and the open-hole strength taken as 85.4 ksi based on previous testing (Bank et al. 2002a). The beam span was taken as 23 ft. The analysis was conducted for a beam in 4-point bending with a shear span of 11.3 ft and a constant moment span of 0.3 ft to provide a worst-case scenario (i.e., a "concentrated load" at the midpoint). Forty-four X-ALH fasters were used in the shear span–a single row at 3 in. on-center spacing. A design load of 1,000 lb per fastener was used. No end anchors were assumed in the modeling.

Table 34
Results of Parametric Study for 0.21 Percent FRP Reinforcement Ratio Design

Yield Strength (psi)	Area (in.^{2})	Whitney Unstrengthened (k-ft)	Strength Model Strengthened (k-ft)	Failure Mode	Moment-Curvature Unstrengthened (k-ft)	Strengthened (k-ft)	Failure Mode
				Concrete Strength 2500 psi			
33.000	2.0				117.0	165.0	
40,000	1.65	94.6	154.8	Conc. Comp.	114.0	164.0	FRP Rupture
60,000	1.1				109.0	162.0	
				Concrete Strength 4,000 psi			
33,000	2.0				131.0	172.0	
40,000	1.65	97.3	161.4	Conc. Comp.	126.0	170.0	FRP Rupture
60,000	1.1				118.0	166.0	
				Concrete Strength 6,000 psi			
33,000	2.0				147.0	175.0	
40,000	1.65	98.8	166.4	Conc. Comp.	140.0	173.0	FRP Rupture
60,000	1.1				127.0	169.0	

Note: All Calculations used E_{frp} = 8.9 ksi, f_{frp} = 85.4 ksi, 44 fasteners in shear span, Shear Span = 136 in., Span = 276 in. Load per fastener = 1,000 lb.

Table 35
Results of Parametric Study for 0.12 Percent FRP Reinforcement Ratio Design

Yield Strength (psi)	Area (in^2)	Whitney Unstrengthened (k-ft)	Strength Model Strengthened (k-ft)	Failure Mode	Moment-Curvature Unstrengthened (k-ft)	Strengthened (k-ft)	Failure Mode
				Concrete Strength 2,500 psi			
33,000	2.0				117.0	142.7	
40,000	1.65	94.6	132.0	Conc. Comp.	114.0	140.8	FRP Rupture
60,000	1.1				109.0	137.5	
Concrete Strength 4,000 psi							
33,000	2.0				131.0	147.3	
40,000	1.65	97.3	138.0	Conc. Comp.	126.0	145.2	FRP Rupture
60,000	1.1				118.0	141.4	
				Concrete Strength 6,000 psi			
33,000	2.0				147.0	149.6	
40,000	1.65	98.8	139.2	Conc. Comp.	140.0	147.5	FRP Rupture
60,000	1.1				127.0	143.6	

Note: All Calculations used E_{frp} = 8.9 ksi, f_{frp} = 85.4 ksi, 44 fasteners in shear span, Shear Span = 136 in., Span = 276 in. Load per fastener = 1,000 lb.

The results show a small variation in ultimate moment for the strengthened section for the different concrete strengths used. In addition, the yield strength of

the steel reinforcement does not affect the ultimate capacity of the section since the area of the steel is scaled so that E_sA_s remains constant. The unstrengthened capacity predicted by the M-C model shows considerable change and is attributed to the strain hardening of reinforcing steel. The two models for the strengthened sections; however, predict different failure modes. The M-C model predicts FRP rupture as the primary failure mode for all designs, while the strength model predicted concrete compression as the primary failure mode. The reason for the difference is a cause for concern and requires further study, however, the strains in the concrete for the M-C model at FRP rupture were found to be close to concrete compression failure of 0.0038 (more than the typical 0.003 used in the Whitney model).

Final Design for Bridge P-53-702

The strengthening of the Bridge P-53-702 with the MF-FRP system for an improved Inventory Rating of HS25 may be achieved with one strip attached every 12 in. o.c. using 40 fasteners spaced equally at 3 in. o.c. on each side of the midspan and 2 anchor bolts on each end of the FRP strip. Since no material safety factors and strength reduction factors for the preliminary design were used, 12 in. FRP strip spacing would provide strengthening sufficiently greater than the required 29 percent. Table 36 shows the final design for the bridge.

Table 36 Final Design for Bridge P-53-702					
Whitney	Strength Model		Moment-Curvature		
Unstrengthened (k-ft)	Strengthened (k-ft)	Inc. %	Unstrengthened (k-ft)	Strengthened (k-ft)	Inc. %
94.6	154.8	63.6	117.0	165.0	41.0

Figure 43 shows the behavior of strengthened unit section of the bridge slab as modeled by the M-C model and provides a 41 percent increase as compared to the unstrengthened section. Note that the unstrengthened section capacity is approximately the same as calculated using the Whitney stress block.
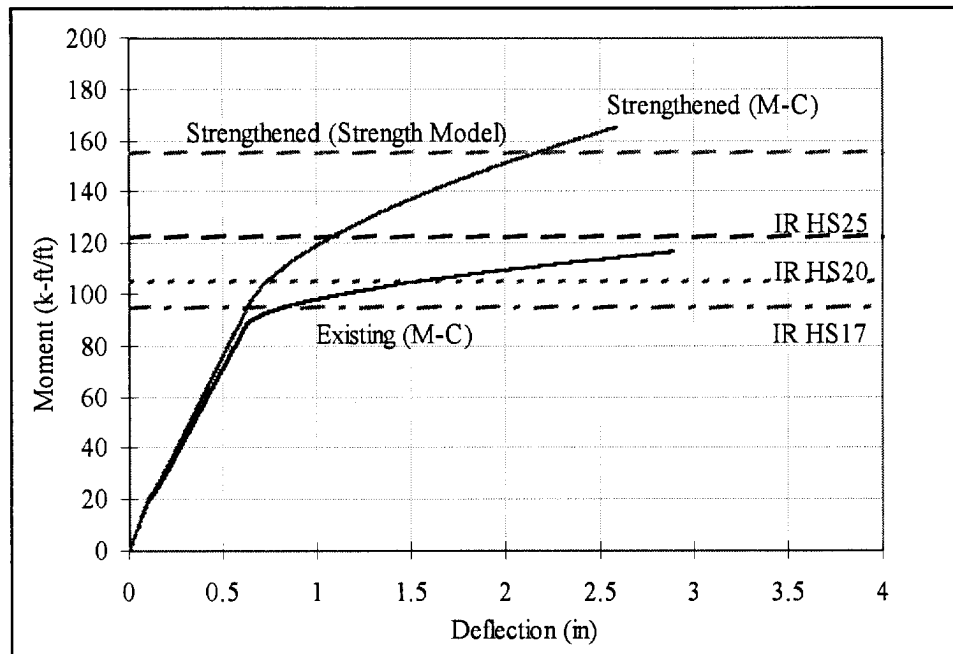
Figure 43. Predicted behavior of strengthened unit width of bridge slab

The final design for the MF-FRP system for the bridge is shown in Figure 44.
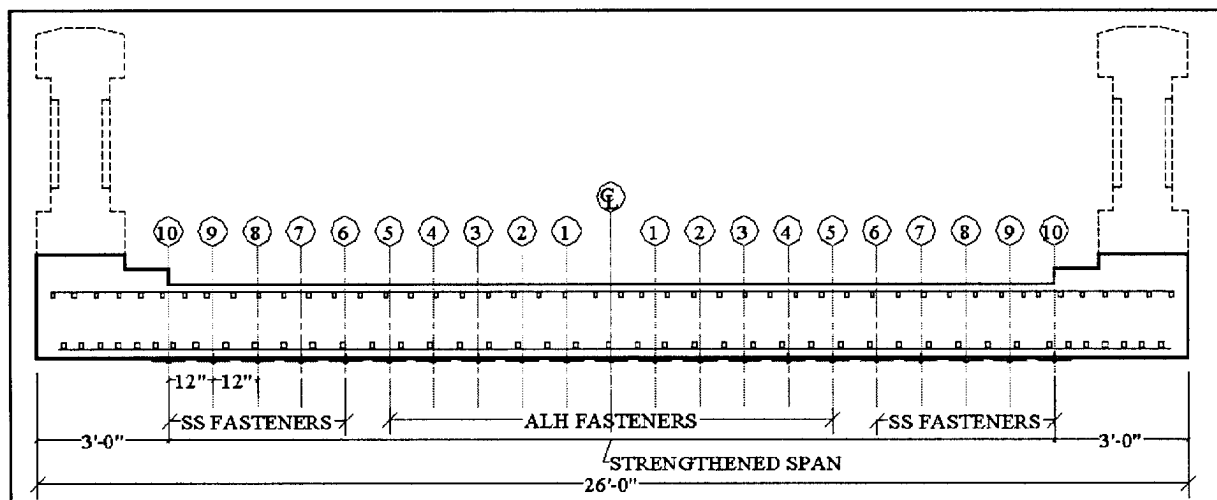
Figure 44. Final design layout of the FRP strips on the bridge

A total of 21 strips are required to be attached to the bridge deck. Eleven strips were designed to be attached using galvanized steel X-ALH fasteners, and 10 FRP strips using stainless steel X-CR-SS fasteners to observe the environmental effects on the fasteners.

Application of MF-FRP System

A plan for the application and testing of the bridge was developed to address issues such as site access, material transportation, strengthening procedure, instrumentation, and data collection. A schedule of the project was developed to accommodate local DOT personnel, scheduled area activities near the bridge, and the window period provided by the DNR. It was an objective of the research team to conduct the strengthening in a two-week period. Table 37 shows the schedule of the 10-day field installation and testing plan.

Table 37
Schedule for Field Application and Testing of Rehabilitation

Week	Day	Date	Proposed Activity
I	1	8/19/02	Site Access, Setup and Clean up of underside
	2	8/20/02	Mark layout of FRP strips and Instrumentation setup for Service Load Testing
	3	8/21/02	Reserve Day
	4	8/22/02	Service Load Test I (Control)
	5	8/23/02	Demonstration of MF-FRP system and certification for local DOT personnel
II	6	8/26/02	Application of FRP strips
	7	8/27/02	Application of FRP strips
	8	8/28/02	Instrumentation setup for Service Load Testing
	9	8/29/02	Reserve Day
	10	8/30/02	Service Load Test II (Strengthened) and cleanup

For the field application and service load testing of the bridge a plan was devised to distribute the activities between the UW-research team and the WisDOT. Table 38 details the distribution of responsibilities between the two teams.

Table 38
UW and WisDOT Roles and Responsibilities

Description	UW Responsibilities	WisDOT Responsibilities
Site Access and Setup	Material for setup and clean up	Personnel to aid UW team
Load Test I	Instrumentation and Setup	Preloaded trucks and personnel for traffic control
Application of MF-FRP	Materials and equipment	Personnel to assist with application
Load Test II	Instrumentation and Setup	Preloaded trucks and personnel for traffic control

The research engineers from UW and the DOT supervised the field installation and load tests. A staff engineer from the ERDC, Vicksburg, MS, also was on hand to witness the second service load test on the bridge. Table 39 shows the DOT man-hours utilized and the tasks completed. Table 40 shows the project material and estimated labor costs.

Table 39
Schedule for Field Application and Testing of Rehabilitation

Week	Day	Activity	Man-hours
I	1	Setup, Clean up underside and Mark Layout	7.5
	2	Instrumentation	NA
	3	Instrumentation	
	4	Service Load Test I (Control) Certification of DOT personnel for PAFS system (One strip attached)	6
	5	Attached 9 strips	18
II	6	Attached 10 strips (10-15 min. attachment time per strip)	12
	7	Instrumentation	NA
	8	Instrumentation	
	9	No Work	
	10	Attach 1 strip for demonstration and Service Load Test II (Strengthened) and cleanup	18
Total			61.5
Total hours for MF-FRP installation only			30
Total labor cost for MF-FRP installation at $60/hr (est.)			$1,800

Table 40
Costs for the Retrofit of P-53-702

Material	Unit Cost	Quantity	Cost ($)
FRP Strips (Strongwell Inc.) (21 Strips 23 ft long ea.)	$ 9 / ft	483 ft	4,347
X-ALH Fasteners + booster + neoprene coated washer (80 per strip, 11 strips)	$ 0.50 ea.	880	440
X-CR SS Fasteners + booster (80 per strip, 10 strips)	$ 1.15 ea.	800	920
Steel Anchor Bolts (4 per strip, 11 strips)	$ 1.14 ea.	44	50
Stainless Steel Anchor Bolts (4 per strip, 10 strips)	$ 4.70 ea.	40	188
Misc. Supplies	$ 10 / Strip	21	210
Total materials cost	$9.84/ft^2	26 x 24 = 625 ft^2	$6,155
Total Labor cost for installation	$2.88/ft^2	625 ft^2	$1,800
Total bridge strengthening cost	**$12.72/ft^2**	**625 ft^2**	**$7,995**

Material and Equipment for Strengthening

Table 41 shows the material and equipment used during the strengthening of the existing bridge.
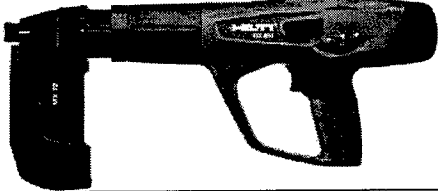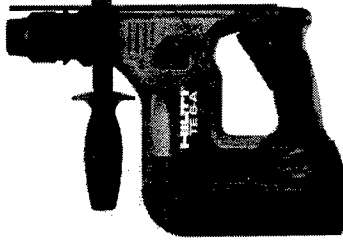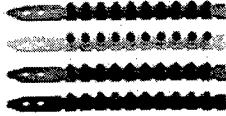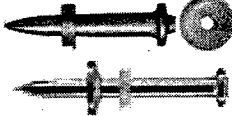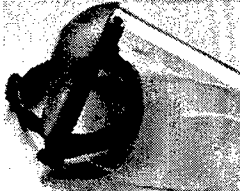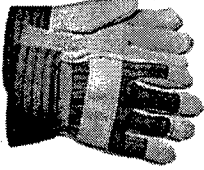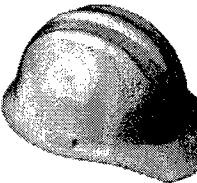
Table 41
Materials and Equipment Used for the Retrofit of Bridge

Material	Type Used	Description
Fastening System	Hilti Powder Actuated Fastening System DX A41 and DX 460 (shown here)	
Predrilling System	Hilti Type TE 6-A Rotary Hammer	
Charge for Fastening System	Hilti 0.27 in. caliber boosters for fastening system with selected power level as per ANSI (1995) guidelines	
Fastener Selection	Hilti Type X-ALH 47 P8 (w/ R-18 5/8 washer) and X-CR44-P8-S12	
FRP Strip	Strongwell FRP strip	STRONGWELL Safstrip®
Expansion Anchors	Hilti Type KBII CS ½ in. x 2-3/4 in. KBII SS ½ in. x 2-3/4 in.	

Table 42 shows the protective gear that was recommended for use during the installation of the MF-FRP system.

Table 42
Protective Gear Used During the Application/Installation of the MF-FRP System

Face Shield	Gloves	Hard Hat	Ear Protection

Installation Procedure

The process used to install the MF-FRP system on the bridge was as follows:

Strip Preparation

The FRP strips supplied by the manufacturer were in 100 ft long rolls. The strips were cut to the desired length of 21 ft 2 in. using a circular saw with a masonry blade. A hacksaw with a masonry blade was used for field cuts if necessary. Figure 45 shows the roll of FRP Strip used for the project as supplied by the manufacturer.
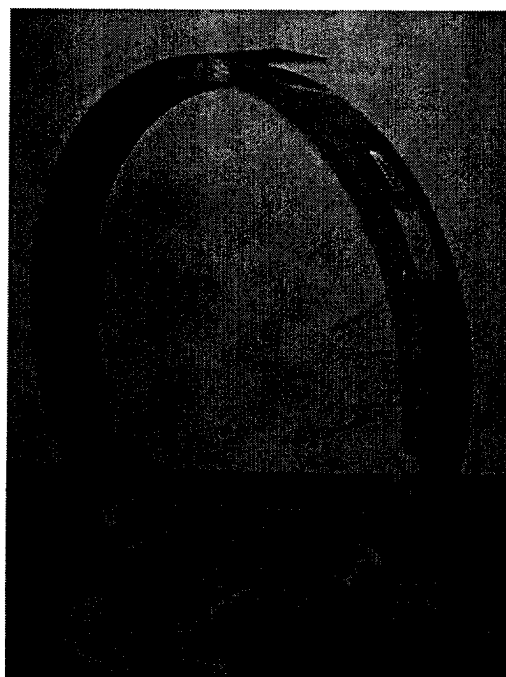
Figure 45. Roll of 100-ft-long FRP strips as supplied by the manufacturer

Mark Center of Strip

The centerline of the pre-cut strip was marked. A horizontal and vertical grid was marked on the FRP strip using a permanent marker to locate the center of the strip and the spacing of the fasteners required by the design (3 in. o.c.).

Predrill Holes in the Strip

The marked grid was then predrilled with a 3/16 in. masonry drill bit at fastener locations.

Setup For Application

A working platform was set up under the bridge. Wooden planks were supported on 4 × 4 lumber placed near the abutments. This was done to maintain an unrestricted flow in the creek. Figure 46 shows the setup of the working platform.

Figure 46. Working platform under the bridge

Surface Preparation

The concrete substrate was cleaned of any residual matter that would have hindered in the application of the FRP strip. A spatula and a wire brush were used to scrape the soft calcium stalactites from under the bridge deck. Figure 47 shows the soft calcium stalactites on the concrete substrate. Figure 48 shows the cleanup using a spatula.
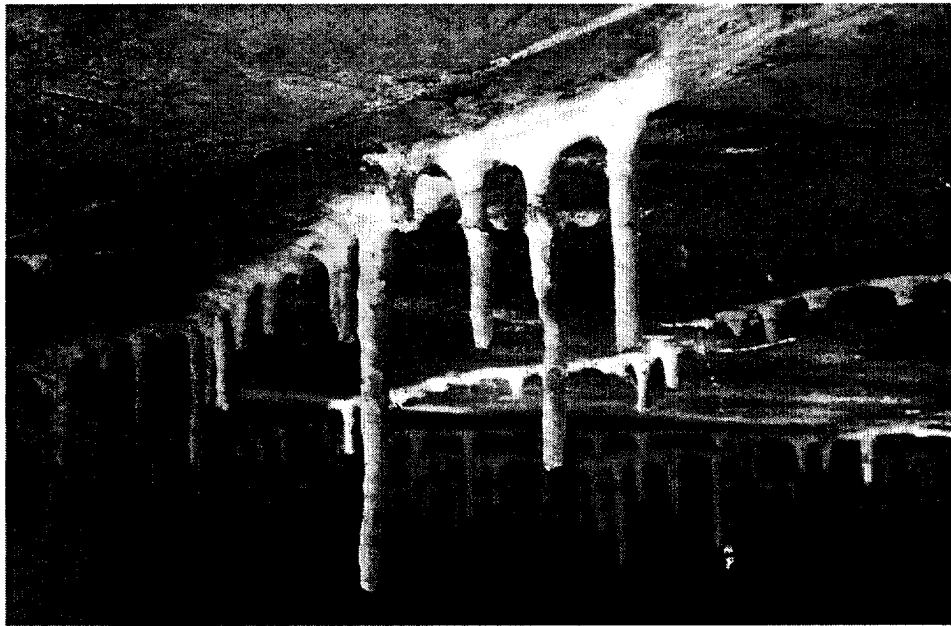
Figure 47. Soft calcium stalactites on the concrete substrate

Figure 48. Surface preparation of the concrete prior to application of FRP strips

Layout of FRP Strips

Using chalk powder and a permanent marker, the desired locations for the FRP strips were marked on the concrete surface.

Suspend FRP Strip on Substrate

The FRP strip was then suspended along the underside of the concrete slab at the appropriate location. Duct tape was used to temporarily position the FRP strip in its desired location. In addition, the strip was manually held in position until the first few fasteners were installed. Working from midspan of the bridge towards one support, the strip was moved into its proper position. Measurements were taken at regular intervals along the length of the strips to ensure the required spacing between the strips was maintained.

Secure Strip at Midspan

Predrilling into the concrete substrate was done through the drilled hole in the FRP strip. A 3/16 in. Hilti type DX-Kwik masonry bit was used with a rotary hammer drill. Figure 49 shows the predrilling at the midspan while the FRP strip is temporarily held up against the soffit.
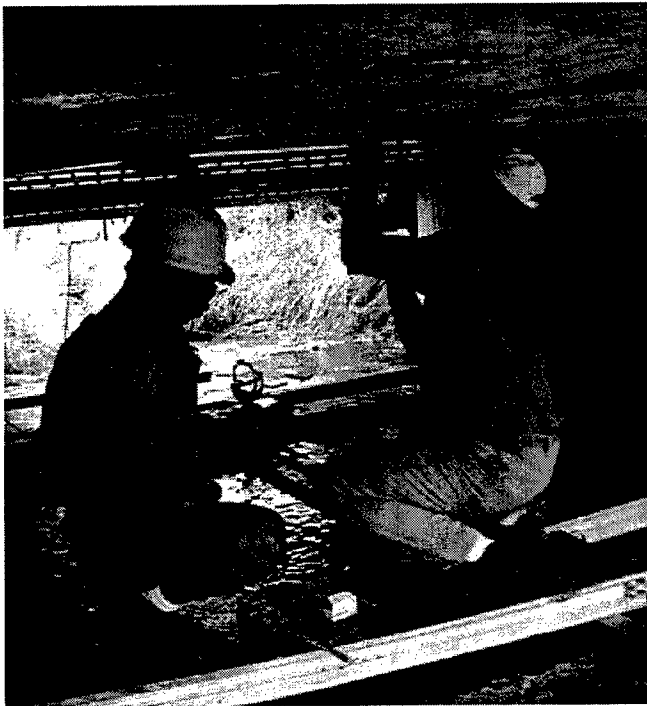
Figure 49. Predrilling into the concrete substrate at the midspan

Power Level for Fastening System

The charge selection for the fastening system was first determined by tests on the surface where the FRP strips were to be attached without predrilling. Starting with lowest power level and booster type a fastener was driven into the concrete with an attached washer. The power level was then increased to fully embed the

fastener and attach the washer snug against the concrete surface. If the highest power setting was not enough to fully embed the fastener, the procedure was then repeated with a higher-level booster.

Attach Fastener

The selected fastener was then inserted with the attached washer into the PAF gun, leaving the fastener point protruding out. The gun was placed perpendicular to the strip and was pressed to unlock the safety mechanism of the gun. The gun was then "fired" to insert the fastener. Figure 50 shows the fastening of the FRP strip at the midspan while it is temporarily held in place. Figure 51 shows a properly secured fastener at the midspan.

Figure 50. Fastening of the FRP strip at the midspan
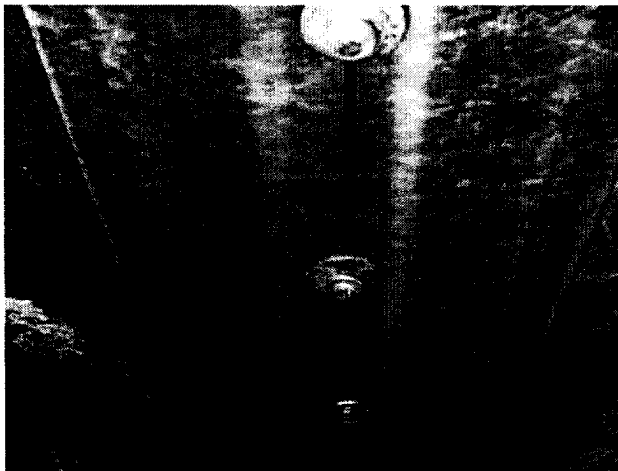
Figure 51. Properly installed ALH fasteners at the midspan

After the midspan fasteners were secured, the next sets of fasteners were installed with alternate predrilling and fastening sets of four fasteners at a time. After four to eight fasteners were installed the position of the FRP strips became fixed. The procedure then continued rapidly with a single person or two people drilling and attaching fasteners towards one end of the strip. When one half of the strip was secure the fastening was then resumed from the midspan towards the direction of the other support. Alternate drilling and fastening was done simultaneously to speed up the process. Figure 52 shows the simultaneous drilling and fastening of the FRP strip after the strip was securely fastened at the midspan.
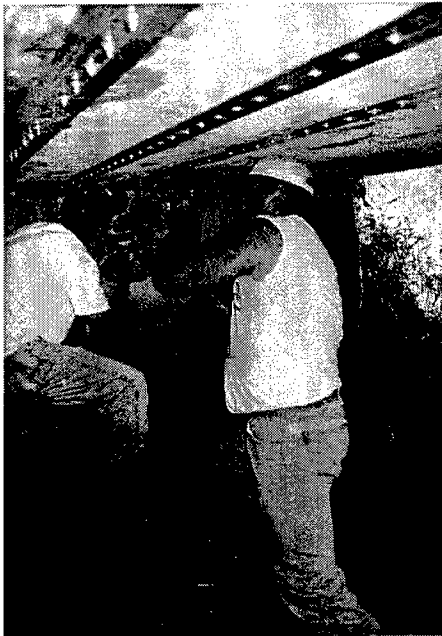
Figure 52. Simultaneous drilling and fastening of the FRP strip

Placement of End Anchors

The strips were predrilled at the locations of the anchor bolts using the rotary hammer drill with the nominal diameter of the anchor bolt. The hole was then cleaned before the anchors bolts were inserted. Once the anchor was inserted in the drilled hole, the anchors were hammered into place (taking care not to damage the FRP strip). The anchor bolts were then tightened using a socket wrench. Figure 53 shows the installed end anchors near the support ends.
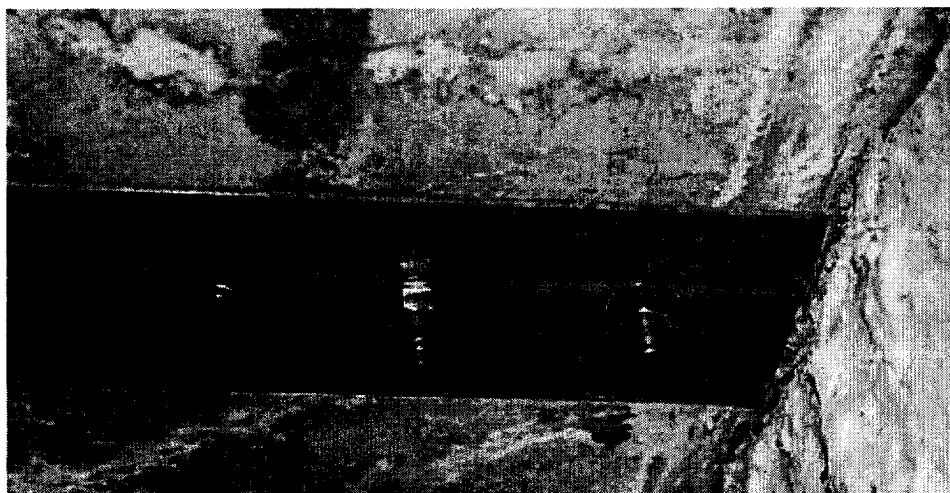
Figure 53. Installed end anchor next to the abutment

The completed retrofit of the bridge is shown in Figure 54 and Figure 55.

Figure 54. Strip spacing (12-in.) between FRP strips

Figure 55. Bridge P-53-702 strengthened using MF-FRP system

Observations During Strengthening

On the construction level, the field installation of the MF-FRP system was similar to that experienced during prior laboratory fastening procedures. However, a number of unique challenges were posed during the field installation. The following difficulties were observed:

It was cumbersome to position the FRP strip at the proper location. At times three to four people were required to temporarily hold the strip at the location before a few fasteners were installed. While the installation of the fasteners through the length of the span (80 fasteners at 3 in. spacing) took not more than 15 minutes, the positioning of the strip took an additional 15 minutes, and this slowed down the rate of installation. Occasionally, instances occurred where the fastener did not fully penetrate the concrete substrate. This was seen when a fastener encountered an obstruction in the substrate. Improper embedment of the fastener was seen. This ranged from incomplete embedment of the fastener to no embedment at all. Incomplete embedment was observed when the fastener ran into the following obstructions:

- Large Aggregate
- Pocket of poor consolidation or deteriorated concrete
- Existing rebar

Figure 56 shows a missing fastener.
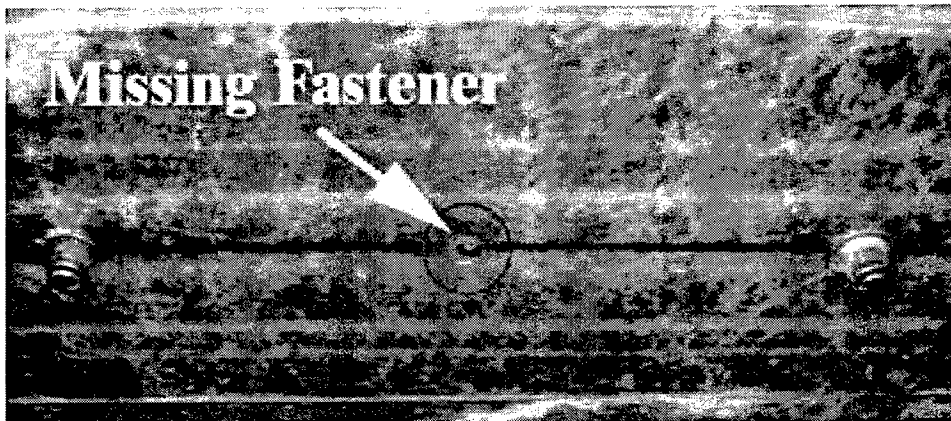
Figure 56. Missing fastener resulting from pocket of poor consolidation in the concrete

In cases where improper embedment was seen a lower power level was used to reinsert the partially embedded fasteners. Extreme caution was used to ensure the fasteners were not over driven. To do this the power level was set to low so that no damage to the strip was caused. In cases when no embedment was seen and the fastener completely came out of the predrilled hole, no further attempts to reinsert the fastener were made. Figure 57 shows an overdriven fastener. Such situations should be avoided.

Figure 57. Over-driven fastener in the FRP strip

In a situation where the row of fasteners was anticipated to achieve improper embedment the FRP strip was slightly re-positioned. Figure 58 shows the position of the FRP strip in close proximity to a local damaged area. The strip was moved a few inches to avoid the damaged area.

Figure 58. Relocated FRP strip near existing local damaged area

Local damage in the existing concrete substrate did not cause a problem with the fastening of the FRP strip. Figure 59 shows an existing damaged area in the bridge with the exposed steel reinforcement.

Figure 59. Existing damaged area in the bridge with the exposed steel reinforcement

Furthermore, locations of localized out-of-plane variations did not affect the fastening procedure. Figure 60 shows a location were original formwork had produced out-of-plane variations.
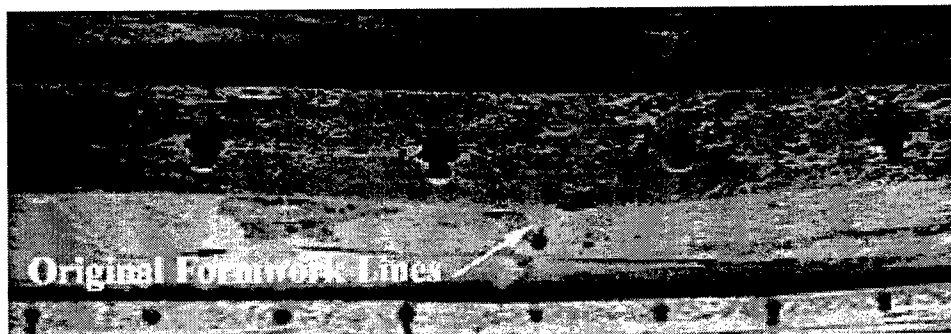
Figure 60. FRP strips fastened over original formwork lines

Service Load Testing

Service load testing of the bridge was conducted to determine if the MF-FRP system was performing appropriately and had increased the flexural capacity of the bridge. The objectives of the tests were to investigate and gather control data on the in situ strength of the bridge before and after the strengthening.

Testing Procedure

The methodology adopted for the service load test was to conduct static diagnostic load tests on the bridge. Figure 61 shows the service load tests on the bridge.

Figure 61. Service load tests on bridge P-53-702

The static diagnostic load method used is a nondestructive test method and has been the method of choice for various studies conducted on bridges (Saraf 1998; Chajes et al. 1997; Stalling et al. 2000). The method employs the positioning of a truck with known configuration and weight at critical locations on the bridge with the response determined by measuring strains in the materials. Strain readings measured in the concrete and the FRP strips were used to verify the composite behavior of the strengthened slab.

A three-axle truck with known wheel configurations was used for the service load testing of the bridge. It was calculated that a truck loaded between 50,000 and 60,000 lb would produce acceptable response without causing any damage to the bridge. The truck was provided by Rock County DOT and was weighed prior to each load test. Figure 62 shows the wheel and axle spacing for the truck used. Table 43 provides the distribution of the weight.
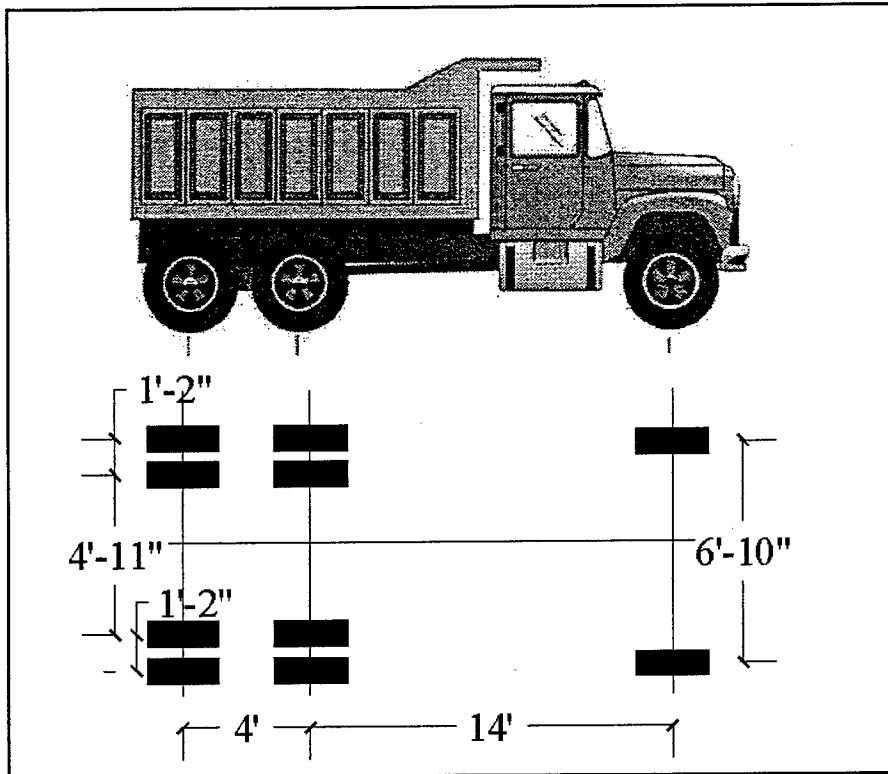
Figure 62. Wheel spacing for the truck used for service load testing

Table 43			
Weights Distribution for the Truck Used for Service Load Testing			
Truck No.	Front Axle (kips)	Rear Axles (kips)	Total Weight (Tons)
1021 WisDOT	12.9	37.8	25.4

Instrumentation and Load Cases

For the service load testing, strain gages, and LVDTs were attached to measure the structural behavior of the concrete slab. Strain gages were also placed on the FRP strips to measure the strains and to confirm the composite action of the strengthened slab. Figure 63 shows the locations of the strain gages attached on the underside of the concrete and the FRP strips. Designations C, E, W, S, and F correspond to Concrete, East, West, South, and FRP, respectively.
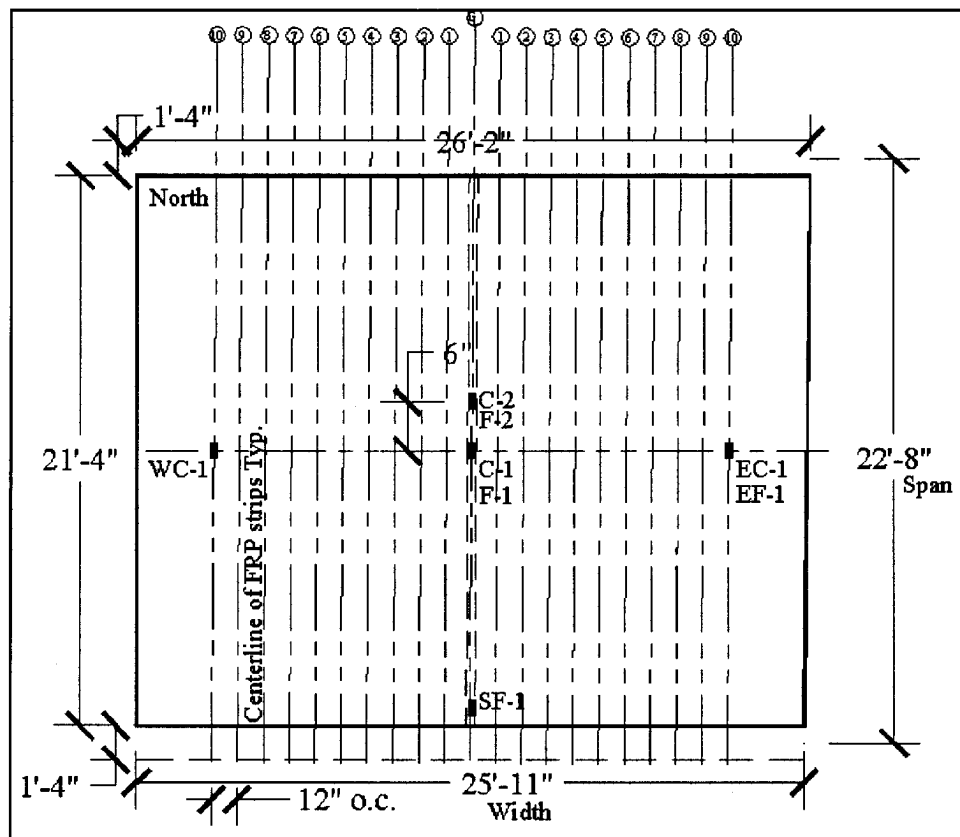
Figure 63. Layout and location of strain gauges on the bridge slab

The strain measurements were made at various locations for different load cases using a portable data acquisition system. Resulting from the lack of a direct current source at the location of the bridge, a generator was used to power the data acquisition system. During the initial load testing, the data acquisition system could not be stabilized resulting from the unstable power source. Therefore, manual strain indicators and switch boxes were used to measure the strains at various locations of the slab. Dial gages (0.0001 in. resolution) were used in place of the LVDTs to measure the deflections of the bridge. However, displacements were too small to be measured.

On the day of the second load tests, rain affected some of the strain gages placed on the concrete surface. While careful precautions were taken to shield the strain gages from direct contact from water, some of the strain gages were affected resulting from seepage seen through the vertical cracks in the slab. While some of the strain gage readings were consistent with those measured during the first series of tests, others were inconsistent and decreased the reliability of the results.

The load cases for both series of service load tests were conducted using the same truck, which was weighed for each series of tests. The load cases used are shown in Figure 64.

Load Case I: Rear axles centered at Midspan of the bridge.

Load Case II: Front rear axle centered at Midspan of the bridge.

Load Case III: Rear axles centered on Eastern edge of the bridge.

Load Case IV: Front rear axle centered on Eastern edge of the bridge.
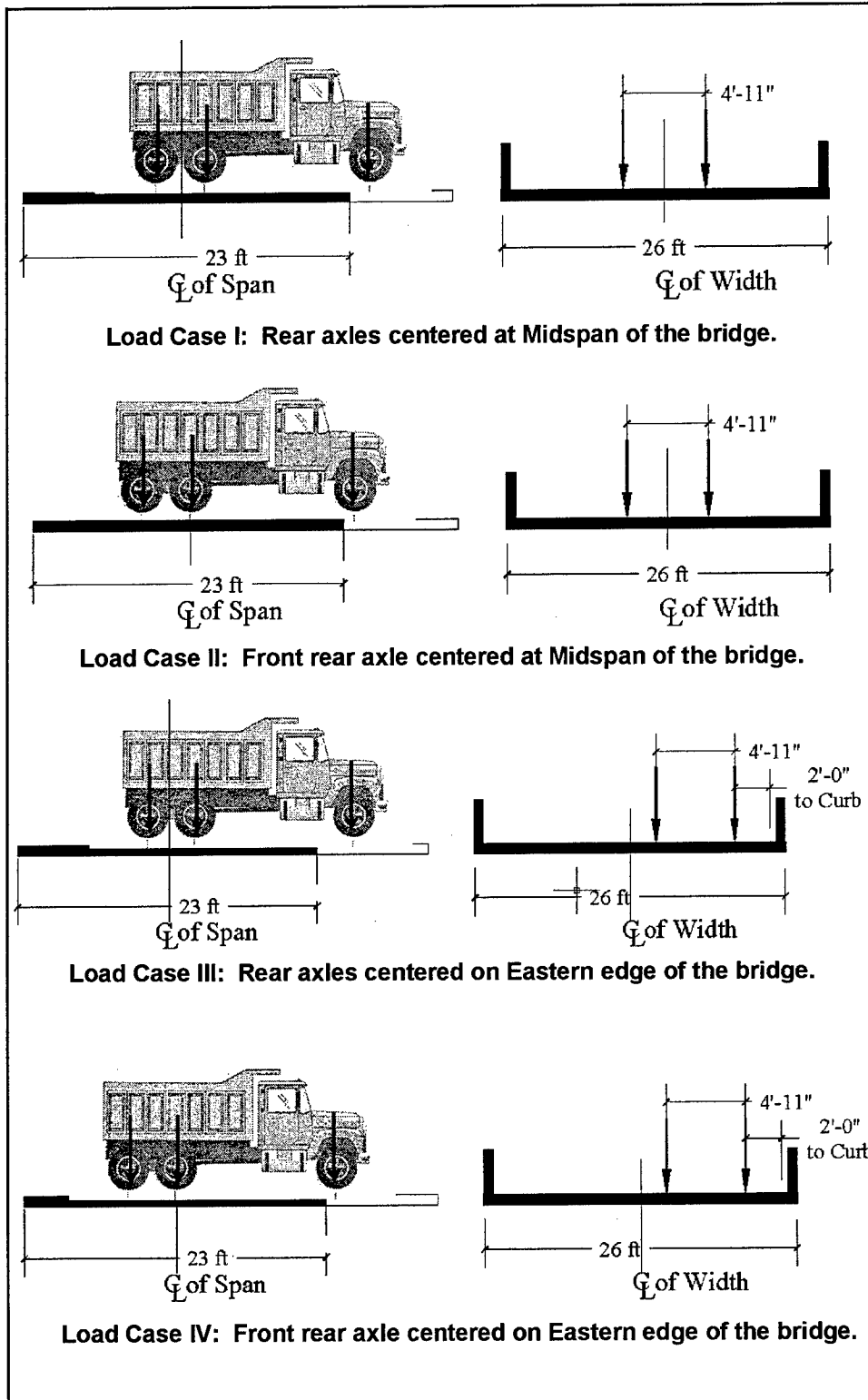
Figure 64. Load cases for service load tests

The load cases were considered to represent the most extreme loading conditions possible. Because of the transverse symmetry of the structure, only one lane was tested. Figure 65 shows Load Case I on the bridge after strengthening.

Figure 65. Load Case I on bridge P-53-702

Results of Service Load Tests

Table 44 and Table 45 summarize the strain readings for the service load tests conducted on the bridge.

Table 44
Strains for Service Load Test I (unstrengthened)

Load Case	WC-1 (με)	C-1 (με)	EC-1 (με)
I	13	15	13
II	2	16	5
III	7	9	13
IV	-9	10	30

Table 45
Strains for Service Load Test II (strengthened)

Load Case	WC-1 (με)	C-2 (με)	F-1 (με)	F-2 (με)	Centerline Avg.	EC-1 (με)	EF-1 (με)	East Avg.
I	5	3	26	12	13.7	-5	11	3
II	6	13	14	7	11.3	29	-	29
III	2	1	-	-	1.0	-6	18	6
IV	1	8	13	5	8.7	30	13	21.5

Figure 66 and Figure 67 show the strain distributions of all the four load cases for the two series of tests. For the strengthened case, the average of the concrete strains and FRP strip strain was taken.
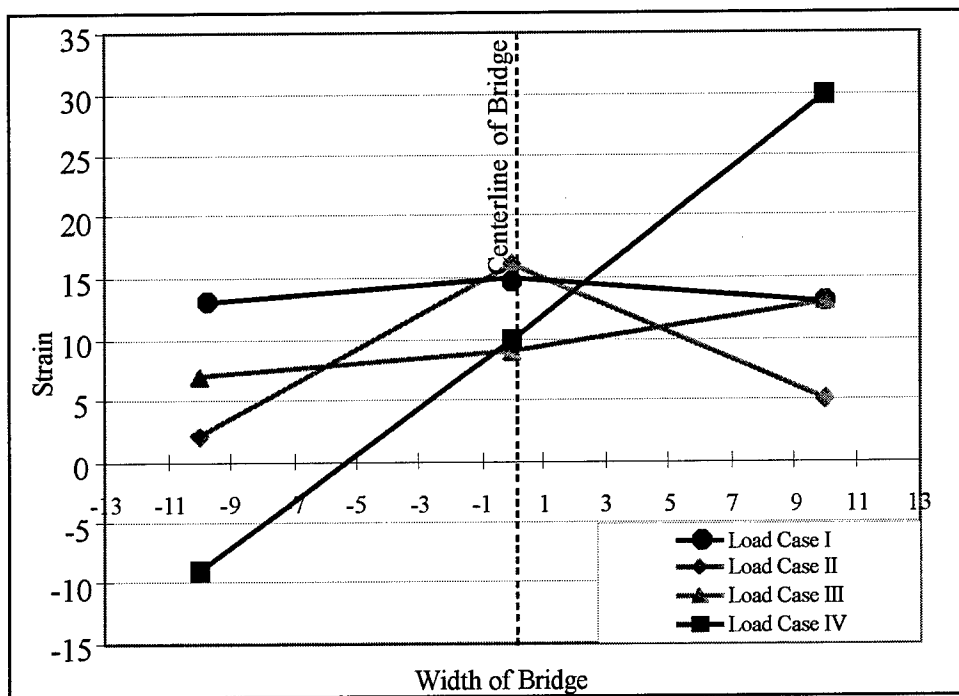
Figure 66. Strain distribution for service load tests I (unstrengthened)
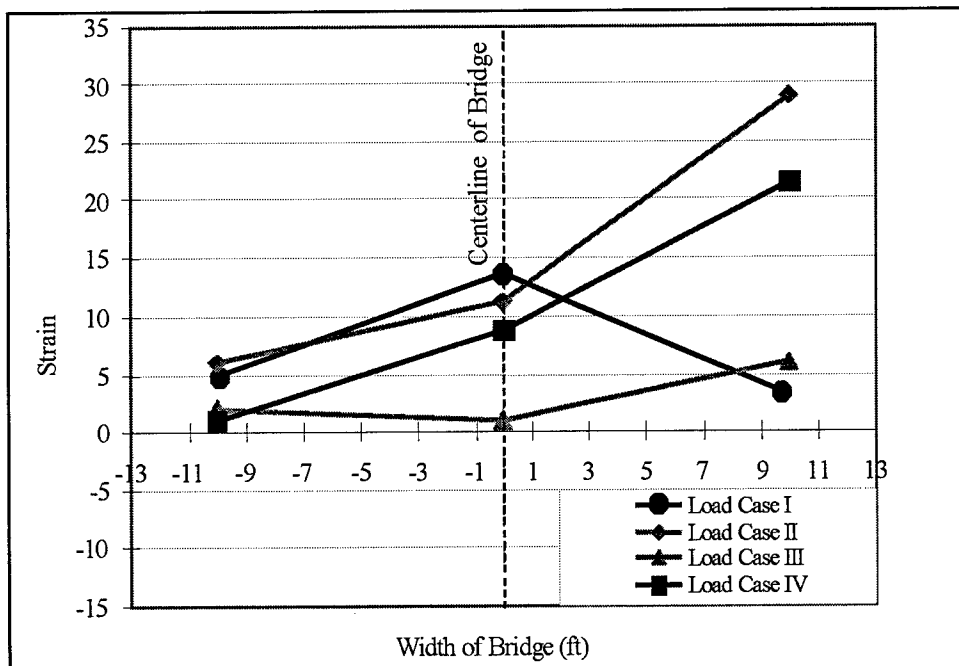
Figure 67. Average strain distribution in concrete and FRP for service load tests II (strengthened)

Discussion of Results of Service Load Tests

The largest average strain reading measured was 30με for Load Case II at the East end of the bridge. Ninety percent of the strain measurements were below the 30με. While such small strain readings may be inconclusive, some general trends were observed. The somewhat symmetrical distribution of the strain in the bridge is observed for the first two Load Cases (I and II). Figure 68 shows the plot of the strain distribution for the two series of tests, before and after the retrofit of the bridge for Load Case I. The reduction in strains is attributed to strengthening.
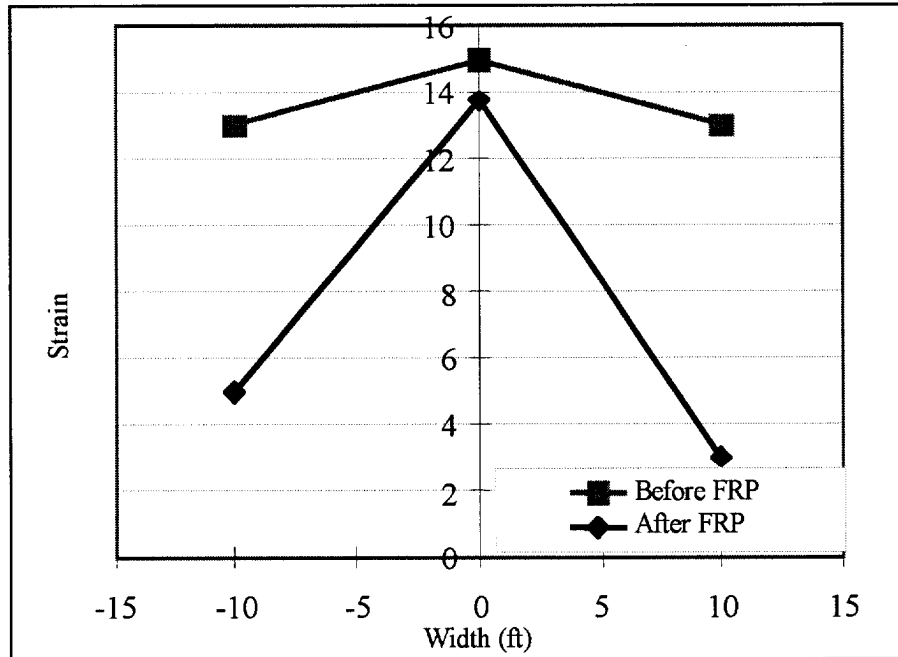
Figure 68. Strain distribution for Load Case I

While as much as a 77 percent reduction in the strain is observed on the east end of the bridge, only a 9 percent decrease in the concrete strain at the middle was observed. The highest measured strain in the FRP strip for Load Case I was 26 με corresponding to a stress in the FRP strip of 231 psi. The corresponding average stress in the FRP strip at the middle was 169 psi.

The unsymmetrical distribution seen in Load Case II after strengthening was peculiar and is difficult to explain. Similar unsymmetrical behavior has been seen in research studies conducted on existing bridges (Stallings et al. 2000). Therefore, Load Case II was not considered in later analysis. For Load Case III and IV, the unsymmetrical behavior is logical resulting from the offset loading of the truck. Figure 69 shows the strain distribution for Load Case III measured before and after the strengthening of the bridge.
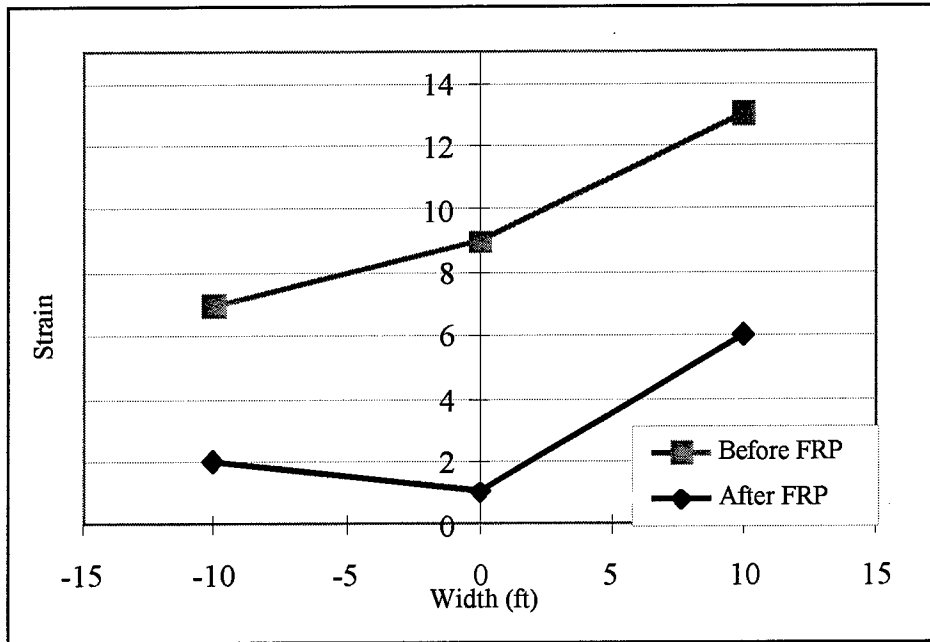
Figure 69. Strain distribution for Load Case III

A 54 percent difference in the strains measured near the load point at the east end was seen. A larger 88 percent strain difference was seen at the center of the bridge for the strengthened section. Figure 70 shows the strain distribution for Load Case IV.
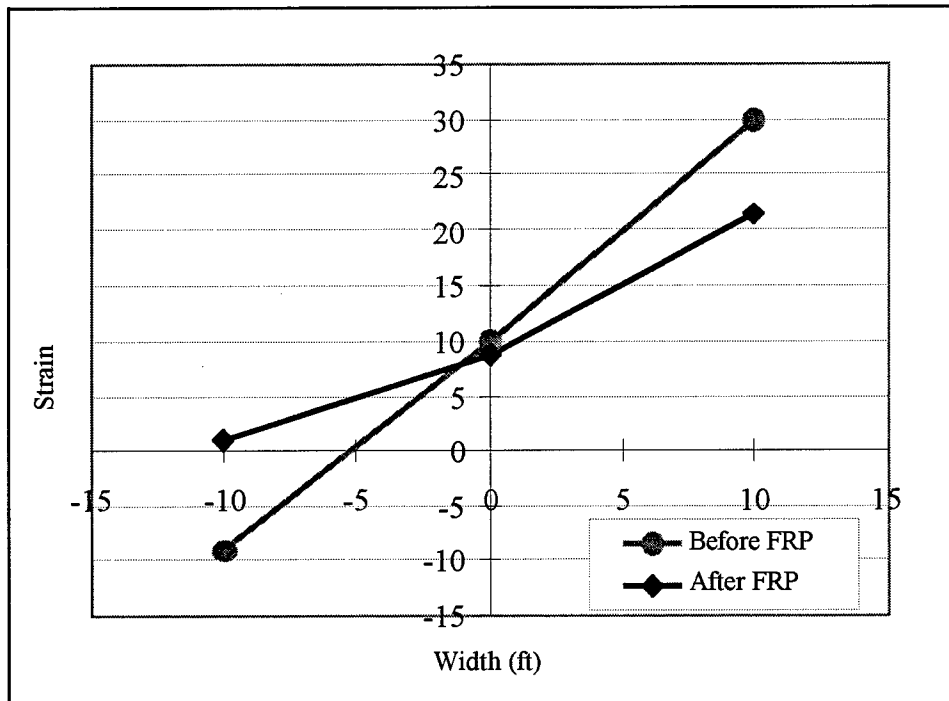
Figure 70. Strain distribution for Load Case IV

The strain distribution for the Load Case IV shows a 20 percent reduction in the concrete substrate strain in the middle of the slab, and a 28 percent reduction at the east end of the bridge where the load was located. The measured strain in the FRP strip was 13 µε corresponding to a stress in the FRP strip of 115 psi. At the west end, a negative strain corresponding to compression is seen in the concrete slab. This may be attributed to some negative bending observed in the west end, when the load was located on the opposite end. After strengthening, a positive strain corresponding to tensile stress in the concrete substrate was seen.

While the results of the service load tests produced some trends that were expected, largely the strain measurements were not significant enough to draw any definitive conclusions related to stiffness or strength increase. Strain data does, however, suggests the composite behavior of the FRP strips with the concrete slab. The reduction in concrete substrate strain and the strain measured in the FRP strips strongly suggest the transfer of stresses to the FRP strip.

Conclusions of MF-FRP Implementation Study

The first-ever full-scale implementation the MF-FRP system on an existing bridge structure proved that the method is easy to apply in the field, is economical, and can be designed using existing AASHTO procedures to increase the load rating of a bridge structure. The following specific observations and conclusions related to the full-scale field implementation can be made:

a. The total cost of materials and labor for the MF-FRP strengthening was $7,995.00. The unit cost for the 625 ft² bridge was $12.72/ft². This is a highly economical strengthening system when compared with existing epoxy-bonded systems.

b. Department of Transportation maintenance workers that had no prior training with the use of FRP composite materials easily installed the FRP strips in the field using commercial fasteners and tools.

c. The FRP strips were attached to a cracked and spalled concrete substrate without any difficulty and with minimal surface preparation (and no surface repair). An epoxy-bonded FRP strip would not have been able to be attached in these conditions.

d. The increase in moment capacity needed to increase the inventory load rating of the bridge from HS17 to HS25 was determined using standard AASHTO procedures. In order to determine the existing live load design capacity of a unit width strip of the bridge, the effective width was back calculated from the reported HS17 load rating.

e. The analysis and design of the MF-FRP strengthening system was preformed using a moment-curvature model and a simplified strength model. Parametric studies were conducted to assess the influence of different existing concrete and steel strengths. It was found that these parameters did not have a large effect on the design when the steel area was scaled for equivalent axial stiffness (EA).

f. The final design of the strengthening system was able to be accomplished in keeping with recommendations developed from prior laboratory testing. These included the use of a single row of fasteners at 3 in. spacing along the length, the use of two anchor bolts at each end of the strip, and the use of a single FRP strip at 12 in. on center spacing across the bridge.

g. Both galvanized steel and stainless steel fasteners were able to be used. No difference in the installation procedure was found for the different fasteners. Stainless steel fasteners are two to three times more expensive than galvanized steel fasteners and their use needs to be justified based on further environmental durability studies.

h. Service load testing was conducted with a 25-ton vehicle. The results of strain readings before and after the strengthening indicate that the MF-FRP system is carrying some load, however, resulting from the very low level of load used in the service load testing final conclusions could not be reached at this stage regarding strength and stiffness increases provided by the MF-FRP system. The results of the ultimate load testing described in what follows were used to demonstrate this aspect of the MF-FRP system.

6   Ultimate Load Testing and Performance of Bridge P-53-702

General

As detailed previously, Bridge P-53-702 in the City of Edgerton, Wisconsin, was strengthened in the summer of 2002 using the MF-FRP system by attaching FRP composite strips with powder-actuated fasteners to the underside of the bridge deck. The purpose of the strengthening was two-fold. First, researchers wanted to demonstrate the practicality of the installation method on a real-world structure. Attaching FRP composite strips had proven efficient in terms of manpower and time in the laboratory, but this efficiency needed to be shown in an implementation on an existing structure. Second, 3 years of studies had proven that the MF-FRP method increased the flexural capacity of laboratory specimens ranging from small-scale model beams to typical full-scale bridge beams (Bank et al. 2002a; 2002b; Borowicz 2002). The aspects of the implementation have been discussed in Chapter 4. In the summer of 2003, ten (10) months after the installation of the FRP strips on the bridge the MF-FRP strengthened bridge was tested to failure prior to its demolition and eventual replacement. In addition to providing data on the capacity and behavior of the strengthened bridge, the effect of 10 months of environmental exposure on the MF-FRP system could be evaluated.

The testing was conducted over a period of 5 days from June 16 to June 20, 2003. The testing was a joint project conducted by the University of Wisconsin–Madison and the University of Missouri–Rolla. Assistance was also provided by the United States Military Academy at West Point. The Wisconsin Department of Transportation and the United States Army Corps of Engineers provided funding for the investigation. This chapter outlines the in-place load testing procedures, documents the results of the testing, and draws conclusions as to the effectiveness of the strengthening method.

Objectives

The objectives of the ultimate load testing of Bridge P-53-702 were as follows:

  a. To conduct load testing of two sections of rehabilitated bridge to failure.
  b. To document failure modes of each test section.
  c. To gather data on the following: load applied to test sections; deflections of test sections; strain in FRP composite strips; and strain in concrete in compression zone.
  d. To synthesize the raw data into load vs deflection and moment vs deflection curves.
  e. To determine the flexural capacity of strengthened test sections and compare them to the capacity of an unstrengthened section tested in the laboratory.
  f. To document any effects on the FRP composite strips or the powder-actuated fasteners resulting from the environment.
  g. To determine the in situ properties of the materials (rebar and concrete) used in Bridge P-53-702.
  h. To characterize the mechanical properties of FRP strips before and after service.

Test Preparation

General

In order to conduct the testing of the strengthened bridge, two test sections were isolated from the rest of the bridge deck, a field loading system was erected, and a data acquisition system and instrumentation were configured. This was accomplished as follows:

Cutting of Bridge Deck

When constructed in 1930, Bridge P-53-702 had a 20-in. thick reinforced concrete deck. Over the years, however, this deck thickness was increased to nearly 26 in. with the addition of an asphalt overlay. As such, the contractor hired to isolate the two test sections had to use a concrete saw with a 54 in. diameter blade. Figure 71 shows the contractor making his initial cut (Cut No. 1) in the bridge deck.
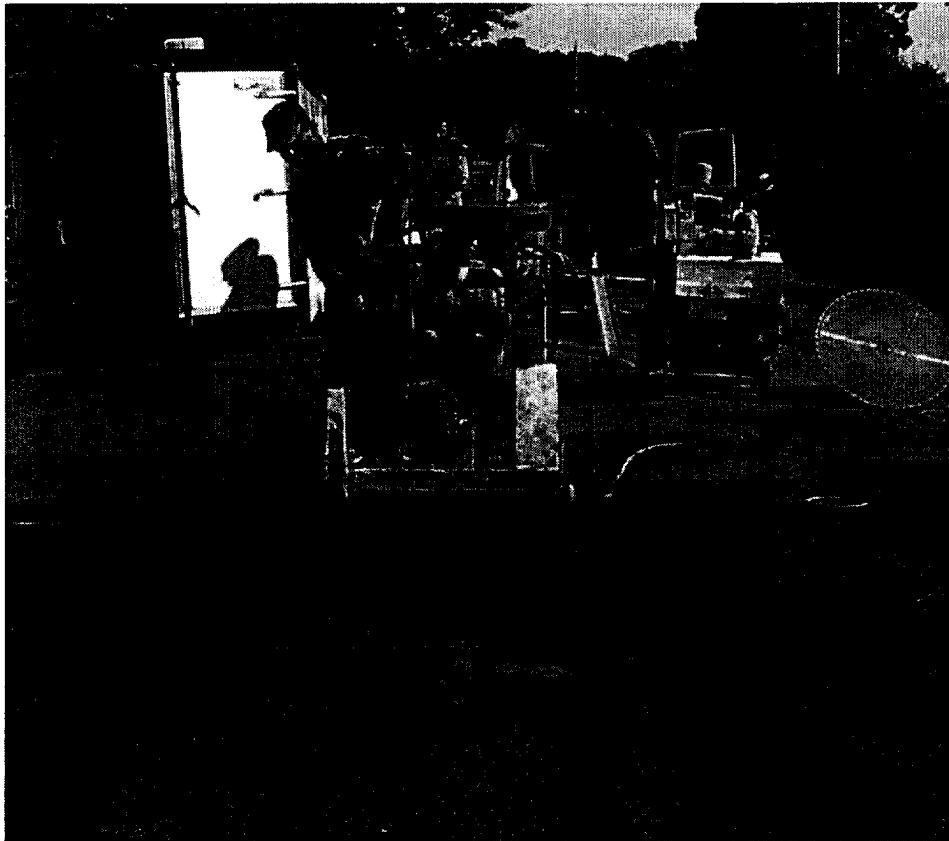
Figure 71. Contractor cutting the bridge deck (Cut No. 1)

Utilizing a rebar locator and construction drawings from the late 1920s, investigators carefully chose the location of the three longitudinal cuts. The first cut was made 6 in. west of the centerline of the bridge and served as the boundary between the two test sections. The second cut was made 43 in. west of the centerline, while the third and final cut was made 33 in. east of the centerline. The result was three cuts running the length of the bridge that separated two test sections. Figures 72 and 73 show views of the isolated test sections along the top of the bridge deck. Since the FRP composite strips were fastened 12 in. on center, both test sections contained three FRP strips spaced evenly across their respective widths. Figure 74 shows the bridge with the test sections marked.
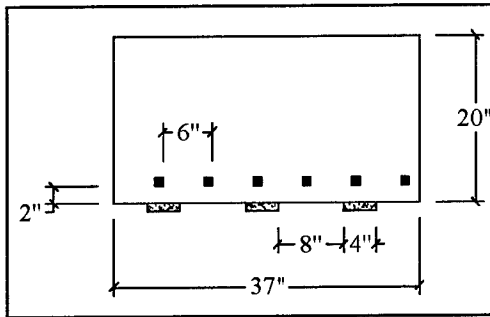
Figure 72. Transverse view of
west section
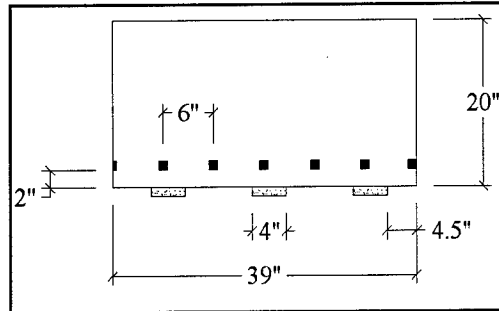
Figure 73. Transverse view of
east section
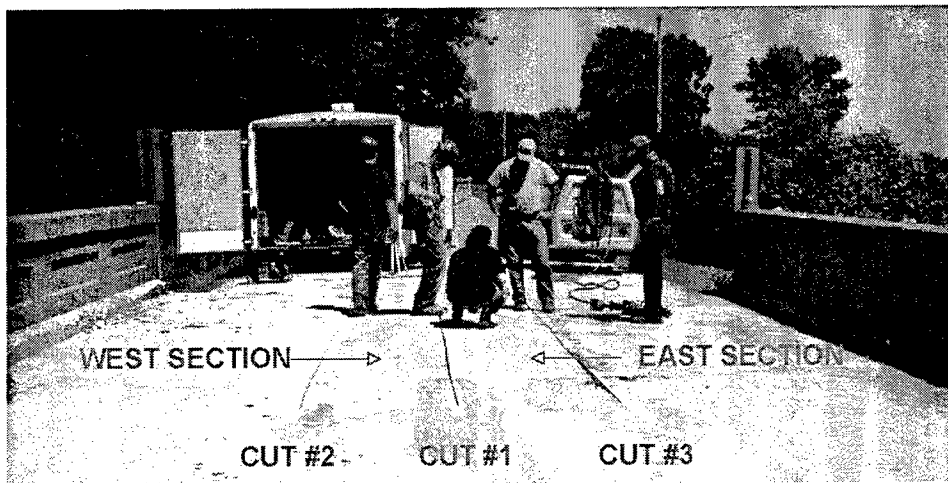
Figure 74. Test sections (looking north)

Despite using the largest concrete saw blade available (25-in. cut depth), the contractor was not able to cut through the entire depth of the bridge deck along cuts one and three (See Figure 75). In fact, the saw blade never pierced the bottom of the bridge deck along cut one. The blade found its way through the entire depth of deck along cut No. 3 four feet from the north and south abutments. The result was that the two test sections were not completely separated. Rather, the east and west sections were connected by 1.5 in. of concrete cover along the entire span length at the bottom of the deck. The east section was also connected to the adjacent untested portion of the deck by less than 1 in. of concrete cover.
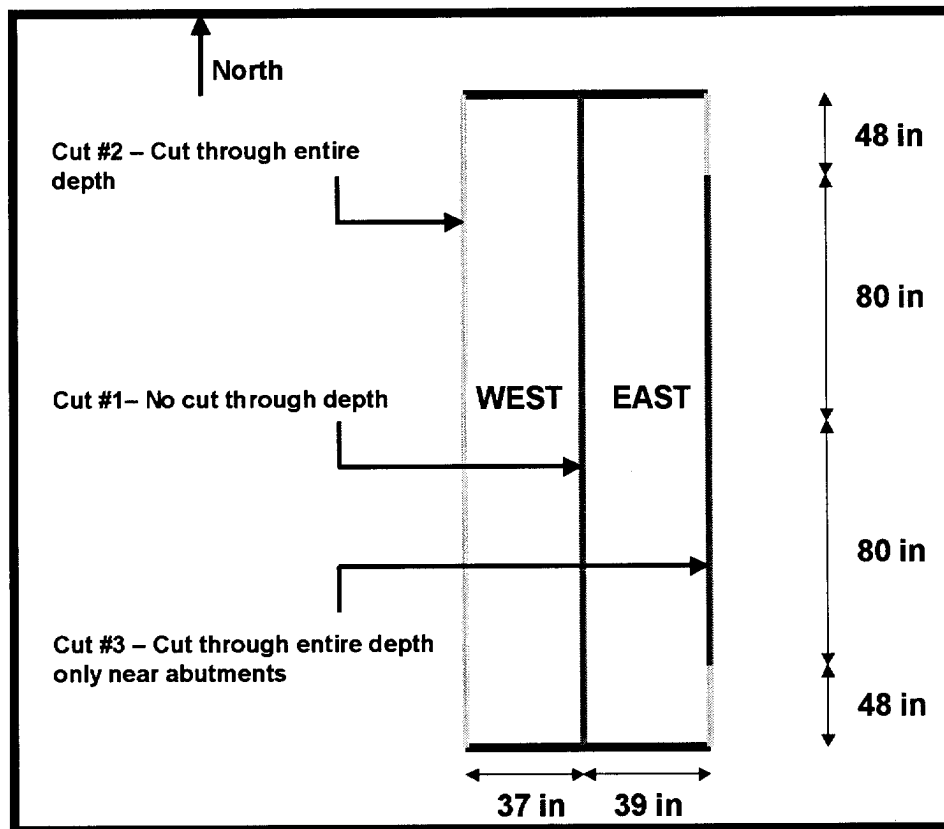
Figure 75. Top view of cut penetration

Drilling of Bridge Deck

Four holes were drilled through the full depth of the bridge deck for the installation of the test apparatus. Locations were positioned in accordance with the test assembly schematic and marked with fluorescent orange paint. In turn, the contractor drilled the 3-in. diameter holes with a standard concrete coring machine. Figure 76 shows the contractor drilling the first hole through the depth of the deck.

Previously, a fifth core had been drilled on an outboard section of the bridge to check the depth of the deck and obtain a suitable concrete core for testing. However, the concrete crumbled and thus prevented researchers from obtaining a specimen suitable for testing.

Figure 76. Contractor drilling through depth of bridge deck

Removal of Asphalt at Center of Test Sections

In order to measure the strain in the concrete at the top of the test sections (compression zone) and observe any compression failures, nearly 6 in. of asphalt overlay on the bridge deck were removed from the central portion of the test sections (See Figure77) using a 40-lb jackhammer powered by a 250 cfm air compressor. The result was a 2-ft long section that spanned both test sections and exposed the original surface of the concrete bridge deck.

Figure 77. Removing the asphalt overlay

Installation of Test Apparatus

The test apparatus consisted of the following components:

a. Two steel reaction beams
b. Two 100 kip hydraulic jacks
c. Four DYWIDAG bars with steel plates

These components were arranged in accordance with Figure 78 to provide the appropriate test configuration. This configuration placed the test sections in four-point bending with a shear span of 102 in. and a moment span of 52 in.

First, the four DYWIDAG bars were inserted through the predrilled holes in the deck and secured with reaction plates and nuts on both the top and bottom of the deck. Then the 1400 lb north and south reaction beams were lifted on to the DYWIDAG bars with a forklift (See Figure 79). When the reaction beams were plumb and level, they were locked them into place by tightening down the appropriate nuts. Next, in order to evenly distribute the applied load across the width of the test sections, the area under the jacks was leveled by placing a 36 in. 3 12 in. 3 1 in. steel plate on top of a layer of high-strength, quick-setting grout. After the grout cured, the jacks were centered on the steel plates, bringing them into contact with the reaction beams. Finally, members of the Rock County (Wisconsin) Department of Roads and Grounds positioned two dump trucks (loaded to a weight of 55,000 lb) on alternate ends of the untested sections of the bridge to prevent these sections from lifting off their respective abutments during the testing.

Assembly Details - Test of West Section (dimensions in inches)
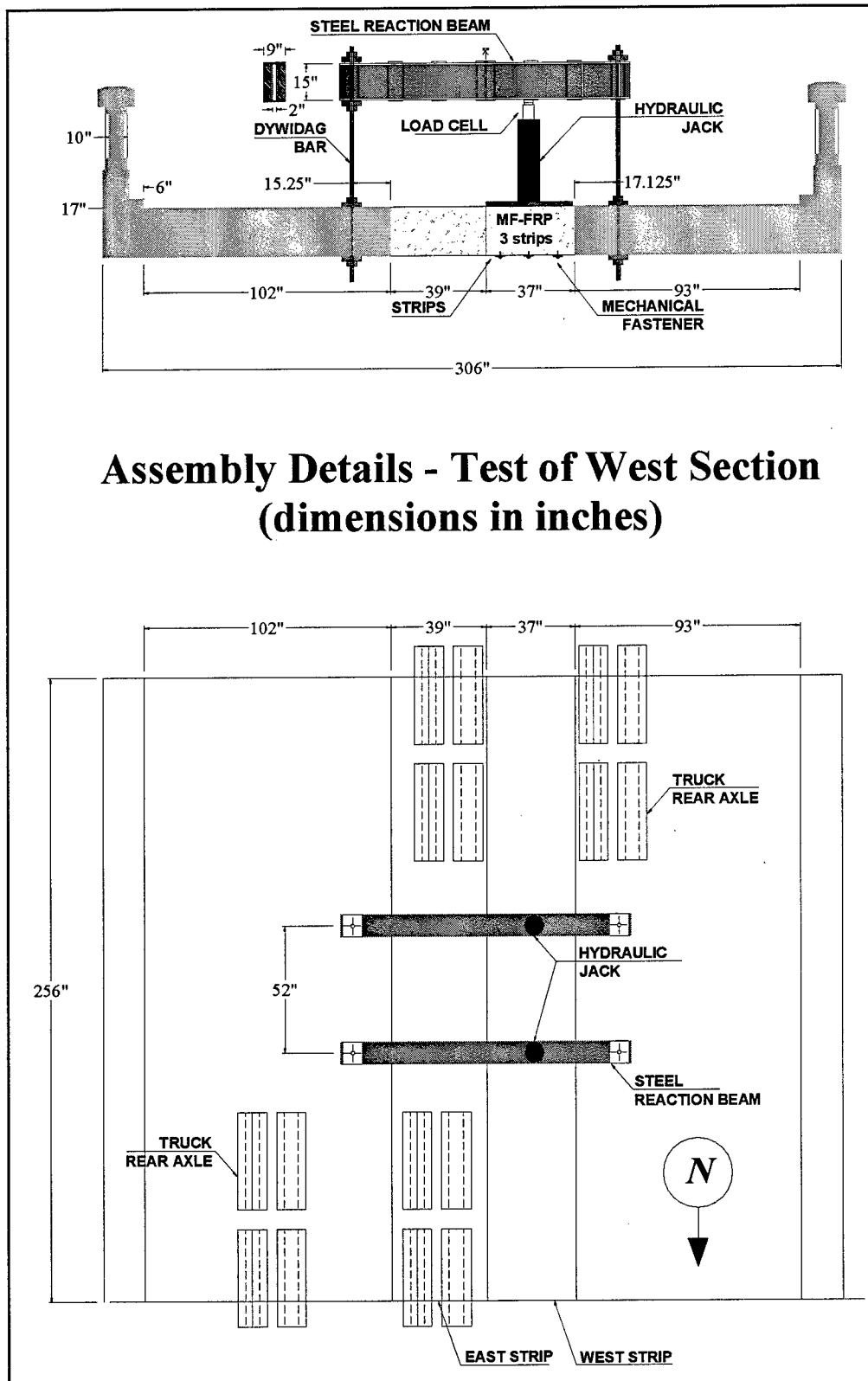
Figure 78. Schematic of test assembly
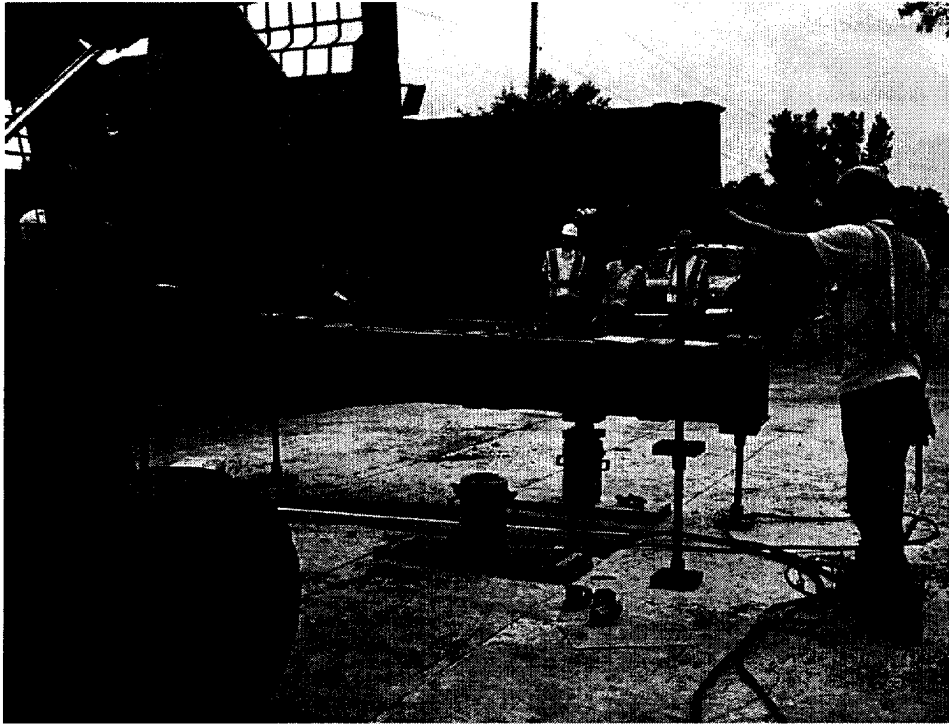
Figure 79. Placing the north reaction beam

Installation of Instrumentation

In order to collect sufficient data, nine DC-LVDTs were used to measure displacement and five 120-ohm strain gages were used to obtain the strain in the FRP composite strips fastened to the bottom of the bridge. Figure 80 shows the layout of the data collection assets for the west section, while Figure 81 shows the arrangement for the east section.
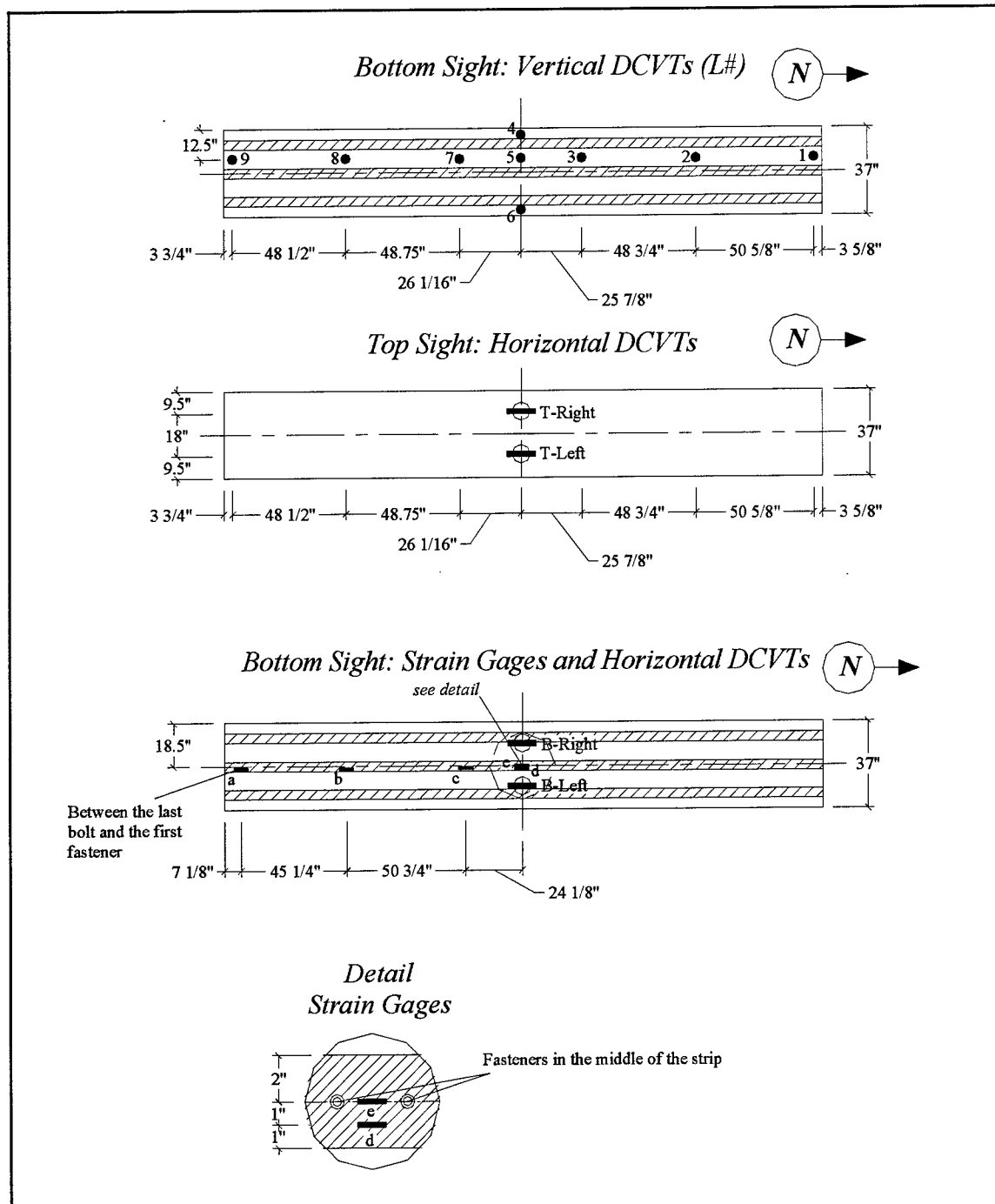
Figure 80. West section instrumentation

Bottom Sight: Vertical (L#) and Horizontal DCVTs (N→)

9 (outside between the 2 loads applied)

17.125"

B-Right

4 — 39"

B-Left

1 (outside between the 2 loads applied)

15.5"

Top Sight: Vertical (L#) and Horizontal DCVTs (N→)

8.96"

B-Right

18"

5

B-Left

9.75"

8● 7● 6 3● 2● 39"

50 1/4" 48.75" 48 3/4" 54 5/16"

26 1/16"

25 7/8"

Bottom Sight: Strain Gages (N→)

see detail

a b c e d 39"

Between the last bolt and the first fastener

7" 47 1/4" 50 7/16" 24"

Detail Strain Gages

Fasteners in the middle of the strip

2"

1"

1"

e

d

Figure 81. East section instrumentation

Test Execution

General

Three major tasks were accomplished during the execution of the load test. First, since both the east and west test sections were still partially attached to adjacent sections, the first load cycle was used to crack the bottom cover that connected the respective sections. Second, a valid load-deflection curve that captured both the yield and ultimate of the rehabilitated test section needed to be obtained. To that end, the manual application of the load (via hydraulic jacks and hand pump) in discrete cycles was carefully controlled. Finally, once the load had reached a plateau at its ultimate, the point at which the FRP composite strips failed needed to be identified. The intention was to accomplish this by continually applying load until a failure in the strips occurred. Figure 82 shows the final preparations prior to testing the west section.
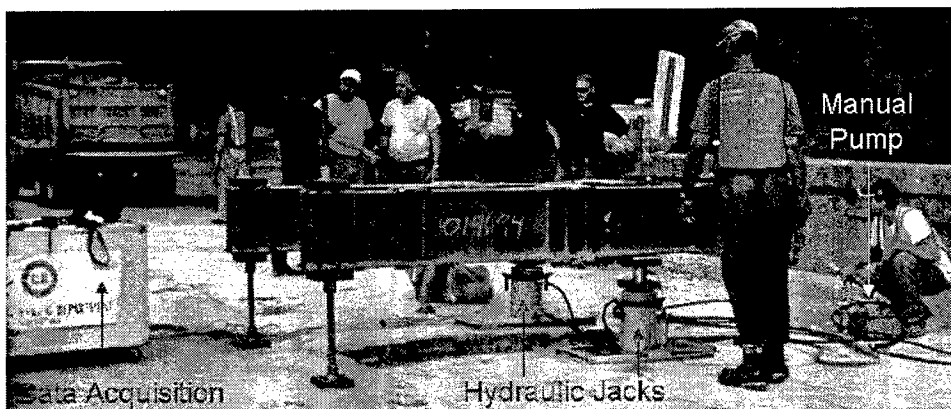
Figure 82. Preparing to execute load test on west section

West Section

Since the west section was still connected to the east section at cut No. 1, the first load cycle was used to crack the 1.5 in. of concrete cover. This load cycle was started at zero and was taken to a total load of 20 kips (10 kips per jack). The load was then removed and a load sequence (See Figure 83) consisting of the following cycles began:

  a. 0 kips to 40 kips total load
  b. 0 kips to 60 kips total load
  c. 0 kips to attempted failure of the west section

Figure 83. Testing the west section

East Section

After analyzing the raw data from the test of the west section, it was decided not to test the east section in its initial configuration (see additional discussion in the Test Results section). In an effort to show the strengthening effect of attaching additional material, two additional 4 in. FRP composite strips were attached to the underside of the east section using a single row of ALH fasteners spaced 3 in. on center (See Figure 84). The result was five total FRP composite strips spaced at 6 in. on center (Figures 85 and 86).
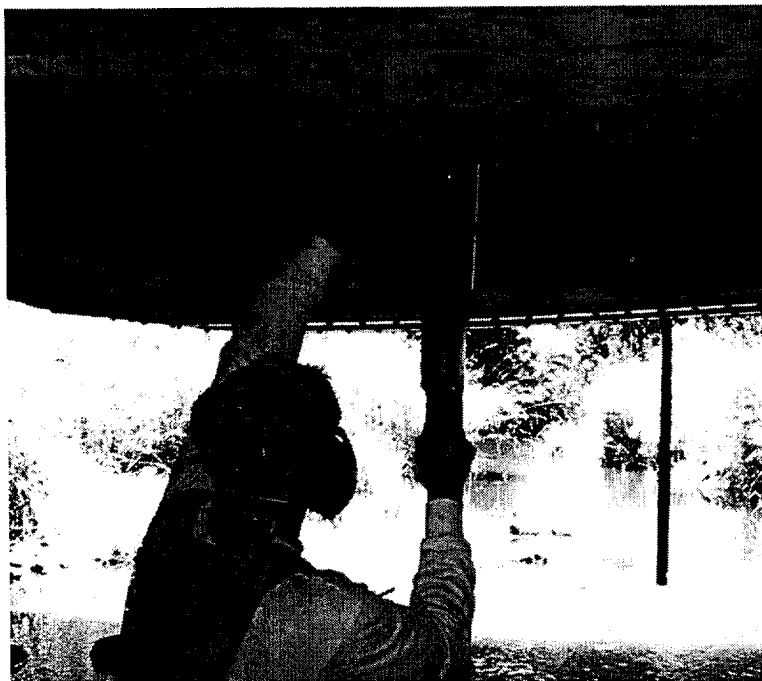
Figure 84. Predrilling the concrete prior to fastening the first additional strip
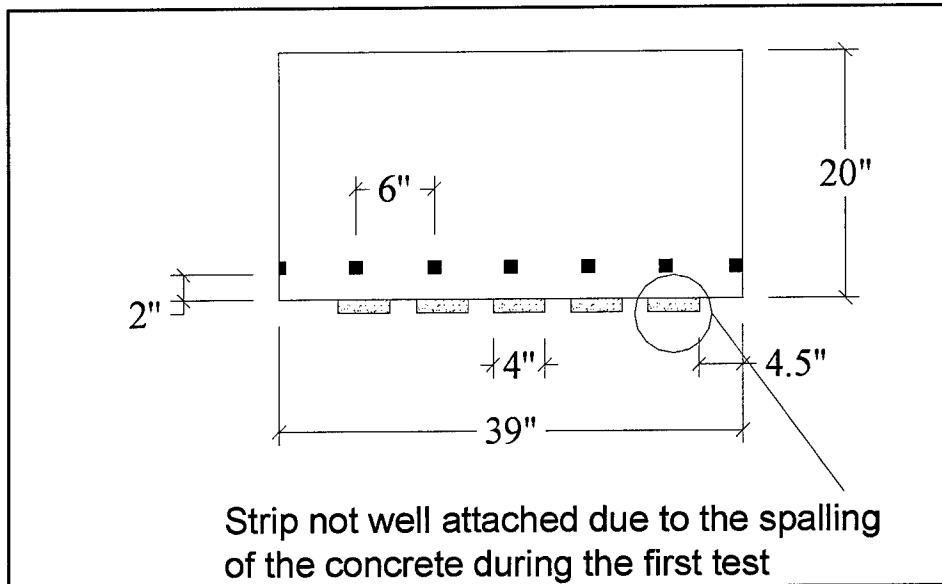
Figure 85. Transverse view of east section after addition of two FRP strips
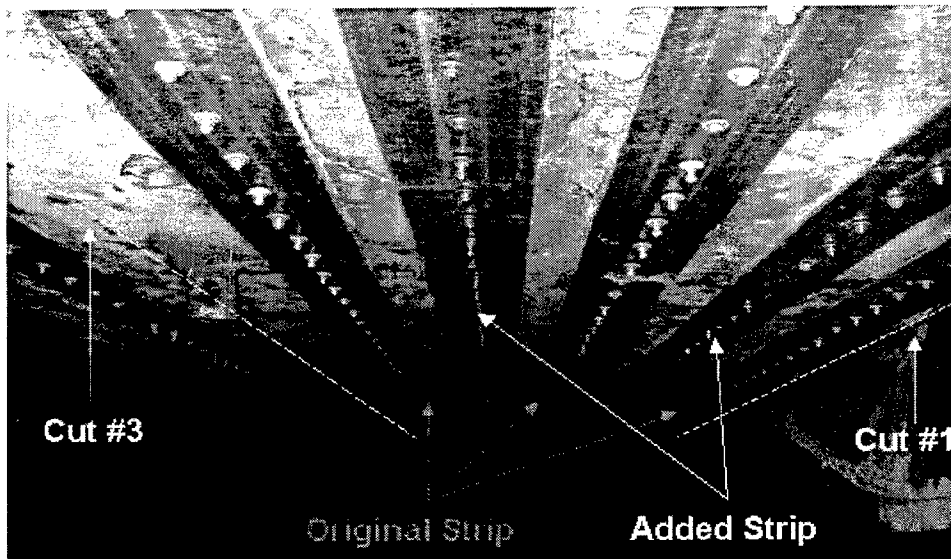
Figure 86. View of east section with two additional FRP strips (looking south)

Since the east section was still connected to the untested section of the deck at cut No. 3, the first load cycle was used to crack the 1.0 in. thick concrete cover along the bottom of the deck. This load cycle was started at zero and was taken to a total load of 20 kips (10 kips per jack). The load was then removed and a load sequence (See Figure 87) consisting of the following cycles began:

    a.   0 kips to 40 kips total load

    b.   0 kips to 60 kips total load

    c.   0 kips to 90 kips total load

    d.   0 kips to attempted failure of rehabilitated east section
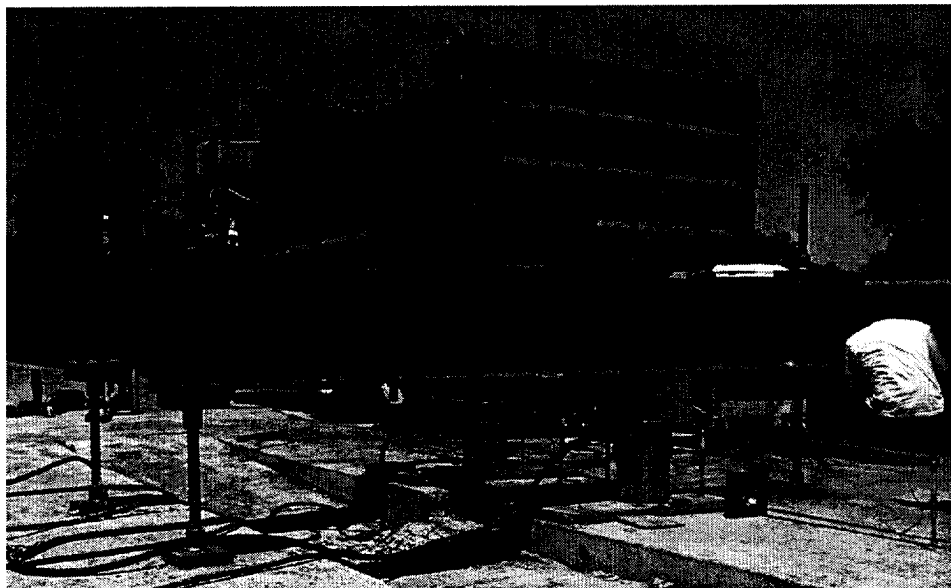
Figure 87. Testing the east section

Data Collection

At approximately 3.5 in. of midspan deflection during both tests, the final load cycle was stopped and the data collection assets were removed from under the bridge so as not to damage the instruments. The test then continued by imposing a large deflection (approximately 8 in.) in an attempt to achieve failure of the FRP composite strengthening system.

Test Results

General

During the testing of each section, load, deflection, and strain data were recorded in accordance with the collection plan outlined. The failure mode of each test section was documented and the condition of the FRP composite strengthening system (including the strips and the fasteners) was noted.

West Section

The west test section failed via concrete crushing in the compression zone. Figure 88 shows the crushed concrete along the top of the west section. Despite this failure, load continued to be applied to the structure in an effort to force a failure in the FRP composite strengthening system. This failure came at a midspan deflection of nearly 8 in. Considerable concrete spalling and a large shear crack opened (Figures 89 and 90) along the southeastern portion of the west test section causing one of the composite strips to detach. Simply stated, the fasteners no longer had any concrete to "hold on" to in this area.
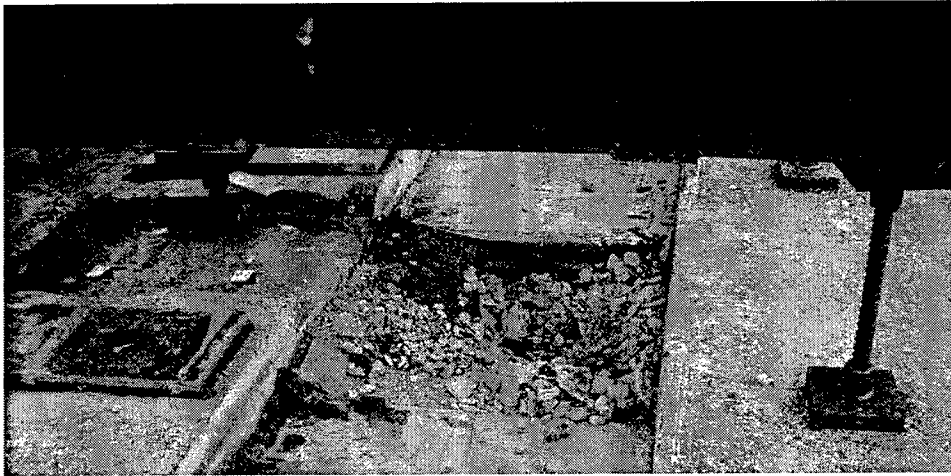

Figure 88. Concrete crushing failure along top of west section
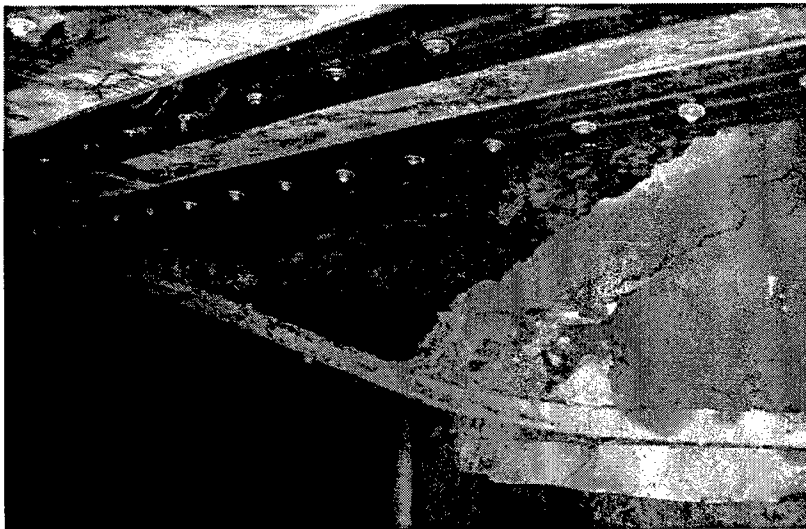
Figure 89. Shear failure and spalling along southeast portion of west section

Figure 90. Flexural cracks at midspan of west section (during test)

Of particular interest during this test was the behavior of the fasteners along the length of the FRP composite strips. As the west test section continued to deflect, the fasteners did not cause a "slotting" or progressive bearing failure in the FRP composite strip as seen in some laboratory tests. Rather, they remained embedded in the concrete and rotated (head of fastener away from midspan of section) as the deflection increased. Figure 91 shows this rotation of the fasteners along the length of the west section.
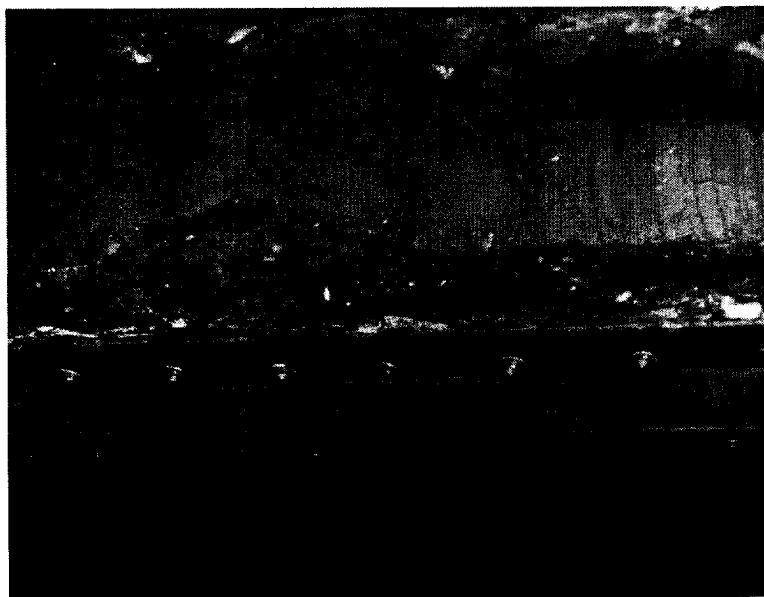
Figure 91. View of rotated fasteners along length of west section

East Section

The east test section failed via concrete crushing in the compression zone (Figure 92). Despite this failure, load continued to be applied to the structure in an effort to force a failure in the FRP composite strengthening system. However, after nearly 7 in. of midspan deflection, the FRP composite strengthening system was still intact (Figure 93). The test was halted at this point for two reasons. First, the east section came in contact with the west section, which started to deflect as well. Consequently, safety became a primary concern. Second, the laptop computer used in conjunction with the data acquisition system lost its charge and could not be recharged on site.
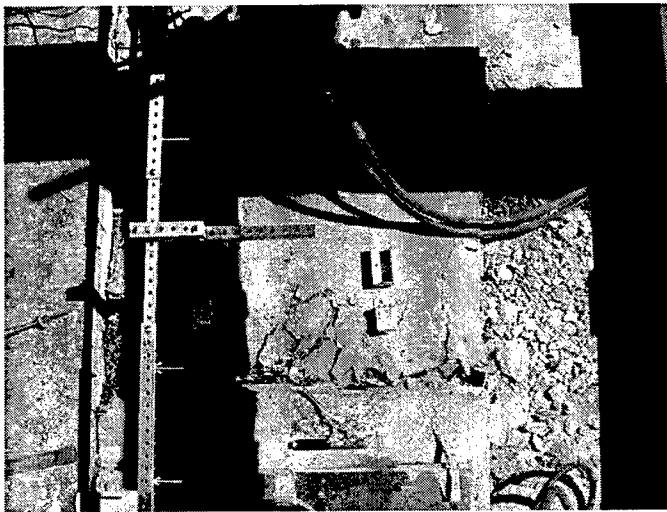
Figure 92. Concrete crushing along top of east section
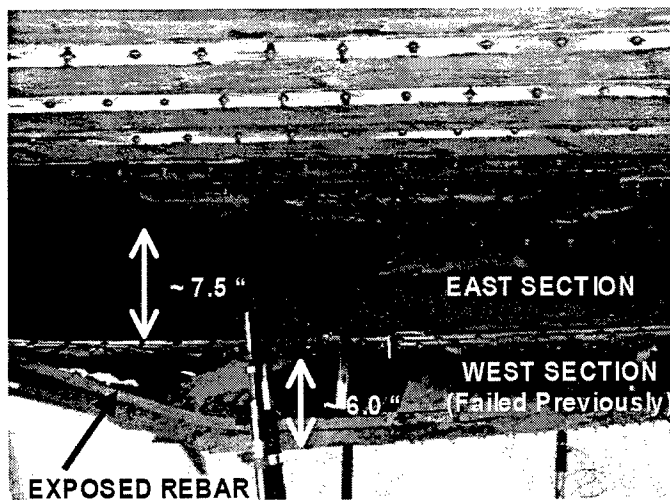
Figure 93. View of deflected east section (foreground)

While the FRP strengthening system remained intact, there were signs that the fasteners and composite strips were under considerable strain (Figure 94). First, the fasteners rotated just as they had in the test of the west section. In fact, this rotation caused some of the fasteners to loosen to the point of falling out of the concrete deck. Second, the large force transferred into the composite strips coupled with the great deflection of the section damaged the strip at some fastener locations. It seemed as if that combination of force and deflection was pulling the strip right through some fasteners.
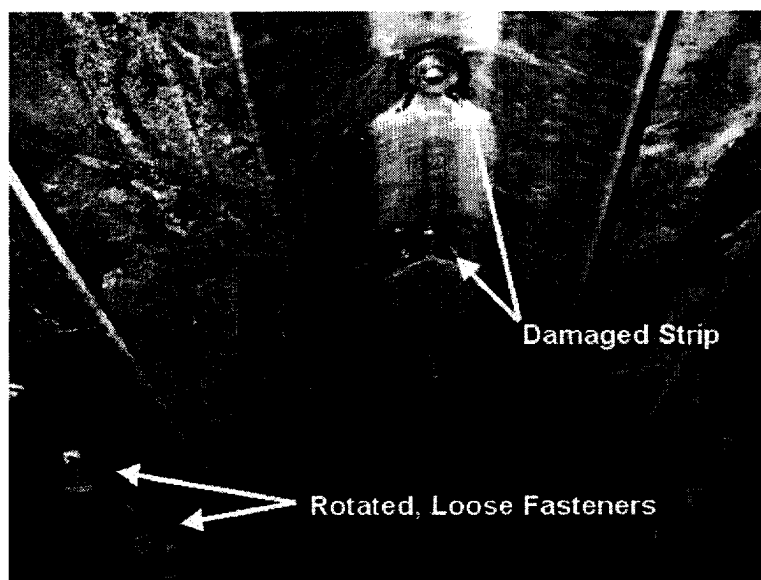
Figure 94. View of strips on east section after test completion

Data Analysis

General

Data analysis included the reduction of raw data to a form that would enable evaluation of the performance of the MF-FRP system. Both the amount of strengthening provided and the long-term durability of the system were of interest. The first step in this process was to determine the material properties of the components of the original bridge and to confirm the mechanical properties of the FRP strips. Next, load vs deflection and moment capacity vs deflection graphs were plotted in order to determine the strengthening effect of the system. The strengthening achieved in practice was compared to the original design requirement for the strengthening system discussed in Chapter 3. Finally, the effect of the environmental on the FRP composite strengthening system was documented.

Verification of Bridge Materials and Original Design

After the testing was completed, a construction contractor demolished the bridge. This proved to a valuable opportunity to gather construction materials and verify the layout of the steel reinforcement in the bridge deck. Plans used to analyze Bridge P-53-702 were not specific to its construction since its plans were no longer on file. That is, the plans were of a typical bridge built during that era and left some doubt as to their applicability to Bridge P-53-702. Figure 95 shows the demolition of the deck. The FRP strips can be seen still partially attached to the test sections.
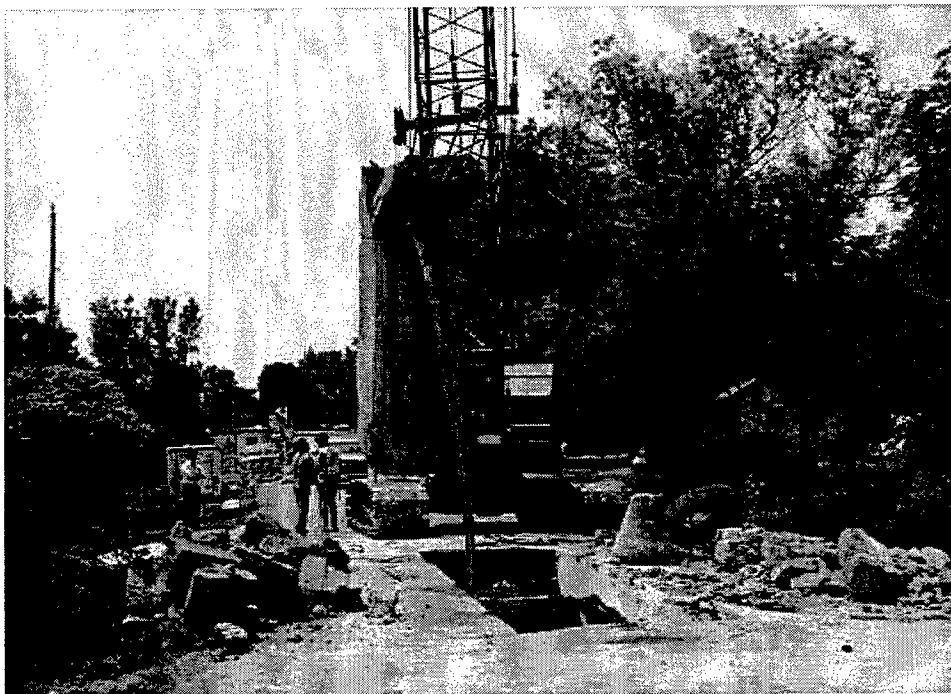
Figure 95. Demolition of the bridge

It was found that the major steel reinforcement was laid out as anticipated. The flexural reinforcement was indeed 1-in. square bars (with deformations) spaced 6 in. on center and covered by 2 in. of concrete along the bottom of the bridge deck. Figure 96 shows the spacing of the steel reinforcement in one of the demolished sections of the bridge. Note that contrary to the initial assumptions there were no bars in the compression zone (top of deck). One-fourth inch square transverse bars spaced 18 in. on center were used to tie the main bars together. Every fourth main bar was bent at the 1/4 point for shear reinforcement. All main bars were hooked on their ends. No reinforcement was found to exist between the abutment and the deck itself. Consequently, the assumption of a simply supported deck (and test sections) was valid.
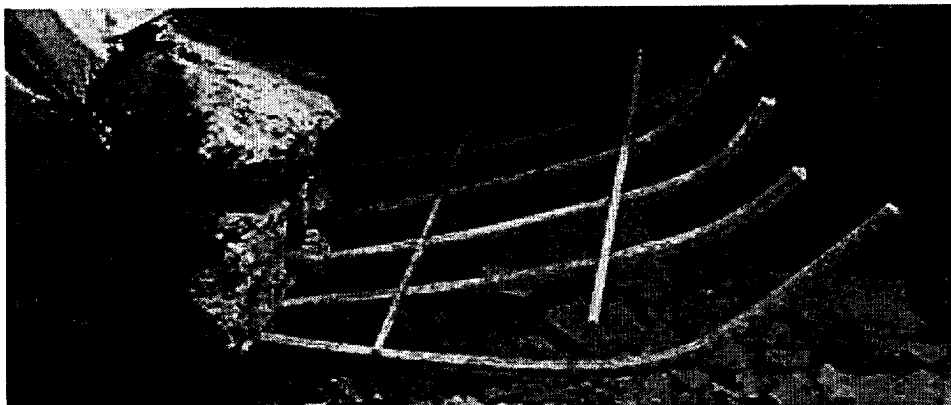
Figure 96. View of flexural steel spaced 6 in. on center

The strength of the steel reinforcement and the compressive strength of the 73 year-old concrete were also determined. The AASHTO Manual for Condition Evaluation of Bridges (2000) recommends using a tensile strength of 33,000 psi for the steel and compressive strength of 2,500 psi for concrete used in construction during this era for the purposes of load rating calculations. These were used in the design of the strengthening system as described previously. Attempts to extract useable concrete cylinders from the bridge deck were unsuccessful, as the concrete crumbled apart during each trial. Instead, large chunks of concrete were taken to the UW laboratory for testing. Varying lengths of the 1–in. square steel bars were also taken for testing.

The concrete was tested using a rebound hammer and was found to have a compressive strength of 2210 psi +\- 553 psi. These results, however, are only a guide in that the effectiveness of the rebound hammer comes into question when it is used on concrete greater than 56 days old and applied to uneven surfaces. Nevertheless, these results imply that using the recommended strength of 2,500 psi is reasonable for analysis.

Two separate lengths of the main steel reinforcement were tested to failure in tension in a universal testing machine. The average yield strength of the steel was 35,000 psi, while the average ultimate strength was 54,000 psi. Figure 97 shows the condition of the two test specimens after failure. This confirms the recommendations of the AASHTO manual for the yield strength of the steel reinforcement from this era.
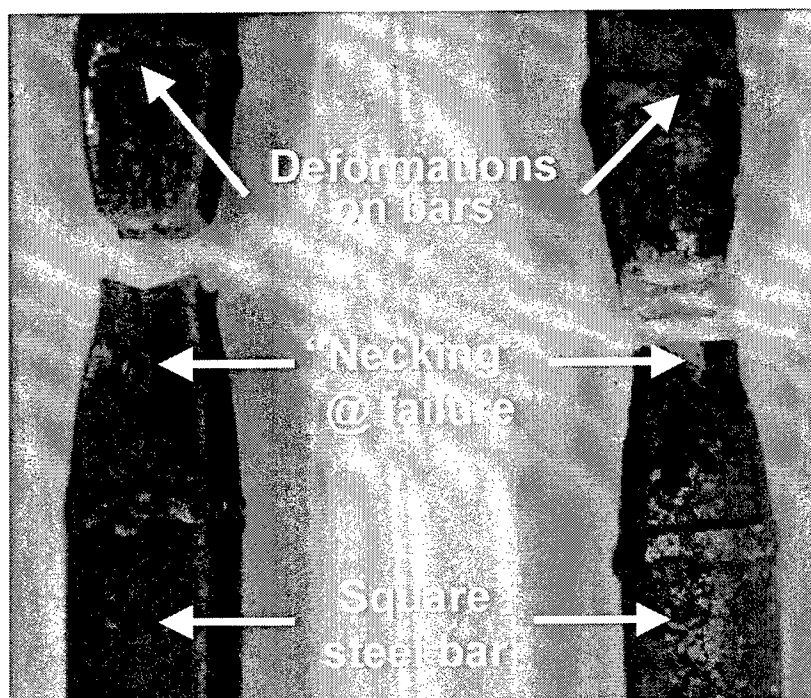
Figure 97. Steel samples postfailure

Load and Deformation of the Strengthened Bridge

The total load vs deflection curve and the bending moment vs deflection curve were plotted to determine the effectiveness of the MF-FRP composite strengthening system. The total load was taken as the sum of the forces from the two separate actuators, while the midspan deflections was taken from the DC-LVDTs located along the bottom of each section from positions L5 and L4, as shown in Figures 80 and 81, for the west and the east sections, respectively.

The behavior of the strengthened sections was compared to an unstrengthened (control) section. One of the sections was originally intended to be tested as a control section to obtain control data for the bridge; however, this was not done. During the testing it was decided that it would be more beneficial to the research study to attempt to increase the level of strengthening by adding two additional FRP strips to the east section (the second section tested), than to do a control test. The reason for this was that the results obtained from the first (west) section tested were felt to be somewhat inconclusive with regard to the strengthening effect and the attachment of the FRP strips. It was thought that the results may have been affected by the fact that the two sections were still partially connected when the section reached its yield load. In order to obtain control data for the unstrengthened bridge, a control beam tested in the UW laboratory was used (Arora 2003). Test results from a 20 3 20 in. beam having the same length as the bridge were scaled to account for the larger size of the bridge sections and the difference in loading configuration and material properties used in the laboratory. It is important to note that the laboratory beam used steel with a nominal 60 ksi yield strength that may have had more postyield

hardening than the existing ~33 ksi yield steel in the bridge (even though the steel area in the control beam was scaled by the ratio of the yield strengths). Therefore, the postyield increase in the control beam shown may not truly represent the real bridge, but nevertheless serves as a good indicator of the unstrengthened bridge's behavior. In addition, the laboratory control beam used 5,000-psi concrete. However, in the parametric studies conducted it was seen that the concrete strength did not significantly influence the load carrying capacity.

While the scaled loads obtained from the laboratory control beam are felt to be representative of the unstrengthened bridge structure, the deflections obtained in the laboratory are not felt to be appropriately scaled to represent the bridge section. It is felt that the overlay on the bridge and the partial fixity it caused at the supports probably increased the stiffness of the bridge sections in the preyield regime.

The results of the load-deflection behavior for the strengthened bridge sections are compared to the scaled laboratory control beam in Figure 98 and 99.
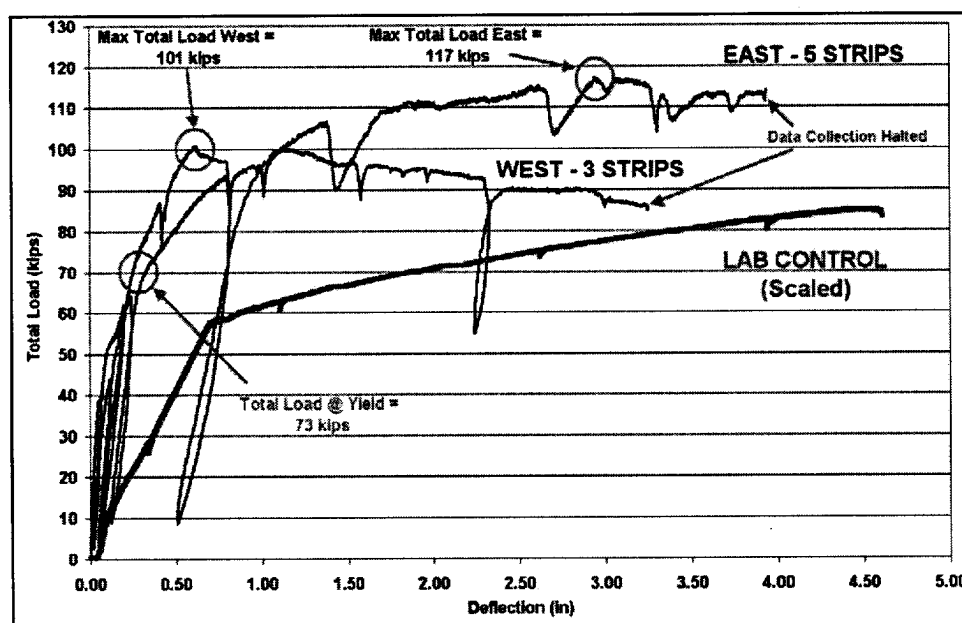

Figure 98. Total load vs midspan deflection results
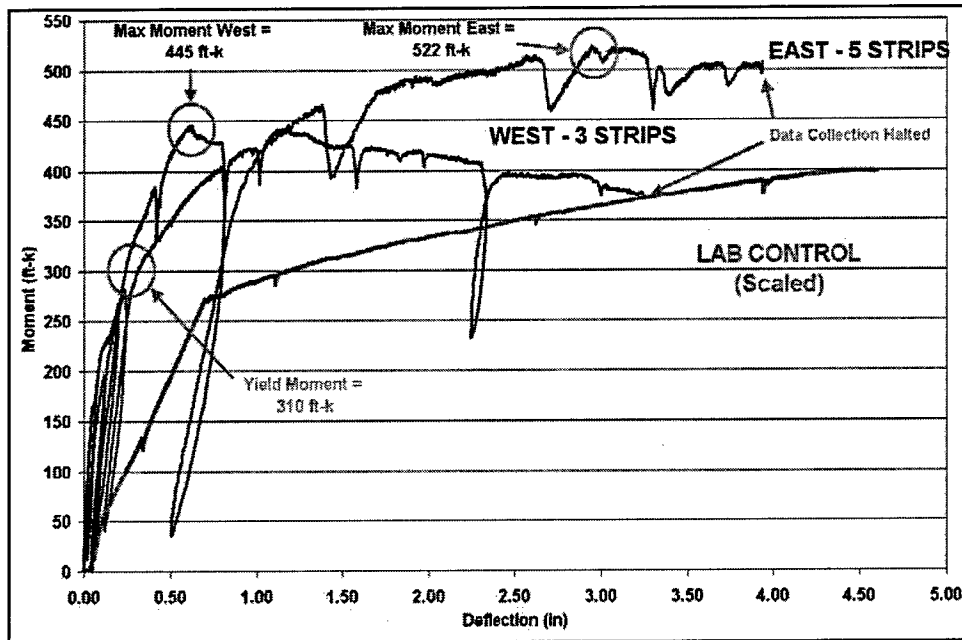
Figure 99. Moment vs midspan deflection results

Figures 98 and 99 clearly show the strengthening effect of the MF-FRP system. Table 46 summarizes the test results for the east and west test sections and compares them to the scaled laboratory control beam. Table 47 provides the results per unit width of the bridge for comparison to the design requirements.

Table 46								
Summary of Ultimate Test Results								
Test Section	No. of Strips	Yield Mom. (ft-k)	% Inc	Ult Mom. (ft-k)	% Inc	% inc wrt. own yield	Mom. @ 2" (ft-k)	% Inc
Control	None	272	-	399	-	-	333	-
West	3	310	14.0	445	11.5	43.5	417	25.2
East	5	310	14.0	522	30.8	68.4	492	47.7
Note: Failure mode for all sections was concrete compression.								

Table 47					
Ultimate Test Results per Unit Width					
Test Section	No. of Strips	Yield Mom. (k-ft/ft)	% Inc	Ult Mom. (k-ft/ft)	% Inc
Control	None	86.1	-	125.2	-
West	3	95.4	10.8	136.9	9.3
East	5	100.5	16.7	169.2	35.1

The predicted nominal strength per unit width for the existing HS17 rating and the required design nominal strength per unit width to increase the load rating to HS 25 were calculated to be (Table 46), 94.6 k-ft/ft and 122.1 k-ft/ft,

respectively. As noted previously a 29 percent increase in nominal moment capacity was required to increase the load rating.

Discussion of Test Results

The yield moments for the two strengthened sections were similar and approximately 14.0 percent higher than that of the scaled control beam. Since both test sections yielded at the same load level, the results appear to be reasonable.

As noted earlier, it is not possible to compare the preyield stiffness of the two beams. It is difficult to explain why the west section (3 strips) is stiffer than the east section (5 strips) in the postyielding regime. The effect of loading and unloading close (60 kips) to the yield load may have had some adverse effect on the behavior of the sections near the yield load.

The strengthening on the east section (three strips) appears to have begun to lose its effectiveness soon after the maximum load was achieved. The fastener rotation described earlier may have occurred at this time. In addition, the shear crack in the concrete section itself probably weakened the section at this time. The strengthening system on the west section (5 strips) appears to have remained attached and effective the full duration of the measured load test. (Recall that the instrumentation was removed at approximately 4 in. of deflection, but that the test was continued without recording data.) Load drops during the loading were resulting from breaks in the load application (and hence load drop-off resulting from the loss of hydraulic pressure in the jacks). This can be confirmed by observing the large hysteresis loop seen at the unloading and reloading cycle at 90 kips.

The ultimate or maximum moments carried by the strengthened test sections were considerably higher than the scaled laboratory control beam. These results not only show the increased capacity of the sections resulting from the MF-FRP composite strengthening system, but also show the benefit of using additional composite strips. With respect to the scaled laboratory control beam, the three strips spaced at 12 in. on center increased the capacity of the west section by 11.5 percent, while five strips spaced 6 in. on center improved the moment capacity of the east section by 30.8 percent. Investigation with respect to their own yield moments reveals that the west section and east section improved by 43.5 percent and 68.4 percent, respectively. Given that the original bridge may not have had such a pronounced strain-hardening regime as the laboratory control beam it is possible that the original ultimate strength of the bridge may have been less than the control. If the original section experienced no strain hardening, the yield strength of the two test sections can be taken as good indicator of the ultimate capacity of the original bridge. Typical deflection limitations for a structure of this type are L/800 (0.32 in. for Bridge P-53-702). Load carrying capacity was also compared at a deflection of 2 in. of deflection (L/128). At this large deflection, the west section showed a 25.2 percent greater capacity, while the east section showed a 47.7 percent greater capacity than the scaled laboratory control.

From the results shown in Table 47 it can be seen that the required increase in strength was achieved by the east section and probably by the west section; however, this depends on the ultimate strength of the existing section, which is open to some question. Analysis of detailed strain data still to be conducted and further modeling of the behavior is expected to clarify this issue.

Environmental Effects on the MF-FRP System

The strengthening system was in place for nearly 10 months and was subjected to the extremes of Wisconsin weather. These extremes included hot, humid summer days with temperatures in excess of 90 degrees and cold winter days with temperatures (including wind-chill) well below zero. Examination of the FRP composite strips and powder-actuated fasteners prior to the ultimate load testing led to the following observations:

a. All the strips were attached firmly to the concrete underside and no sign of any damage was seen.

b. The underside was in good condition and no additional deterioration was seen as compared to the year before.

c. No stalactites were seen on the soffit near or around the FRP strips and the substrate seemed in fair condition. Figure 100 shows the overall view of the underside after one winter.
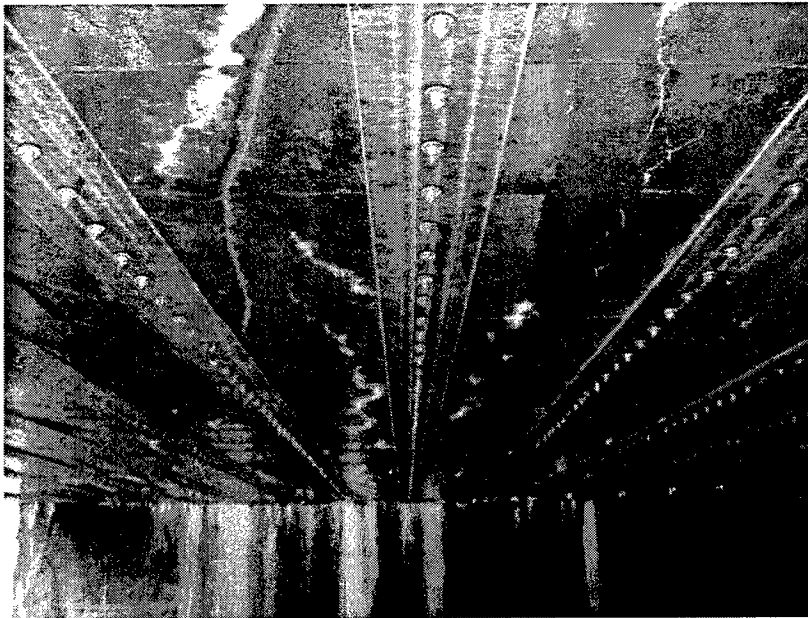

Figure 100. Overall view of the retrofitted bridge deck after 10 months

d. In the spring of 2003, the FRP strips were covered with water and some strips were covered with frost. Figure 101 shows a high amount of moisture on the FRP strip. However, this did not seem to affect the strips.

e. Some corrosion was seen in most of the washers on the X-ALH fasteners and the carbon steel anchors. The southern end of the bridge showed less corrosion as compared with the northern end of the bridge near the abutment. Figure 102 shows the corrosion of the ALH fasteners at the southern end of the bridge and Figure 103 shows the corrosion seen at the northern abutment. The variation in the rate of corrosion was attributed to the larger amount of existing deterioration of the substrate near the North abutment. Figure 104 shows the original damaged area near the north abutment.

Figure 101. FRP strips covered with moisture (Spring 2003)
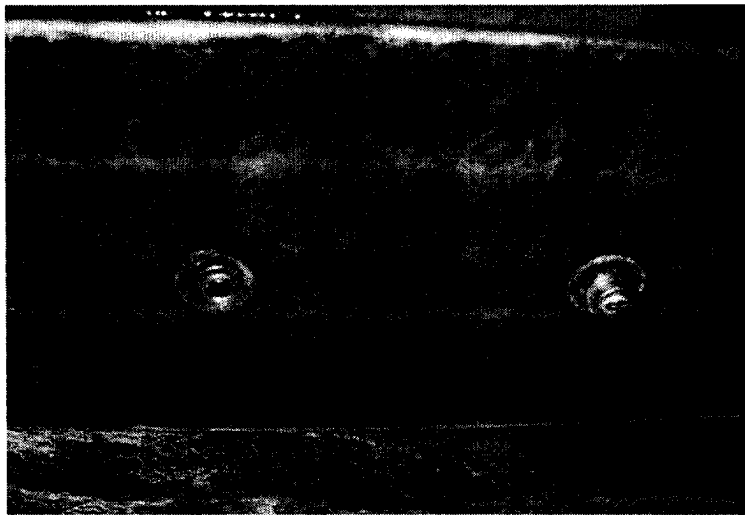

Figure 102. Small amount of corrosion seen at the southern end
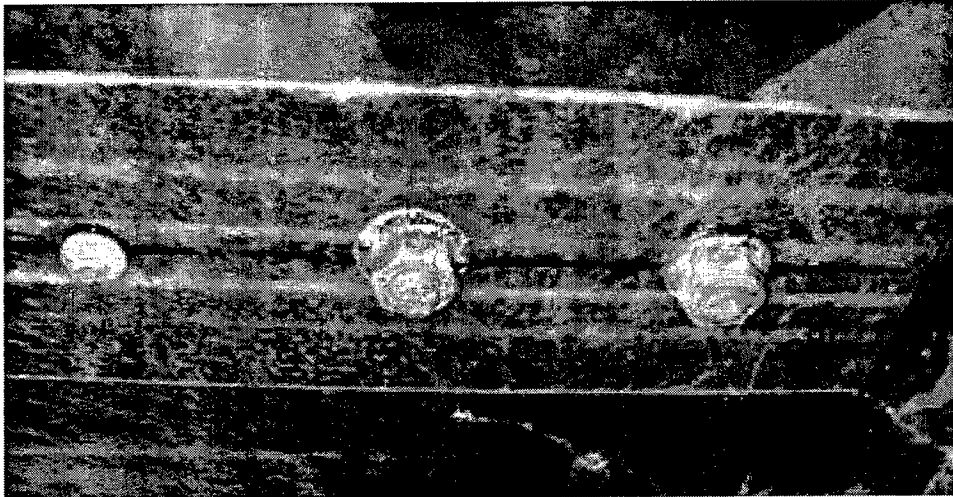
Figure 103. Corrosion seen at the northern abutment

Figure 104. Original damaged area near the northern abutment

f. No corrosion was seen on the stainless steel X-CR fasteners and the anchor bolts. Figure 105 shows the unaffected stainless steel fasteners and anchor bolts.

Figure 105. Stainless steel fasteners and anchors bolts

g. A small amount of corrosion on the ALH fastener shank was observed on fasteners that had achieved improper embedment during the installation of the system. Figure 106 shows one of the fasteners exhibiting some corrosion on the fastener shank. The corroded fastener, which was bent originally when the fastener struck hard aggregate, was pulled out to observe the extent of deterioration. Figure 107 shows the bent fastener after one winter.
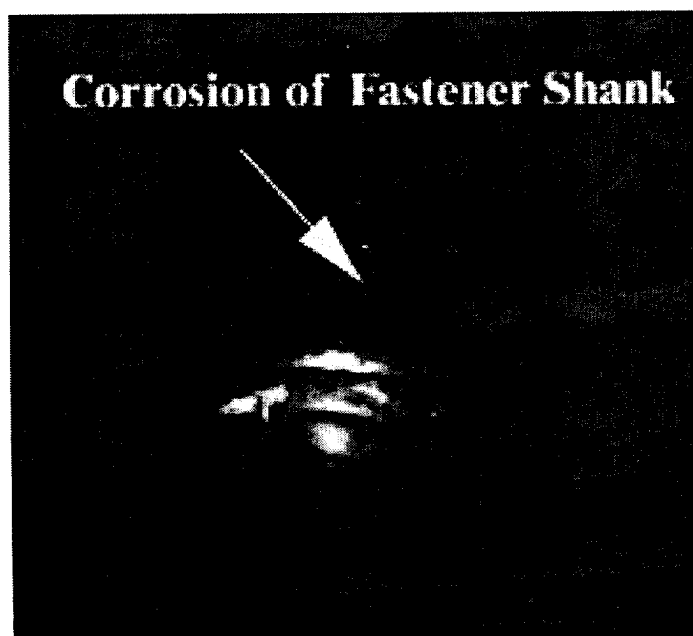

Figure 106. Corrosion of ALH fastener shank with incomplete embedment
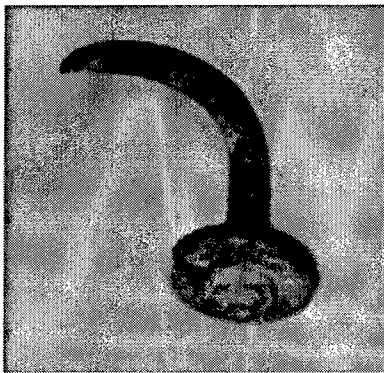
Figure 107. Corrosion on X-ALH fastener seen after 10 months

    h. At the locations of the missing fasteners the FRP strips showed some signs of deterioration. Figure 108 shows some deterioration at the location of the missing fastener.
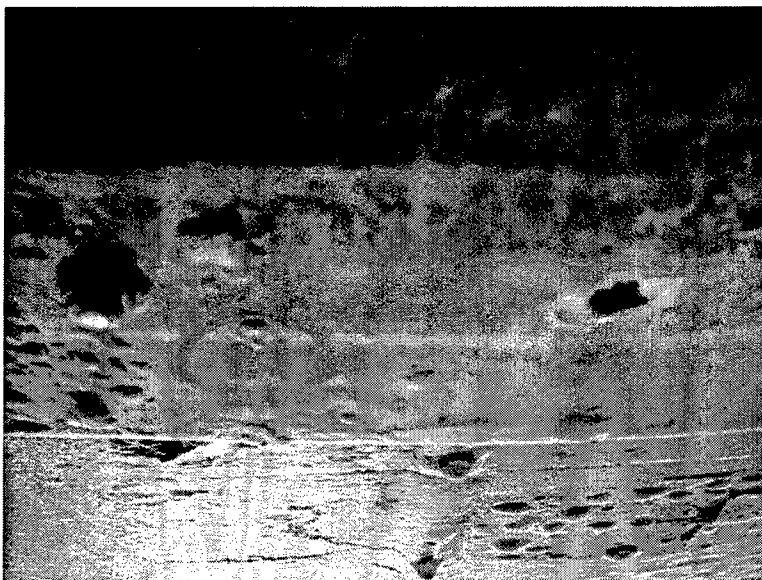

Figure 108. Deterioration of FRP strip at location of missing fastener

    i. The overall condition of the bridge seemed to have been unchanged after one winter. Some additional corrosion of the exposed rebar was seen and it was observed that water had penetrated in between the FRP strips and the concrete deck. This can be seen in Figure 109 where the edge of the FRP strips was covered with water.
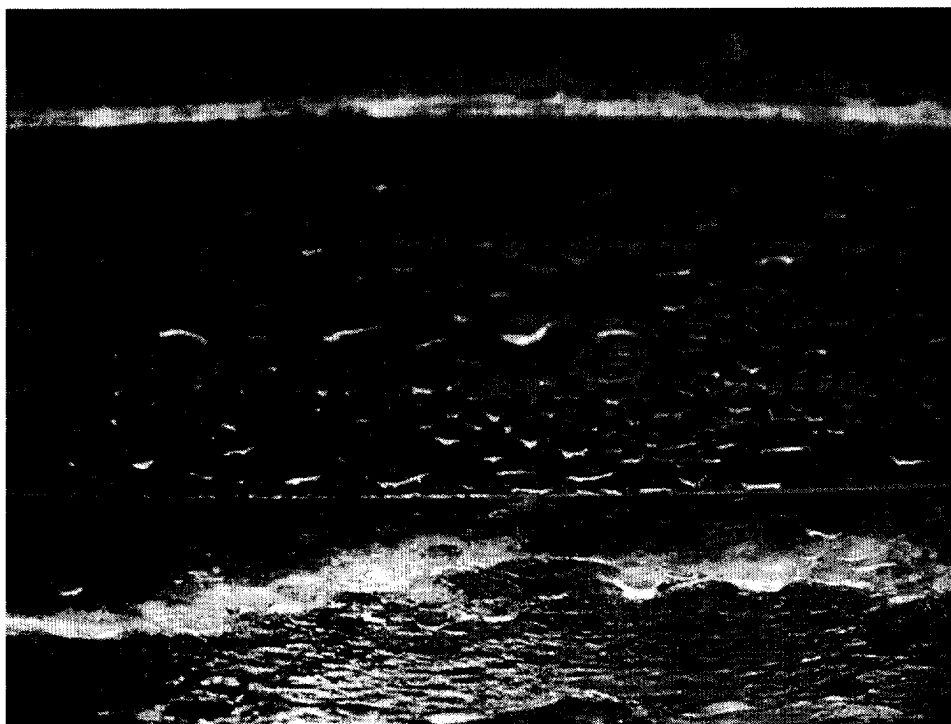
Figure 109. Edge of FRP strips covered with water

The survey of the MF-FRP strengthening system can be described as in "Good" condition as defined by the condition evaluation guidelines by FHWA (2000). The qualitative performance of the FRP strips after one winter was encouraging as no indication of any significant damage to the fastened connection was observed.

Material Properties of FRP Strips

Not only was it important to visually inspect the FRP composite strips, but also it was necessary to determine if 10 months of exposure had degraded the properties of the FRP material. As such, both virgin FRP strips and FRP strips recovered from Bridge P-53-702 were tested in tension to determine their ultimate strength, open-hole strength, and modulus of elasticity.

Tension test conducted on coupons that were 14 in. long by 1 in. wide with a gage length of 10 in. (2 in. on the ends of the coupons were enclosed by the grips of the test apparatus). Open-hole strength tests had the same dimensions, but a 0.188 in. hole was drilled in the center of the coupons (7 in. from either end) prior to the tensile test. Width and thickness were measured to calculate the average cross-sectional area of each specimen for calculation of the strength and stiffness following ASTM D3039 and ASTM D5766. The strain in each coupon was measured with an extensometer, which was removed at approximately 75 percent of the ultimate load to prevent damage to the equipment. Figure 110 shows the test apparatus, while Figure 111 shows typical failed samples.
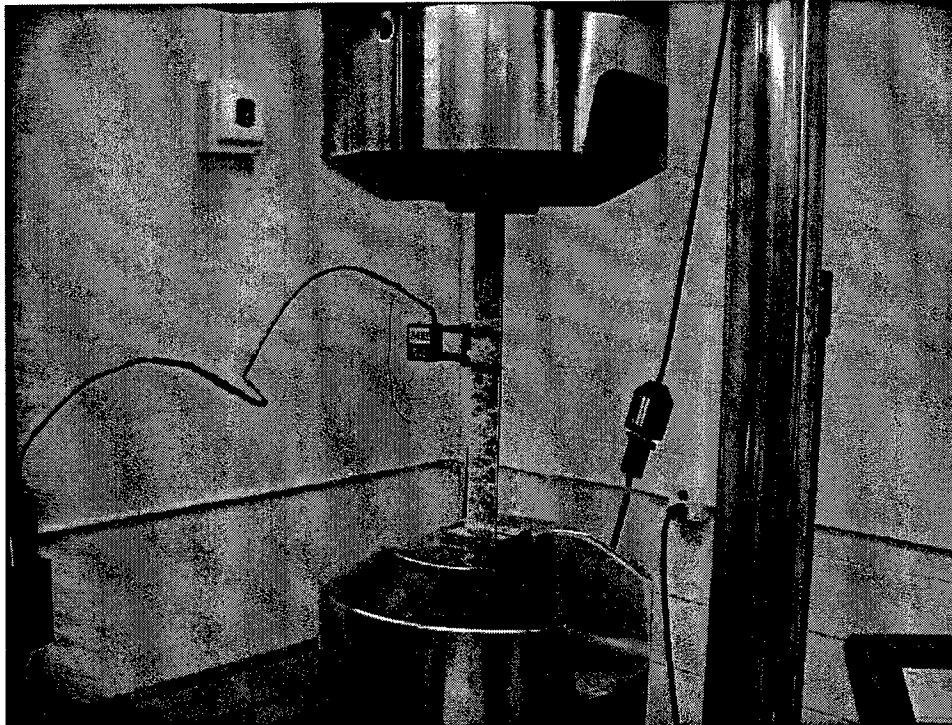
Figure 110. Testing a coupon of recovered material (no hole)
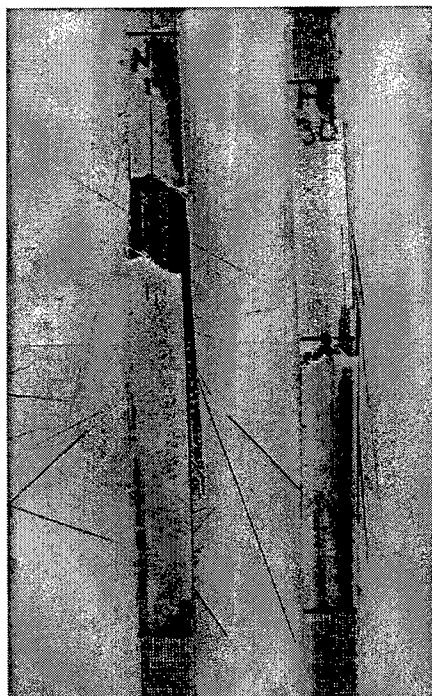
Figure 111. Failed coupons of virgin material (left–no hole; right–central hole)

The ultimate load, strain data, and cross-sectional area provided the basis for analysis. The ultimate load divided by the cross-sectional area gave the ultimate strength, while a linear regression of the stress vs strain curve provided the modulus of elasticity. The results of the two rounds of tensile testing are shown in Table 48. Table 49 compares the properties of the two materials.

Table 48
Average FRP Tensile Test Data

FRP Sample	No. of Tests	Ultimate Strength			Modulus of Elasticity		
		Average (ksi)	Std Dev (ksi)	COV (%)	Average (ksi)	Std Dev (ksi)	COV (%)
Virgin D3039	30	121.0	5.4	4.5	8,511	634	7.5
Recovered D3039	5	122.7	6.4	5.2	8,729	667	7.6
Virgin D5766	30	94.4	5.7	6.0	--	--	--
Recovered D5766	5	94.5	2.3	2.4	--	--	--

Table 49
Material Property Comparison

FRP Sample	Strength (ksi)	% Difference from Virgin	Modulus of Elasticity (ksi)	% Difference from Virgin
Virgin D3039	121.0	--	8,511	--
Recovered D3039	122.7	+1.4	8,729	+2.6
Virgin Open Hole	94.3	--	--	--
Recovered Open Hole	94.5	+0.2	--	--

From the above results, it can be seen that the 10 months of exposure to the elements had a statistically insignificant impact on the mechanical properties of the FRP composite strips. The ultimate strength, the open-hole strength, and modulus of elasticity of the recovered strips remained relatively unchanged with respect to the virgin material. It should be noted, however, that the coupons used for the "recovered" FRP material were cut from the side portions of the strips away from the holes in the strip where some damage may have occurred resulting from environmental effects or resulting from the load testing on the bridge. These measured material properties for the FRP strips also compared well with those obtained in testing conducted at UW (Gulbrandsen 2002) prior to installation of the strips on the bridge. These tests reported an ultimate strength of 122.4 ksi, an open-hole strength of 92.8 ksi, and a modulus of 8,893 ksi.

Conclusions of Ultimate Load Testing Study

The ultimate load testing conducted on a flat slab bridge in Edgerton, Wisconsin, which had been strengthened previously with the MF-FRP system,

was the first in situ test of the MF-FRP system. The following conclusions can be drawn for this phase of the study:

a. Specially designed FRP composite strips attached with powder-actuated fasteners and expansion anchors were able to increase the ultimate strength of test sections of a 73-year-old concrete bridge.

b. The level of strengthening was shown to be a function of the number of strips. A test section with five strips had a higher ultimate load than a section with three strips.

c. Both test sections were shown to have improved strength over a scaled laboratory control beam. Both sections also had significant increases in strength after yield of their internal steel.

d. The FRP strips remained attached to the underside of the concrete bridge well past the yield point and well into the inelastic large-deformation range. The FRP strips remained attached to the concrete well beyond the compressive strength of the concrete.

e. The FRP strips did not appear to be as well attached to the concrete at the locations of the powder-actuated fasteners as had been seen in prior laboratory experiments. Progressive bearing failure, or slotting, of the FRP strips was not seen. Fasteners tended to rotate rather than shear through the strips. This is attributed to the poor properties of the concrete substrate. Nevertheless, significant load was transferred into the FRP strips.

f. Both test section failed resulting from concrete compression with the strips still firmly attached.

g. The FRP composite strip did not appear to have been degraded by 10 months of in situ environmental exposure.

h. The in situ properties of the steel reinforcing bars and the concrete were measured on samples extracted from the demolished bridge. Properties of the steel and concrete were similar to those recommended by AASHTO and as assumed in the design studies.

i. During the design phase of the research it was determined that a 29 percent increase in the nominal strength of the bridge was required to increase the inventory load rating of the bridge from an HS17 to an HS25. Based on the results of the in situ ultimate load testing this increase in strength was felt to have certainly occurred in the east section strengthened with five FRP strips and most likely to have occurred in the west section strengthened with three strips.

j. The predicted strength of the existing section using AASHTO recommended strengths for steel and concrete the 1930's and using an effective width corresponding to the inspection inventory load rating show reasonable agreement with the results of the load tests.

7 Conclusions

The tests conducted on the full-scale T-beams and an existing reinforced concrete flat slab bridge strengthened with the MF-FRP system consisting of powder-actuated fasteners, expansion anchors and FRP composite strips lead to the following conclusions:

a. Experimental and analytical investigations undertaken to demonstrate the rapid strengthening of an existing deteriorated reinforced concrete bridge using MF-FRP have proved the ability of the system to rehabilitate under-capacity structures and improve their load carrying capacity. The addition of end anchors to the system greatly enhanced the effectiveness of the system.

b. The cyclic loading of a full-scale T-beam and the 10 months of in service load on the full-scale bridge demonstrated the ability of the MF-FRP system to be durable under fatigue loading. In both tests, the composite strips showed no signs of degradation, and all fasteners remained embedded in the concrete.

c. The implementation of the MF-FRP system on a bridge in a timely manner with the aid of conventional labor demonstrated the rapid installation and adaptability of the system on a deteriorated structure. The field-application of the system on the deteriorated surface of the bridge also demonstrated benefits over conventional techniques, which require extensive surface preparation and profiling. The MF-FRP system required no surface preparation besides the removal of extra matter from the bridge soffit. The adaptability of the system was demonstrated at locations of high out-of plane variations where conventional techniques would have been susceptible to local failures.

d. Service load testing of the bridge showed the composite behavior of the system with the existing bridge deck and data indicate a reduction in stresses in the existing materials.

e. The tasks undertaken for the experimental verification of the strengthening and to obtain control data on the complete load-deformation behavior of the beams representative of the bridge section met the objectives and showed encouraging results. The test results of representative sections of the bridge slab demonstrated the increase in the load carrying capacity of the bridge from the existing HS17 to HS25

corresponding to at least 29 percent increase in strength.

f. The theoretical model developed for the strengthened reinforced concrete members with the MF-FRP system predicted strengthening improvements. The strength model depends on a desirable bearing failure mode of the fastened FRP strip, which was shown to be proportional to the number of fasteners used.

g. The preliminary design procedure and the application guidelines for proper detailing of the proposed method developed, provide a basis for the application of the system to strengthen existing deteriorated reinforced concrete bridges and other reinforced concrete structures.

h. The research indicates the efficacy of the proposed system for rehabilitation of existing under-capacity bridges which in combination with repair techniques may offer a potential for the temporary upgrading of highway and non-highway bridge infrastructure before budgets for eventual replacements of such structures are available.

i. The method of in place load testing used in the research is practical and efficient. It affords researchers the opportunity to investigate real-world structures and provides the opportunity to gather pertinent data including applied loads, deflections, and strains.

j. Both test sections of the strengthened flat slab bridge exhibited an increased flexural capacity over a scaled laboratory control beam. The increase in the yield moment for both test sections was 14.0 percent, while the increase in ultimate moment ranged from 11.5 percent for the west section (3 strips) to 30.8 percent for the east section (5 strips).

k. The FRP composite strengthening method maintains an increased flexural capacity over an unstrengthened section even after large deflections. The flexural capacity of the west section (3 strips) was 25.2 percent higher at 2 in. of deflection (L/125), while the east section (5 strips) was 47.7 percent greater at the same deflection. This also demonstrates that the addition of more FRP composite strips increases the strengthening effect of the system.

l. The qualitative survey of the strengthened bridge after 10 months demonstrated the durability of the system under exterior exposure. The system showed some minor signs of deterioration but performed well without any significant loss of strength of the fastened connection.

m. The mechanical properties of the FRP composite strips were not degraded by 10 months of exposure to the elements. The failure stress and modulus of elasticity (for both the standard tension test and open-hole tension test) of the recovered FRP composite strips remained consistent with the virgin material.

8 Recommendations for Future Work

This investigation has indicated that the MF-FRP strengthening method is viable for application to real-world structures. The following recommendations look towards refining the method and furthering its development:

a. X-ALH fasteners are recommended for use; however, under exterior exposures the use of stainless steel fasteners X-CR-SS fasteners is recommended only if washers with a neoprene backing are used. The use of stainless steel fasteners with neoprene backed washers needs to be further investigated prior to use on full-scale applications.

b. Additional bearing strength tests with different fasteners and anchors to experimentally determine the bearing strengths and force per fasteners corresponding to bearing failure of the FRP strip should be conducted.

c. An experimental investigation of the bearing strength of the FRP strip under clamped conditions to simulate the fastened connection should be conducted to obtain more understanding of the effects of clamping pressure on the fastener load.

d. Connection tests with multiple fasteners and single fasteners should be studied to further obtain information on load distribution and reasons for low-level concrete pry out failures.

e. The effects of shear failures at the ends and in between mechanical fasteners of the fastened FRP strips to sustain higher loads should be studied in order to determine minimum and maximum spacing requirements.

f. The predictions of the strength model should be compared with all existing experimental test data before the strength model is adopted as a design procedure.

g. A comprehensive moment-curvature model based on the strength model with the inclusion of the slip to accurately predict the complete load-deformation behavior of the strengthened member should be developed for research purposes.

h. A statistical analysis of the appropriate safety factor that should be used for the contribution of the MF-FRP system to the flexural capacity of the member should be conducted.

i. Additional full-scale tests with the MF-FRP system on different types of bridge structures (for example T-beam bridges) and with different span lengths should be conducted. This may further reveal benefits of stiffness increase by the MF-FRP system.

j. The long-term effects of the environment on the MF-FRP system should continue to be studied. After 10 months, there were local adverse effects such as corrosion on the fasteners and deterioration of the composite strip at open-hole locations. A study of environmental impacts on a rehabilitated real-world structure is necessary to verify the practicality of the system for long-term applications.

k. The installation process for use on longer span structures should be studied. Workers were able to strengthen Bridge P-53-702 using 21-ft-long composite strips rather easily. The relatively short length of the strips made them easy to handle and attach. A longer span structure, however, would not prove as easy. Refinements, to include the investigation of splicing the composite strips, need to be explored to make the method practical for all structures, regardless of length.

References

American Association of State highway and Transportation Officials. (1996). "Standard specifications for highway bridges," 16th ed., Washington, DC.

_____. (1998). "LRFD bridge design specifications,: 2nd ed., Washington, DC.

_____. (2000). "Manual for condition evaluation of bridges," 2nd ed., Washington, DC.

American Concrete Institute Committee 440.2R. (2002). "Guide for the design and construction of externally bonded FRP systems for strengthening concrete structures," Farmington Hills, MI.

American National Standards Institute. (1995). "American national standard for construction and demolition: powder-actuated fastening systems–safety requirements," Chicago, IL.

American Society for Testing and Material D638. "Standard test method for tensile properties of plastics," West Conshohocken, PA.

American Society for Testing and Material D953. "Standard test method for bearing strength of plastics," West Conshohocken, PA.

American Society for Testing and Material D3039. "Standard test method for tensile properties of polymer matrix composite materials," West Conshohocken, PA.

American Society for Testing and Material D5766. "Standard test method for open hole tensile strength of polymer matrix composite laminates," West Conshohocken, PA.American Society for Testing and Material D5961. "Standard test method for bearing response of polymer matrix composite laminates," West Conshohocken, PA.

Arora, D. (2003). "Rapid strengthening of reinforced concrete bridge with mechanically fastened–fiber reinforced polymer strips," M.S. thesis, University of Wisconsin-Madison, WI.

Bank, L.C., Lamanna, A.J., Ray, J.C., and Velazquez, G.I. (2002a). "Rapid strengthening of reinforced concrete beams with mechanically fastened, fiber-reinforced polymeric composite materials," Technical Report ERDC/GSL TR-02-4, U.S. Army Engineer Research and Development Center, Vicksburg, MS.

Bank, L.C., Borowicz, D.T., Lamanna, A.J., Ray, J.C., and Velazquez, G.I. (2002b). "Rapid strengthening of full-size reinforced concrete beams with powder-actuated fastening systems and fiber-reinforced polymer (FRP) composite materials," Technical Report ERDC/GSL TR-02-12, U.S. Army Engineer Research and Development Center, Vicksburg, MS.

Borowicz, D.T. (2002). "Rapid strengthening of concrete beams with powder actuated fasteners and fiber reinforced polymer (FRP) composite materials," M.S. thesis, University of Wisconsin-Madison.

Chajes, M. J., Mertz, D. R., and Commander, B. (1997). "Experimental load rating of a posted bridge", Journal of Bridge Engineering, 2(1), 1-10.

Federal Highway Administration. (2000). "Recording and coding guide for the structure inventory and appraisal of the nations bridges," Report No. FHWA-PD-96-001.

Federal Highway Administration. (2001). "National bridge inventory (NBI)," http://www.fhwa.dot.gov/bridge/nbi.htm.

Gulbrandsen, P.W. (2002). "Tensile and bearing tests of FRP composite strengthening strips," Hilldale Undergraduate Research Report. University of Wisconsin-Madison, WI.

Lamanna, A.J. (2002). "Flexural strengthening of reinforced concrete beams with mechanically fastened fiber-reinforced polymer strips," Ph.D. diss., University of Wisconsin–Madison, WI.

Lamanna, A.J., Bank, L.C., and Scott, D.W. (2001a). "Flexural strengthening of reinforced concrete beams using fasteners and fiber-reinforced polymer strips," ACI Structural Journal, 98(3), 368-376.

Lamanna, A.J., Bank, L.C., and Scott, D.W. (2001b). "Rapid flexural strengthening of RC beams using powder actuated fasteners and FRP strips," 5th ed. International Symposium of FRP in Reinforced Concrete Structures, Cambridge, UK, July 16-18, 389-397.

Saraf, K.V. (1998). "Evaluation of existing RC slab bridges", Journal of Performance of Constructed Facilities, 12(1), 20-24.

Shahrooz, B.M., Miller, R.A., Saraf, V.K., and Godbole, B. (1994). "Behaviour of RC slab bridges during and after repair", Transportation Research Record 1442, 128-135.

References

Stallings, J.M., Tedesco, J.W., El-Mihilmy, M., and McCauley, M. (2000). "Field performance of FRP bridge repairs," *ASCE Journal of Bridge Engineering*, 5(2), 107-113.

State of California. (1998). "Pontis Element Level Inspection Manual," Department of Transportation Engineering Service Center, Division of Structures. Office of Structures Maintenance and Investigation.

U.S. Department of Commerce. (1956). "Standard plans for highway bridge superstructures," Bureau of Public Roads, Washington, DC.

Velázquez, G.I., Ray, J.C., Borowicz, D.T., Lamanna, A.J., and Arora D., and Bank, L.C. (2002). "Tests of reinforced concrete T-Beams retrofitted with mechanically anchored fiber-reinforced polymer (FRP) plates," *1st International Conference on Bridge Maintenance, Safety and Management*, IABMAS, 2002, Barcelona, SPAIN, July 14-17, CD-ROM.

WBM. (1994). "Wisconsin bridge manual," *Wisconsin Department of Transportation*, Madison, WI.

Appendix A
Bridge Inspection Report and Rating Sheet for P-53-702 provided by WisDOT

Bridge Inspection Report

EM30 - 0198   Section 84.17 Wis. Stats.

Wisconsin Dept. of Transportation

Feature On: LRD STOUGHTON RD	Maintainer: City/Municipal Hwy Agenc	Structure Number: P-53-0702
Feature Under: SAUNDERS CREEK	Sect/Twn/Rng: S04 T04N R12E	

location: 0.6M N JCT STH 59	County: Rock	Municipality: CITY OF EDGERTON	

Inv Rating: HS17	Rdwy Width: 23	Deck Width: 25.9	Existing Posting:	Suff Rating: 32.7
Oper Rating: HS29	Total Length: 24	Deck Area: 621	Recom Posting:	Rate Score: 64

Overburden in.: 3	Date: 1/1/1901	Section Loss %:	ADT On: 600	Year: 1980	ADT Under:	Year:

Bridge Element — **Quantity in Condition State**

Num	Description	Env	Unit	Tot Qty	1	2	3	4	5	Comments
39	Concrete Slab -	4	(SF)	646	646	0	0	0	0	Deep deter. on deck edges
215	Reinforced Conc	2	(LF)	46	36	10	0	0	0	Cracks and deep spalls both abut. @ corners
322	Bituminous Approach	3	(EA)	2	2	0	0	0	0	
331	Reinforced Conc Bridge	3	(LF)	49	0	49	0	0	0	
359	Soffit of Concrete Deck	4	(EA)	1	0	0	0	1	0	SHOWS HUNDREDS OF STALAGTITES W/
400	Concrete Wingwall	2	(EA)	4	0	4	0	0	0	CRACKS & SPALLS IN ALL WINGWALLS.
405	Drainage	2	(EA)	2	0	2	0	0	0	NEED DOWN SPOUTS.
410	Curb	2	(LF)	49	0	49	0	0	0	spalls entire length

Structure Notes:

CHECK FOR LOAD RATING CAP. POSSIBLY RE-RATED. This bridge should be considered for replacement 2002-2003.

	Old New		Old New		Old New		Old New
NBI RATINGS	Deck 3	Superstructure	3	Substructure	5	Culvert	N

Should structure be re-rated for load carrying capacity? (yes/no) [Y]   **Structure Number: P-53-0702**

Other Items	Rating Old	Rating New	Comments	Marking/Signing	Rating Old	Rating New	Comments
Approach Alignment	8			Bridge Markers	Y		1 - needs repairs
Channel Condition	6			Narrow Bridge			Need narrow bridge signs
Waterway Adequacy	6		Some silting	One Lane Bridge			
Construction Joints	6			Vertical Clearance			
Utilities				Weight Limit Post			

Clearance	Meas. (ft)	Date	New Meas.
Min Vert Clear. Under Cardinal (N or E)		1/1/1901	
Min Vert Clear. Under Non-cardinal		1/1/1901	
Min Vert Clear. Over			
Measured by:		Date:	

EXPANSION JOINTS				STRUCTURE TYPE			
Location	In.	Temp	Type	Material	Configuration	# Spans	Length
A.				CONCRETE	FLAT SLAB	1	23
B.							
C.							
D.							
E.							
F.							

Inspection/Maintenance Notes:

This bridge should be rerated for load carryibg capacity.
Recommend - replacement of bridge or other.

Recommendations	Estimated Cost	Year Programmed
BRIDGE REPLACEMENT	56160	1999
Repair bridge marker and install narrow bridge signs	200	

CONSTRUCTION HISTORY			
Year	Work Performed	Year	Work Performed
1930	NEW STRUCTURE		

Routine Inspections		Fracture Critical Inspections		Underwater Inspections						Other Special Inspections	
				Visual/Probing		Diving		Profile/Soundings			
Last Insp	Freq (mo)	Last Insp	Freq (mo)	Last Insp	Freq (mo)	Last Insp	Freq (mo)	Last Insp	Freq (mo)	Last Insp	Freq (mo)
11/15/00	24			11/15/00	12	1/1/01		1/1/01			

Equipment Needs:

Routine	
Fracture Critical	
Underwater	
Other Special	

Inspector:	Date:	Inspection Agency: City/Municipal Hwy Agenc

**** SIMPLE SPAN AXLE RATINGS ****

P-702 CTH N ROCK COUNTY

22.000	0.205	0.205	0.286	16.000	0.800	10.000
2.000	2.000	0.0	0.0	0.0	36.000	
0.0	0.0	0.0	0.0	19.500	12.000	
0.0	0.0	0.0	0.0	0.0	0.0	

SECTION MODULI - REINFORCED CONCRETE SECTION

CONCRETE - 570.2
STEEL - 30.9

LONGITUDINAL GIRDER RATINGS
ALLOWABLE PERMIT GROSS WEIGHT OF SINGLE AND TANDEM AXLES IN KIPS

MULTIPLE AXLES ARE SPACED AT FOUR FEET.

30 PERCENT IMPACT
1 AXLES = 46.9
2 AXLES = 56.7
3 AXLES = 61.9
4 AXLES = 72.7

ALLOWABLE PERMIT GROSS WEIGHT OF AXLE GROUP COMBINATIONS IN KIPS

TWO SINGLE AXLES
6 FT.SPAC.   61.1   12 FT.SPAC.   85.2   18 FT.SPAC.   ****

ONE SINGLE AXLE AND ONE 2-AXLE TANDEM
6 FT.SPAC.   64.2   12 FT.SPAC.   84.8   18 FT.SPAC.   ****

ONE SINGLE AXLE AND ONE 3-AXLE TANDEM
6 FT.SPAC.   70.6   12 FT.SPAC.   ****   18 FT.SPAC.   ****

TWO 2-AXLE TANDEMS
6 FT.SPAC.   73.0   12 FT.SPAC.   ****   18 FT.SPAC.   ****

ONE 2-AXLE TANDEM AND ONE 3-AXLE TANDEM
6 FT.SPAC.   83.7   12 FT.SPAC.   ****   18 FT.SPAC.   ****

TWO 3-AXLE TANDEMS
6 FT.SPAC.   ****   12 FT.SPAC.   ****   18 FT.SPAC.   ****

H-RATING= 17.6   30 PERCENT IMPACT.
R-RATING= 29.3   30 PERCENT IMPACT.

HS-RATING= 17.6   30 PERCENT IMPACT.

P-702

2

RS-Rating = 29.3   30 Percent Impact (reverse)

REPORT DOCUMENTATION PAGE				Form Approved OMB No. 0704-0188

Public reporting burden for this collection of information is estimated to average 1 hour per response, including the time for reviewing instructions, searching existing data sources, gathering and maintaining the data needed, and completing and reviewing this collection of information. Send comments regarding this burden estimate or any other aspect of this collection of information, including suggestions for reducing this burden to Department of Defense, Washington Headquarters Services, Directorate for Information Operations and Reports (0704-0188), 1215 Jefferson Davis Highway, Suite 1204, Arlington, VA 22202-4302. Respondents should be aware that notwithstanding any other provision of law, no person shall be subject to any penalty for failing to comply with a collection of information if it does not display a currently valid OMB control number. **PLEASE DO NOT RETURN YOUR FORM TO THE ABOVE ADDRESS.**

1. REPORT DATE (DD-MM-YYYY) July 2004	2. REPORT TYPE Final report	3. DATES COVERED (From - To)

4. TITLE AND SUBTITLE	5a. CONTRACT NUMBER
Strengthening of Concrete Beams with Fasteners and Composite Material Strips–Scaling and Anchorage Issues	5b. GRANT NUMBER
	5c. PROGRAM ELEMENT NUMBER
6. AUTHOR(S)	5d. PROJECT NUMBER
Lawrence C. Bank, David T. Borowicz, Dushyant Arora, Anthony J. Lamanna, Gerardo I. Velázquez, James C. Ray	5e. TASK NUMBER
	5f. WORK UNIT NUMBER

7. PERFORMING ORGANIZATION NAME(S) AND ADDRESS(ES)	8. PERFORMING ORGANIZATION REPORT NUMBER
Department of Civil and Environmental Engineering University of Wisconsin-Madison Madison, WI 53706; U.S. Army Engineer Research and Development Center Geotechnical and Structures Laboratory 3909 Halls Ferry Road Vicksburg, MS 39180-6199	ERDC/GSL TR-04-5

9. SPONSORING / MONITORING AGENCY NAME(S) AND ADDRESS(ES)	10. SPONSOR/MONITOR'S ACRONYM(S)
U.S. Army Corps of Engineers Washington, DC 20314-1000	11. SPONSOR/MONITOR'S REPORT NUMBER(S)

12. DISTRIBUTION / AVAILABILITY STATEMENT

Approved for public release; distribution is unlimited.

13. SUPPLEMENTARY NOTES

14. ABSTRACT

A system to rapidly strengthen concrete beams and slabs, known as the Mechanically-Fastened Fiber-Reinforced Polymer (MF-FRP) system, has been developed. In the fourth year of research on the subject, the focus was on scaling and anchorage issues. The effect of increasing the number of strips, the fastener spacing, termination distances, and the use of expansion anchors at the strip ends were considered. The scaling study also investigated the use of the MF-FRP system on a full-scale highway bridge.

A second series of tests was conducted on large-scale T-beams at the U.S. Army Engineer Research and Development Center, Vicksburg, MS, in the summer of 2002. The results of this testing and of parametric design studies conducted were used to design the strengthening system for a flat-slab bridge built in 1930 in the city of Edgerton, WI, and slated for replacement in 2003. The bridge was strengthened with the MF-FRP system in the summer of 2002 and tested to failure in the summer of 2003. An investigation was also conducted into the properties of the FRP strips with different constituent material properties. An optimal strip design to produce the best ultimate longitudinal strength and stiffness, as well as bearing strength, has been recommended to the manufacturer.

(Continued)

15. SUBJECT TERMS			
Beam retrofit	Bridge retrofit	Fiber reinforced polymeric	FRP plates
Beam upgrade	Bridge upgrade	FRP	Mechanical fasteners

16. SECURITY CLASSIFICATION OF:			17. LIMITATION OF ABSTRACT	18. NUMBER OF PAGES	19a. NAME OF RESPONSIBLE PERSON James C. Ray
a. REPORT UNCLASSIFIED	b. ABSTRACT UNCLASSIFIED	c. THIS PAGE UNCLASSIFIED		154	19b. TELEPHONE NUMBER (include area code) (601) 634-3265

Standard Form 298 (Rev. 8-98)
Prescribed by ANSI Std. 239.18

14. (Concluded).

The research conducted revealed a number of important scaling related issues with the MF-FRP system. It was found that multiple strips were not as effective as single strips, that a double row of fasteners at 2 in. on center is less effective than a single row of fasters at 3 in. on center, and that mechanical anchor bolts at the ends of the strip significantly improved performance and delayed the onset of end-delamination failures. The importance of a small termination distance from the support was confirmed in testing. Fatigue testing to 2 million cycles showed no degradation of the MF-FRP strengthening system. The full-scale bridge application proved the versatility of the system. Strips were easily and rapidly attached to a severely deteriorated concrete soffit that would not have permitted the use of an epoxy-bonded FRP (EB-FRP) strengthening system.

Ten (10) months of environmental exposure did not appear to reduce the effectiveness of the system, and no degradation in material properties of the FRP strips was seen. The ultimate failure test on the bridge proved the ability of the MF-FRP system to increase the strength of a reinforced concrete bridge. Analytical models to predict the strengthening were shown to produce reasonable predictions. These models can be used for design purposes.